Friction and wear of the Durham finger prosthesis

Vandelli Dott. Ing. Cinzia

Friction and wear
of the Durham finger prosthesis

By

Vandelli Dott. Ing. Cinzia

Submitted for the degree of

Master of Science

University of Durham,

Centre of Biomedical Engineering,

School of Engineering

2002

Abstract

Rheumatoid arthritis of the hand can cause deformities that may severally impair hand function. Surgical procedures including total joint replacement have been developed over the last thirty years to treat patients with metacarpophalangeal deformity. The Centre of Biomedical Engineering at Durham University contributed to this field of research by designing a new artificial metacarpophalangeal (MCP) joint intended to operate in the same manner as the natural joint. The Durham MCP prosthesis is a non constrained two piece all XLPE device which allows flexion-extension, adduction-abduction and little rotation movements. In order to test the wear behaviour of the Durham MCP prosthesis before implanting it, a new finger wear simulator was also designed at Durham University and the prosthesis gave acceptable results from a wear point of view. In 1997 clinical trials started and to date five people have been implanted with the Durham MCP prosthesis.

In order to investigate the *in vitro* wear behaviour of the Durham MCP prosthesis further, nine wear tests were undertaken during this research using the finger wear simulator. For the first time EtO-sterilized XLPE prostheses were tested and their performances in bovine serum were very promising. This might indicate that ethylene oxide gas is a valid alternative to gamma irradiation for sterilizing the Durham MCP prosthesis as it doesn't seem to influence its wear properties. Wear debris was also analyzed showing that the majority of the particles detected were less than 1μm in size.

In order to investigate the frictional properties of the Durham MCP prosthesis, a new finger friction simulator has been designed, manufactured and validated during this research. Various tests were undertaken using different pairs of materials in order to compare the results with literature and validate the simulator. The new finger friction simulator appears to give consistent results and might then be used to record the variations of the coefficient of friction in the all XLPE Durham MCP prosthesis during the wear tests.

Contents

List of Figures

List of Tables

This work is dedicated to my sister: may it contribute towards the understanding of juvenile rheumatoid arthritis and give some hope to those threatened by it

"The science of total joint replacement was just a side road in progress until the real science of joint restoration/healing advances. Such restoration is likely to be aided by the use of degradable and biologically active temporary support materials."

Author unknown

1. Introduction

The very complex mechanical structure of the human hand (Tubiana, 1980) and its subtle system of control units allow for a great variety and high adaptability of movement. It is therefore evident that this normal human hand performance is very important in basic and professional activities of daily life. Unfortunately the small joints of the hand can be affected by arthritis, especially rheumatoid arthritis, and this disorder can lead to severe degenerative changes limiting the normal functions of the hand. When the small joints of the hands are seriously affected by rheumatoid arthritis, the main indication for its cure is arthroplasty.

Arthritis and rheumatic disease affects around eight million people in the UK and more than three million of them have a significant disability. In 1997 more than 26 million prescriptions were issued for musculoskeletal and joint diseases, with a total cost of £205m (Arthritis and Rheumatism Council, 1997).

The aim of this research project was to investigate the *in vitro* wear and frictional properties of biomaterials for artificial finger joints with a particular interest in the two piece all cross-linked polyethylene (XLPE) Durham metacarpophalangeal joint. The Durham prosthesis has been designed to be implanted into patients with rheumatoid arthritis at an early stage of the disease and it was therefore expected to act as a low friction shield to the undamaged bone beneath. The bearing surfaces were also required to articulate with a low wear rate and produce the minimal amount of wear particles in order to avoid adverse tissue reactions. Simple wear theory predicts that wear is proportional to load (Archard, 1953), thus since few situations occur when high loads are accompanied with movement, it would seem that wear would not be a significant problem in MCP prosthetic design. However, since the wear rate for similar polymer bearing surfaces is high in comparison to other material combinations, the choice of the material becomes very important.

In artificial joints, mechanical and biological phenomena are simultaneous and synergistic in the process of loosening: the articular movements under load provoke wear with production of debris, and generate destructive shearing stresses at the bone-implant interface. Then the breakage of the anchorage leads to movement, causing wear at the bone interface and increasing the penetration of fluid which carries debris. The bone resorption caused by foreign body reaction to the particles accelerates the loosening and increases the movement.

A very important parameter for evaluating the choice of the pair of materials is the coefficient of friction, which depends on the contact conditions of the materials, the surface finish and on the lubrication. The affinity of one surface towards the other depends on the nature of the materials and can be influenced by the ambient conditions: nature of the medium, pH, temperature and pressure. The lubrication depends on the presence and the quality of the lubricant and on the wettability of the surfaces.
The natural human joints have a very low coefficient of friction between the cartilage/cartilage coupling (0.002 to 0.007). On the other hand, prostheses produce higher friction (coefficient of friction metal/polyethylene: 0.05 to 0.2).

The aim of this research was to investigate further the wear and frictional properties of biomaterials for finger joints. For this reason various tests involving the two piece all XLPE Durham MCP joint were run using the wear simulator. The influence of method of sterilisation, motion, lubricant and long-term performances were investigated. A test was also run to compare the Durham prosthesis behaviour under the same conditions as the Swanson prosthesis.

In order to investigate the *in vitro* frictional properties of XLPE rubbing against itself, a new finger friction simulator was designed and validated. Tests under the MCP loading and motion conditions were run using different pairs of materials.

2. Review of published work

2.1 Metacarpophalangeal Joint

2.1.1 Anatomy

The three planes that describe the spatial relationships of the hand anatomy are shown in fig. 2.1.

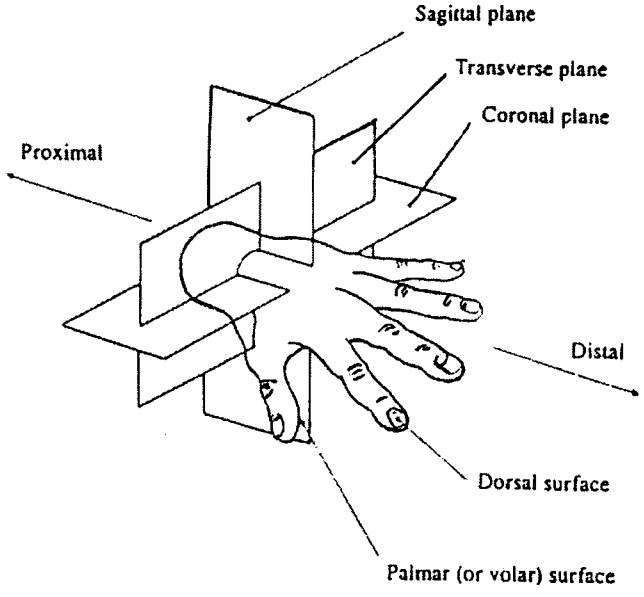

Fig. 2.1 Planes of the anatomy of the hand (Beevers and Seedhom, 1993)

The anatomy of the hand is shown in fig. 2.2.

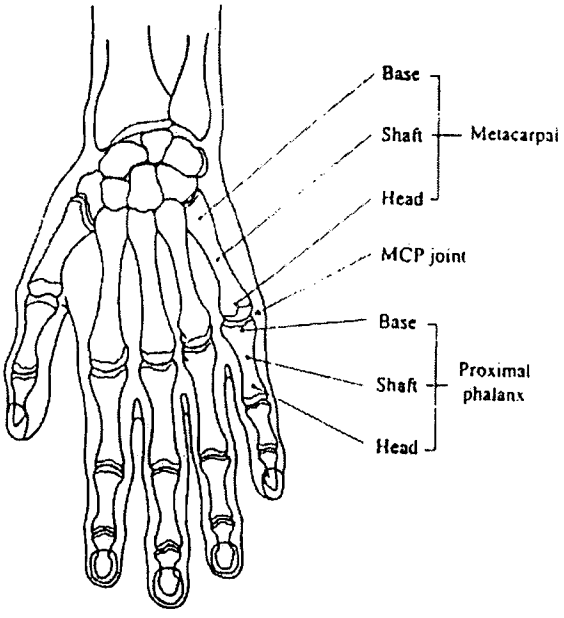

Fig. 2.2 Anatomy of the hand (Beevers and Seedhom, 1993)

The normal MCP joint is a diarthodial, condylar-type joint. The metacarpal head has a greater surface area than the base of the proximal phalanx. The articular surface of the head is convex and has a wider palmar surface. The eccentric attachment of ligaments accounts for the tightening of the collateral ligaments when the joint flexes.

The normal metacarpophalangeal joint allows an active range of motion from 20° extension to 90° flexion and a 40° arc of abduction-adduction while also permitting passive rotation (Walker and Erkman, 1975; Youm et al., 1978).

As it has been described previously, the metacarpophalangeal joint has three planes of motion: the sagittal plane where flexion-extension occurs, the coronal plane for the abduction-adduction movement and the transverse plane around which a limited degree of axial rotation is allowed.

The major stabilisers of the MCP joint are the collateral ligaments located on the ulnar and radial sides of the joint and the volar plate positioned between the head of the metacarpal and the proximal phalanx. The two collateral ligaments act as

stabilising elements allowing flexion-extension and abduction-adduction without any joint subluxation, while the volar plate provides support for the MCP joint in extension by being strongly attached to both the proximal phalanx and the metacarpal via the metacarpo-glenoidal ligament.

2.1.2 Biomechanics of MCP joints

During a normal activity of the hand like pinch grip using the index finger and the thumb, the flexor mechanism passes through a flexor tunnel, then insert into the proximal phalanx and also continues to the middle and distal phalanges (Tubiana, 1969). When this occurs, the metacarpo-glenoidal ligament acts as a pulley and turns the flexor tendons through the appropriate angle of flexion and through an inclination to the ulnar side (Smith et al., 1966) as shown in figure 2.3.

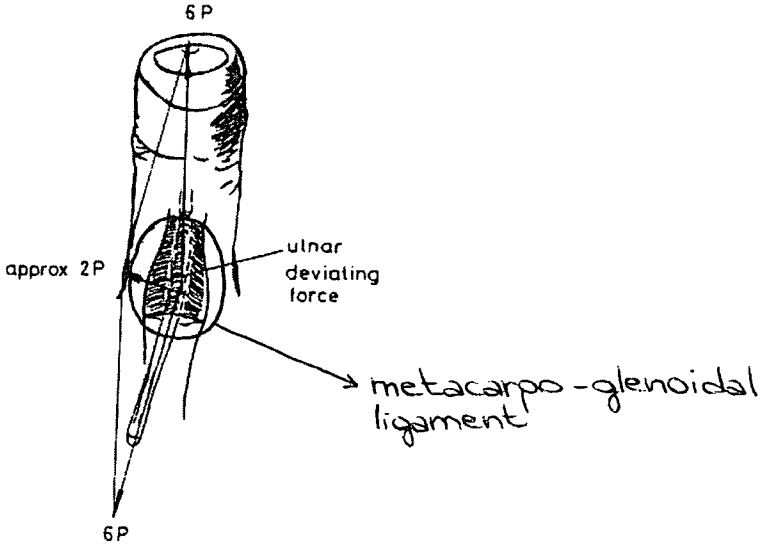

Fig. 2.3 Ulnar deviating forces due to flexor action in pinching (Unsworth In Dowson and Wright, 1981)

If the whole finger is then considered while "pinching" a small ball, then the just explained mechanical disadvantage of the system, causes the flexor tendons to exert very large forces compared with the original pinch force (fig. 2.4).

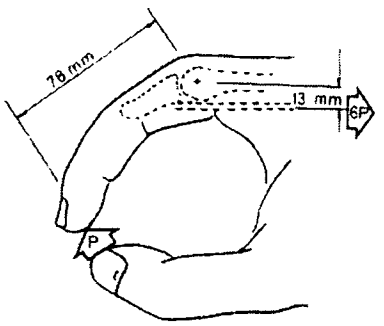

Fig. 2.4 Flexor tendon forces when pinching with a force of P (Unsworth In Dowson and Wright, 1981)

If the pinch force required is P, then the tendon pull is six times P having assumed that the tendon force acts about the centre of rotation of the metacarpophalangeal joint. As a consequence of this particular force configuration, the metacarpo-glenoidal ligament feels a resultant force, which tries to extend in the palmar direction. The magnitude of this palmar force depends on the angle of flexion of the metacarpophalangeal joint and can be expressed in terms of the pinch force P as

$$S = 12\ P \sin\left(\frac{\vartheta}{2}\right)$$

therefore when $\theta = 45°$, $S = 4.59\ P$.

Whatever P is in daily life activities, this force is easily carried by an healthy joint, but the same cannot be said for a rheumatoid hand where the metacarpo-glenoidal ligament is stretched because of the disease. In this case the palmar force is transferred to the collateral ligaments of the metacarpophalangeal joint resulting in a subluxation of the base of the proximal phalanx (fig. 2.5). This is a common

deformity in a rheumatoid hand and it can be totally explained in terms of the bio-mechanics of the joint.

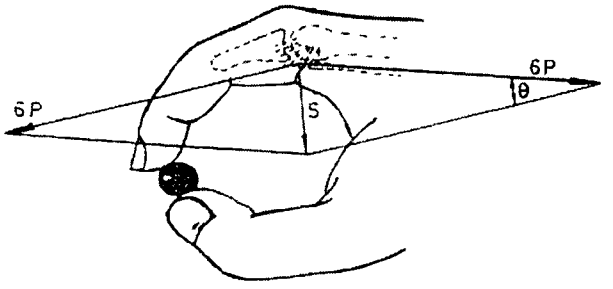

Fig. 2.5 Forces causing subluxation in the metacarpophalangeal joint (Unsworth In Dowson and Wright, 1981)

Using the same form of analysis in the dorso-volar plane, the tendon forces deflect the flexor sheath towards the ulnar side resulting in ulnar deviation in case of stretching of the metacarpo-glenoidal ligament.

A simple way to help rheumatoid patients to prevent subluxation or ulnar deviation deformities is to teach them to grip with the metacarpophalangeal joint in full extension in order to reduce the subluxing force to zero.

2.1.3 Pathology of rheumatoid MCP joints

Rheumatoid arthritis of the hand causes multiple deformities (Nordin and Frankel, 1898). The vast majority of indications for MCP arthroplasty and the focus of the literature are patients with RA. Destruction of the MCP joint in RA begins with a proliferative synovitis and progressively leads to a volarly subluxed proximal phalanx with ulnar deviation and destruction of the articular cartilage (fig. 2.6).

Fig. 2.6 Rheumatoid hands (http://www.worldortho.com/database/exam-orth/index.html)

The primary causative factor producing the characteristic joint deformities remains controversial. A study by Zancolli et al., 1979 suggested the proposal of a deformity, which exists before articular destruction. Synovial inflammation of the carpometacarpal joints exaggerates the spread of the metacarpals and the tendency for the metacarpophalangeal joints to move into ulnar deviation with flexion. In addition, contracture of the interosseous muscles on the ulnar side and early synovial infiltrations along the collateral ligaments lead to the stretching out of the radial collateral ligament and cause further ulnar deformity. The synovial proliferation within the joint contributes to attenuation of the radial sagittal bands and facilitates migration of the extensor tendons (McMaster, 1972).

The theory of deformity preceding the development of metacarpophalangeal articular changes is not universally accepted, as some authors (Stirrat, 1996) have thought that, due to inflamed synovium, the articular destruction comes before deformation. The initial changes seen in the articular cartilage are softening and a loss of the normal translucent appearance of articular cartilage. With further joint inflammation, erosion of bone and articular cartilage occurs leading to some metacarpal head destruction. As deformity due to chronic synovitis appears, the extensor tendons lose their ability to extend the metacarpophalangeal joints fully

and the ulnar intrinsics gradually may tighten to induce ulnar-deviated subluxed deformity (Stirrat, 1996).

2.1.4 Clinical assessment

Evaluation of a patient with RA of the MP joints requires an assessment of the global function of the extremity and in particular the deformities of the adjacent joints. With wrist deformity for example, radial MC deviation might cause rapid failure of any corrective procedure performed in the MP joints (Taleisnik, 1989; Shapiro et al., 1971). Therefore a patient limited by wrist deformity may not benefit from the MP reconstruction.

Once decisions have been made about parts of the hand unrelated to the MP joint, then it is suggested to consider the MP joint conditions and classify the MP involvement in four stages (Millender and Nalebuff, 1973). The advantage of thinking in terms of stages of the disease is that it facilitates directing treatment towards the pathology that exists rather than trying to fit the pathology to the operation. Stage I disease shows MP synovitis, the ability to extend the joint fully, and little ulnar deviation or articular changes. Typically patients are managed medically for the synovitis, with splinting and corticosteroid injection for symptomatic relief. Stage II is marked by the development of early erosions. An extensor lag commonly exists, but flexion is well preserved. Surgical intervention is infrequently performed, but could include synovectomy and soft tissue balancing. Stage III disease is characterized by advancement in joint destruction and an increase in the deformity. The surgical decision is whether arthroplasty or tendon centralization and synovectomy is appropriate. The patient's level of pain and the function of the affected hand typically guide this decision. In stage IV disease there is considerable destruction as seen on radiographs, with fixed volar subluxations of the proximal phalanges, therefore an MP arthroplasty is considered the treatment of choice.

2.1.5 Small joint arthroplasty of the hand

Arthritis of the small joints of the hand are due primarily to rheumatoid, traumatic and degenerative changes. Rheumatoid arthritis is an inflammatory disease that is systemic and likely to be due to problems with the autoimmune system. It leads to articular, periarticular and soft tissue inflammation, frequently involving the MCP joints. Resection arthroplasty was the first method used to maintain mobility in the metacarpophalangeal joint (Fowler, 1962; Vainio, 1989).
A number of prosthetic replacements have been used during the past forty years and they can be classified in three basic types: hinged prostheses, flexible prostheses and surface prostheses.

2.1.5.1 Hinged prostheses

The first generation of hinged prostheses consisted of simple uniaxial designs, all made of metal and they only allowed the flexion-extension movement. In 1953 Brannon and Klein implanted the first prosthesis in the MP joint. The prosthesis was assembled from five titanium components and the intramedullary stems had a triangular cross section in order to prevent rotation (fig. 2.7).

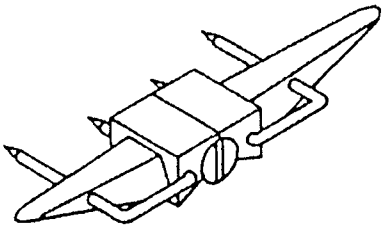

Fig. 2.7 Brannon and Klein prosthesis

This prosthesis quickly showed different problems essentially connected with the hinged-type design and with the material chosen for manufacturing the prosthesis. In fact the flexion movement was difficult because the hinge axis was higher than that found in the natural joint and the metallic components produced high friction coefficients. Abrasive-corrosive wear could also quickly damage the oxide layer on the surface of the titanium alloy if metallic wear debris became trapped between the bearing surfaces and acted as third body particles.
Only one report discussed the clinical results of this prosthesis showing that the two patients treated increased their ROM from 32.5° to 75° of flexion, but this was only during a short follow-up period. Furthermore one of the two prostheses also sank into the bone nearly a year after surgery (Brannon and Klein, 1959).

The Flatt prosthesis was considered as a modified Brannon and Klein prosthesis in an attempt to overcome the problems encountered with the first one. In this three-component, all stainless steel prosthesis, the centre of rotation of the hinge was offset from the mid-line of the metacarpal shaft in order to match the natural joint centre and therefore allow an easier flexion movement. Instead of having a single medullary stem, the design consisted of twin spikes used to allow bone ingrowths and also to prevent rotation of the prosthesis (fig. 2.8).

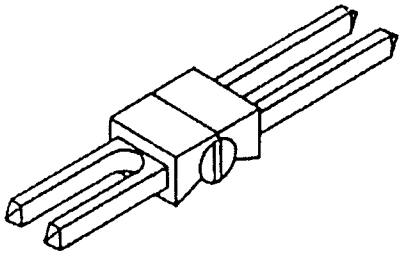

Fig. 2.8 Flatt prosthesis

Flatt first commented on the promising clinical results of this prosthesis in metacarpophalangeal joints in 1961 (Flatt, 1961), and also in a later study (Flatt, 1967) he reported the ROM as being satisfactory. Although Flatt's six-years follow-up results showed an improvement in the ROM from 32.3° to 51.3° (Flatt and Ellison, 1972), a later 11.5-years clinical study (Blair et al., 1984a) reported that the average ROM dropped to 24°. After a good initial period, recurrent ulnar deviation occurred in 57.5% of the joints and the rate of fracture was 47.4%.
The most serious problem of this prosthesis was due to the elastically deformed prongs, which were constantly exerting pressure on the inner walls of the medullary canals, leading to rapid bone erosion. For this reason the Flatt prosthesis failed even under the lower forces acting on the rheumatoid hand compared with a normal hand. Furthermore, it is interesting to note that Flatt has suggested the criteria that are still applicable for small joint arthroplasty. These are: biological compatibility, adequate fixation, adequate material wear and strength characteristics, simulation of normal joint kinematics, provision for accurate alignment for preservation of tendon moment arms, and allowance for soft tissue reconstruction.

The next concept in hinge design was that of the "roller and socket", first used by Griffith and Nicolle (Griffith RW and Nicolle FV, 1975). The proximal phalanx design included a stainless steel cylinder which allowed both flexion-extension and adduction-abduction movement. The polypropylene stems were not fixed in the intramedullary canals. The two years follow-up study showed a ROM of only 38° and recurrent ulnar drift (Nicolle FV and Gilbert S, 1979).

The Schetrumpf prosthesis consisted on a polyacetal proximal phalanx "roller" component and on a polypropylene metacarpal "socket". The elaborate three-fin shape of the stems was expected to resist rotational forces better, but this has no influence in rheumatoid hands where the cancellous bone becomes very soft. The small clinical trial was satisfactory, but no independent follow-up series have been reported (Schetrumpf, 1975).

The Schultz prosthesis is another two component "roller and socket" device, but a cemented one. A 10.9 years follow-up study has been described (Adams et al., 1990) reporting a reduced ROM of 21.6°, which is not sufficient for an MCP joint. The neck of the proximal phalanx component fractured in 39% of the joints and this might be due to the cement fixation that might induce a higher loading on the joint mechanism. Moreover the prosthesis was found not to be strong enough to transmit the ulnar deviating forces induced on the prosthesis by the flexor tendons because ulnar drift recurred in all joints.

The Type 2 Steffee prosthesis was another cemented "roller and socket" design. Different clinical trials have been reported on both Type 1 and Type 2 designs and in particular during a 2 years follow-up study, the ROM was reported only slightly improved at 42° while recurrent ulnar drift was found in 7.7% of the Type 2 prostheses (Steffee et al., 1981). A Type 3 Steffee prosthesis has recently been developed, but no clinical trials have been reported (Beckenbaugh and Linscheid, 1993).

The first ceramic prosthesis implanted in the MCP joint was the KY Alumina ceramic prosthesis (Doi et al. 1984), followed by the Minami alumina ceramic prosthesis (Minami et al., 1988). Both were made of three components. The metacarpal stems of both prostheses were obtained from polycrystal alumina and the proximal phalanx stems from a single-crystal alumina and were pushed into the intramedullary canals without the use of cement. Both types had a HDPE bearing to fix the two stem components together and they allowed flexion-extension and abduction-adduction movements. The weak point of these prostheses was the quality of the ceramic's structure that could not be controlled during manufacturing in terms of porosity, uniformity of grains and presence of inclusions. This might explain the high fracture rates reported (Mahoney and Dimon, 1990).

In long term clinical follow-up studies, all these hinged design prostheses presented a high rate of recurrent deformity which indicated that the prostheses could not transmit the forces that occur in the hand. The post-operative range of

motion was also found to be small at approximately 30°. At present hinged prostheses are infrequently used.

2.1.5.2 Flexible prostheses

In order to solve the problems encountered with the metallic hinged prostheses, the attention moved towards the development of new polymeric materials for manufacturing the prostheses.

Introduced in 1966 the Swanson prosthesis is a single-component implant made from silicone elastomer, a flexible material, which allowed both the flexion-extension and the abduction-adduction movements (fig. 2.9).

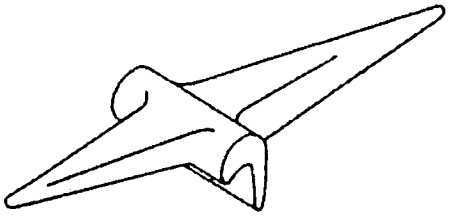

Fig. 2.9 Swanson prosthesis

The prosthesis is fixed in the joint by a firm fibrous capsule, therefore no further fixation is required (Swanson, 1968; Swanson, 1969; Swanson, 1972a; Swanson, 1972b). The intramedullary stems, being free to slide into the medullary canals during the flexion-extension movement, can undergo a pistoning motion which is supposed to increase the ROM and prolong the prosthesis life by reducing the stresses acting on it (Gillespie et al., 1979; Swanson, 1968). This motion however, is also reported to cause bone erosion (Levack et al., 1987) that might lead to prosthesis failure.

The main problems found with the use of this prosthesis are essentially due to the material and to the hinged design. The silicone rubber is in fact a very flexible material and therefore doesn't have the strength to stop the process of ulnar drift deformation, often recurrent. It can also allow the fracture of the implant with the patients being unaware of it (Beckenbaugh et al., 1976; Kirschenbaum et al., 1993). Furthermore, the hinged-type design can easily lead to fracture if the prosthesis doesn't flex about the right centre of rotation (Gillespie et al., 1979; Swanson, 1972a; Swanson, 1972b).

Many short clinical trials using the Swanson prosthesis have been reported (Swanson, 1972a; Rhodes et al., 1972; Mannerfelt and Andersson, 1975; Ferlic et al., 1975; Hagert et al., 1975a; Millender et al., 1975; Beckenbaugh et al., 1976; Blair et al., 1984b; Fleming and Hay, 1984; Jensen et al., 1986) and they showed a post-operative ROM of 29-61.5° average, correction of ulnar drift deformation (98.1%-57.4%) and low rates of fracture (0.8-26.2%).

However, long term follow-up studies (Wilson et al., 1993; Kirschenbaum et al., 1993; Schmidt et al., 1996; Hansraj et al., 1997) reported a post-operative arc of motion inferior to 45° flexion, therefore as motion only occurs at central hinge portion when prosthesis flexes beyond that angle (Gillespie et al., 1979), the prosthesis would never flex in the right place throughout the duration of its life. This might quickly induce the prosthesis fracture (3.2-27%) (Beevers and Seedhom, 1995).

The Niebauer prosthesis was a contemporary and similar device to the Swanson silastic metacarpophalangeal prosthesis, first implanted in 1966 (Niebauer et al., 1968; 1969). It was a single component silicone prosthesis reinforced with Dacron on the hinge. This tougher material was introduced in order to achieve stability and increase the flex life of the prosthesis with the strength being mainly supplied by the Dacron core. Unfortunately this prosthesis presented all the same problems of the Swanson prosthesis. In 1971 Niebauer and Laundry reported an arc of motion of 39° and no fracture. However later short follow-up trials (Hagert, 1975b; Beckenbaugh et al., 1976) reported a failure of half of the prostheses implanted. Furhermore a 11.5 year follow-up study (Derkash et al., 1986) reported the failure for fracture of the 87% of the prostheses and recurrent

deformities on the 58% of the prostheses. The high fracture rate might be explained with the mismatch in moduli between the silicone and the Dacron mesh, which leads to yield of the softer material.

Many other flexible prostheses have been designed, but they all have similar problems to the Swanson.

Modifications of the Calnan-Reis (1968) prosthesis led to the Calnan-Nicolle prosthesis, which consisted of a single-component polypropylene hinge and stem design surrounded by a silicone capsule. In a one-year clinical study (Nicolle and Calnan, 1972) an arc of motion of 59.3° and recurrent ulnar drift was observed. In a later trial (Griffiths and Nicolle, 1975), the ROM was found to deteriorate to 34.7° after a follow-up of 1.7 years. Infection and fracture rates of 1.8 and 32.1% respectively were also observed.

Other flexible prostheses include the Helal flap prosthesis with a 1.5 year clinical study (Levack et al., 1987) and the Sutter prosthesis (Linscheid and Beckenbaugh, 1991; 1993). Their short follow-up trial indicated behaviour similar to the Swanson implant. Another recent study (McArtur and Milner, 1998) however, showed a worse performance of the Sutter spacer compared with the Swanson.

At present flexible prostheses, especially the Swanson joint, are most widely used and this is due to the fact that they are relatively inexpensive, easy to implant and to remove if revision is required. However they have many disadvantages: the flexible material is required to prevent deformation, but it resists flexion and inhibits finger motion. Furthermore, the articulating area has to have a large thickness, but in this way the prostheses are inclined not to flex at the desired hinge area. Most of the flexion motion is therefore supported by the stem-hinge junction, which offers less resistance and can lead to prosthesis fracture. This is evident in the long-term clinical follow-up series analysed, which have found high rates of recurrent deformity (approximately 50%), fracture (approximately 30%) and small range of motion (approximately 40%) (Beevers and Seedhom, 1993; 1995).

2.1.5.3 Third generation prostheses

This third group includes devices with no common design aspect like surface prostheses and hybrid implant of the hinged and flexible types. Flexion-extension and abduction-adduction movements were possible. The articulating portions of the surface prostheses are also referred as non-constrained because the two articulating components are not connected by mechanical constraints.

Hinged or silicone rubber implants can be satisfactory in elderly patients with gross deformity, but they are certainly inadequate for implantation in younger patients who expect to restore more accurate anatomy of the joint. These patients, if ligaments and muscles that surround the joint are still functional at this stage, might benefit from surface replacement prosthesis which better replicate the anatomy of the MCP joint. All MCP prostheses that have undergone clinical trials generally provide pain relief and cosmetic improvement, possess low rates of infection and give high patient satisfaction. However, they cannot restore stability and function comparable to that of the natural joint. They have high rates of deformity and fracture, together with a diminishing range of motion with time, as observed in long-term follow-up reports. Therefore, there are no prostheses currently available, which can replace MCP joints that have been damaged by rheumatoid arthritis and which can restore the biomechanics of the joint.

The Kessler prosthesis is a silicone rubber implant for the replacement of the metacarpal head with Dacron-coated intramedullary stems (Kessler, 1974). Only a short clinical trial was performed, therefore the results cannot be regarded as sufficient. The problems expected in a long-term follow-up refer to the non-spherical geometry that cannot provide the precise bearing surface and to the Dacron material that might cause the fracture of the silastic stems.

Hagert et al (1986) designed a UHMWPE metacarpal head with a titanium proximal phalangeal socket prosthesis that allowed the flexion-extension and the adduction-abduction movements. In a 3.5 years follow-up, the authors observed an arc of motion of 65° of flexion, no recurrent deformity, but a high fracture rate.

A longer clinical trial is suggested as it might determine the validity of the results described in the paper.

Beckenbaugh developed a non-cemented, unconstrained two component prosthesis manufactured using pyrolitic carbon (Cook et al., 1983; Beckenbaugh, 1983; Linschied and Beckenbaugh, 1993). In a 1-year follow-up trial, the ROM was found to be 47° and no infection was reported. An 8-year clinical study (Cook et al., 1999) observed an increased arc of motion, correction of deformities and very low fracture rate. This might lead to the conclusion that a pyrolitic carbon prosthesis is a wear-resistant, biocompatible and durable implant for the metacarpophalangeal joint.

2.1.5.3.1 Durham prosthesis

As it has been reported previously, the numerous prosthetic designs that so far have been developed cannot restore stability and function comparable to that of the natural joint, either in a clinical or mechanical context. In order to try and solve this problem, a non-constrained, non-cemented, modular prosthesis had been manufactured for replacement of the damaged articular cartilage of the MCP joint (Fig. 2.10).

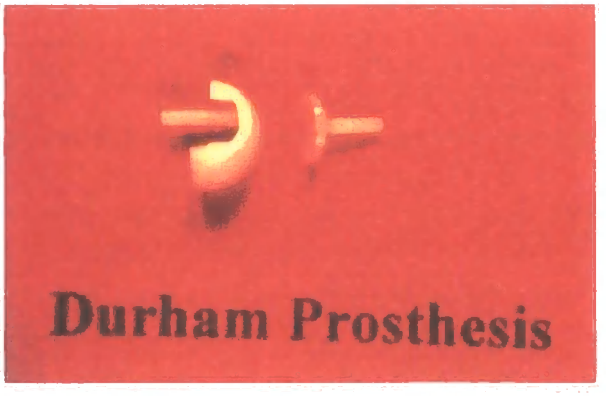

Fig. 2.10 Durham prosthesis

The bearing surfaces were required to allow the collateral ligaments to remain intact and to transmit the internal joint forces to the bone ends, as in the natural

joint, rather than to the medullary canals. They were also required to articulate with a low wear rate and produce the minimal amount of wear particles to avoid adverse tissue reactions. The prosthesis has also been designed slightly thicker than the natural articular cartilage it replaces to allow re-tension of the ligaments which tend to become lax in rheumatoid arthritis. Finally the Durham prosthesis is low cost and easy to implant and to remove.

Size and shape

Ideally the radii of the prosthetic bearing surfaces should be compatible with the articulating cartilage surfaces which they will replace. However, since each MCP joint has unique dimensions, a large range of prostheses would be required. As this is obviously impractical, a range of sizes was defined. From the available data on the anatomical dimensions of the metacarpal and proximal phalanx bones (Unsworth et al., 1971; Pagowski and Piekarski, 1977; Unsworth and Alexander, 1979; Tamai et al., 1988), three sizes were chosen with R equal to 6.5, 7.5 and 8.5mm respectively, where R is the radius of the outer articulating surfaces.

Table 2.1 Metacarpal component dimensions (mm)

R	6.5	7.5	8.5
r	5.0	6.0	7.0
w	8.75	10.5	12.25
t	2.65	2.95	3.25

where

R = articulating surface radius

r = internal radius obtained subtracting the thickness = R – 1.5 (1.5mm is the prosthesis thickness)

w = width. From Stokoe (1990): w = 1.75r

t = thickness of the lower lip

Table 2.2 Phalangeal component dimensions (mm)

R	6.5	7.5	8.5
s	8.0	9.0	10.0
a	9.66	10.82	11.98
b	7.53	8.72	9.91

where:

R = articulating surface radius

s = distal prosthesis radius

= R + 1.5mm (1.5mm is the prosthesis thickness)

b = minor axis length. From Stokoe (1990): r = 0.84046b – 1.33145,

where r = metacarpal bone radius

a = major axis length. Based on Stokoe (1990): a = 0.9772b + 2.2982

The metacarpal head and proximal phalanx base are approximately spherical in shape (Unsworth et al., 1971; Pagowski and Piekarski, 1977; Unsworth and Alexander, 1979; Tamai et al., 1988). However, the radius of the proximal phalanx base is slightly larger than the radius of the metacarpal head (Unsworth et al., 1971; Pagowski and Piekarski, 1977; Tamai et al., 1988). The question arises as to whether the spherical prosthetic bearing surfaces should be unequal, as in the natural joint, or equal in radii. The Durham prosthesis however, has been designed as conforming spherical articulating surfaces and the reason for this choice is related to consideration of the centre of rotation, contact pressure and lubrication. The face of the metacarpal head component when viewed from distally to proximally is shaped as a trapezium while the face of the phalangeal component is that of an ellipse (Stokoe, 1990). Both prosthetic components have a wear face of 1.5mm thickness together with a 3mm square section stem that is 12mm long. The square section of the intramedullary stem is an important design feature as it influences the rotational stability of the prosthesis. If the metacarpal component rotated in the bone, the bearing surfaces would no longer be in contact when the prosthesis is at full extension. The centreline of the metacarpal stem is 2.6mm offset in the sagittal plane to fix the stem in the centre of the medullary canal (Unsworth and Alexander, 1979) and help prevent rotation of the prosthesis.

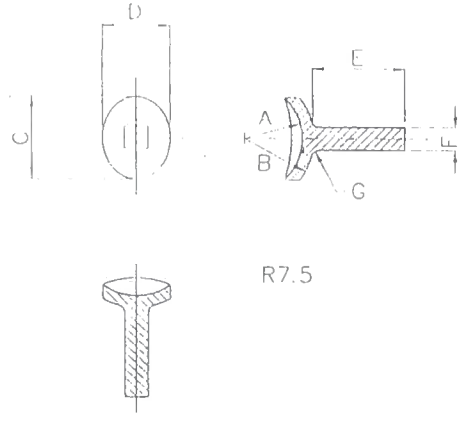

A	B	C	D	E	F	G
5.5	7.0	8.50	6.34	12.0	3.0 SQ	R1.0
6.5	8.0	9.66	7.53	12.0	3.0 SQ	R1.0
7.5	9.0	10.82	8.72	12.0	3.0 SQ	R1.0
8.5	10.0	11.98	9.91	12.0	3.0 SQ	R1.0
9.5	11.0	13.14	11.10	12.0	3.0 SQ	R1.0

PHALANGEAL TABLE OF DIMENSIONS.

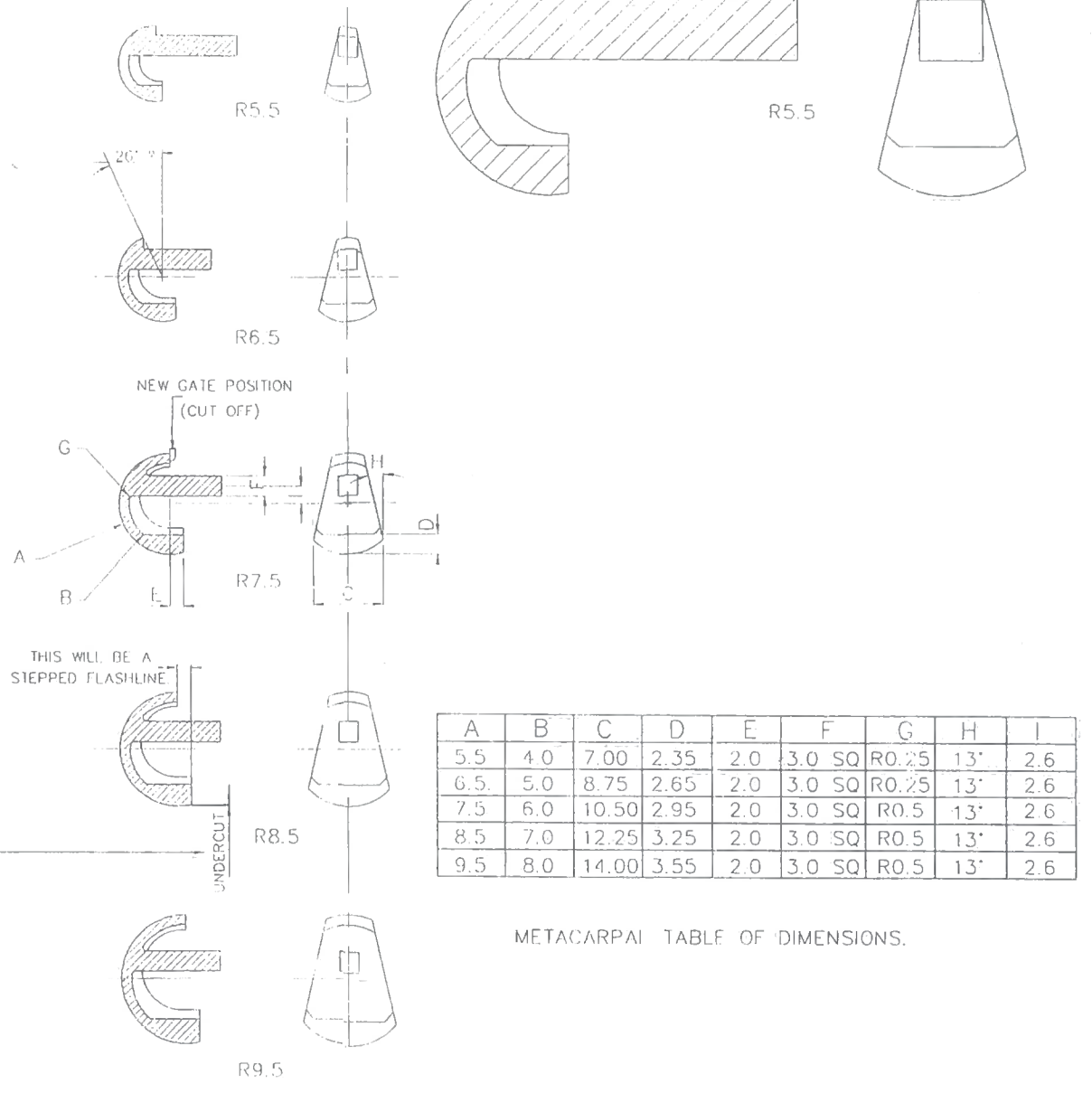

A	B	C	D	E	F	G	H	I
5.5	4.0	7.00	2.35	2.0	3.0 SQ	R0.25	13°	2.6
6.5	5.0	8.75	2.65	2.0	3.0 SQ	R0.25	13°	2.6
7.5	6.0	10.50	2.95	2.0	3.0 SQ	R0.5	13°	2.6
8.5	7.0	12.25	3.25	2.0	3.0 SQ	R0.5	13°	2.6
9.5	8.0	14.00	3.55	2.0	3.0 SQ	R0.5	13°	2.6

METACARPAL TABLE OF DIMENSIONS.

All unspecified dimensions are mm

To Dept
Prod Eng
Prod Cont
Qual Cont
Date Issued

Catalogue Number

Computer Number

Alterations
Number Issue Signed

Material X.L.P.E

Quantity Per Ass'y

Scale

Drawn G.M Date

Checked Date

Project Leader P.KILBURN Date

General specifications

Surface Finish BS N7

Metric tolerances

Imperial tolerances

Angular tolerance

Geometrical tolerance

Product Title
PHALANGEAL AND METACARPAL COMPONENTS.

Drg. Title
COMPONENT DRAWING

DePuy International Ltd.

Drg.No B000294A

Fixation

Fixation is the coupling of the prosthesis to the host bone. The stems can be designed to move freely in the medullary canals or be fixed in position by using adhesion, mechanical fixation, polymethylmethacrylate (PMMA) cement or bone ingrowth methods.

The most common method to fix prosthetic components to the bone is using PMMA cement. Cement has many advantages including that the surgical preparation of the medullary holes does not have to be exact, since the cement acts as a filler material to provide a good fit between the bone and the prosthesis. High stress concentrations are also avoided. However, bone cement debris left behind during surgery can cause damage to the bearing surfaces and increase the wear rates (Caravia et al., 1990). Furthermore, high temperatures around 50°C occur in the cement when it sets, due to the exothermic polymerisation process (Schultz et al., 1987). Those temperatures have been shown to be critical as they can induce bone necrosis. Therefore, cement could induce thermal necrosis of adjacent bone. This is an important factor since necrosis occurs at a bone depth up to 1mm and the cortical bone of the metacarpal and proximal phalanx in a rheumatoid hand can be thinner (Swanson et al., 1986).

An ideal method of fixation would be the one that relies on bone ingrowth. Two method of bone ingrowth can be used: porous surfaces and hydroxyapatite coatings. Hydroxyapatite coating has recently been used with polymers (HAPEX®) and it might be interesting to test its application on the Durham prosthesis.

Since both components are always in compression in the Durham MCP prosthesis, it was decided to use no firm fixation. Furthermore, if the intramedullary stems are not fixed to the bone, the implantation procedure would be quick and simple.

Centre of rotation

While several authors conclude that the centre of rotation is fixed (Unsworth and Alexander, 1979; Youm et al., 1978; Bartel et al., 1968; Flatt and Fisher, 1969), others argue that it is variable (Pagoski and Piekarski, 1977; Tamai et al., 1988, Walker and Erkman, 1975).

Flatt and Fisher's work was on living hands instead of cadavers and this was quite important because the centre of rotation depends not only on the geometry of the joint surfaces, but also on the ligaments. The *in vitro* study by Unsworth and Alexander concluded that the MCP joint has a single centre of rotation in both sagittal and transverse planes and the same result was also achieved by Youm et al. using an X-ray technique and an analytical method.
Pagowski and Piekarski discussing the results obtained from cadavers argued that the centre of rotation is not fixed as it moves on a 1.5mm radius arc. However, they assumed the collateral ligaments to be always taut, while they are slack when the joint is in extension, to become tighter as the joint is flexed (Flatt, 1983). The other two studies were also on cadavers, but while Tamai et al. concluded that there isn't a fixed centre of rotation in the MCP joint without giving the dimensional variance of the centre of rotation, Walker and Erkman graphically determined its position within 3mm in the centre of the metacarpal head.

A theory section on the contact pressure, lubricating conditions and material choice referring to the Durham prosthesis is given in Appendix A.

2.2 Wear

2.2.1 Definition

While total joint replacement is regarded as the major development in orthopaedic surgery in the twentieth century, the most difficult problem connected with these implants relates to wear. Therefore there is much interest in extending even further, early in the twenty first century, the life of implants by understanding the wear mechanisms and possibly improving the materials resistance to wear.

Wear can be defined as the mechanical removal of material from surfaces by their relative motion under load. Thus, the wear will induce a weight loss in the sliding components, topographical and dimensional changes and also the appearance of wear debris. Therefore it is very important to characterise both the materials and the surface prior to the commencement of a test so that changes which take place can be related back to a known starting state.

Wear can be defined as belonging to two main types: cohesive and interfacial (Lancaster, 1990). Cohesive wear includes abrasive wear where the surface asperities of the harder bearing material abrade the softer material digging grooves into the surface and inducing the release of wear debris. Interfacial wear on the other hand, is a result of adhesion or fatigue or a combination of them. Adhesion is generally defined as the transference of material from the softer surface to the harder surface during relative motion and this is due to the compressive force that creates connections between the surface asperities. Fatigue wear is the removal of particles due to the dynamic behaviour of the surface pressure as a result of repeated cyclic stress of the asperities. Furthermore, third-body particles can be generated by the different wear mechanisms at the prosthetic articulating interface and they can contribute to an acceleration of the wear mechanisms. In addition, transition between different wear regimes can occur and the relative importance of a particular wear mechanism can alter during the progression of a test.

The most commonly used materials for total joint replacement is the metal on polymer combination, first introduced by Sir John Charnley in hip replacement

(Charnley, 1961). Charnley used a 22-mm diameter metallic femoral head articulating against a PTFE (polytetrafluoroethylene) acetabular cup with the intention of minimising the frictional torque transmitted to the surrounding bone. Unfortunately the wear rate of this polymer was unacceptably high, therefore Charnley replaced PTFE with UHMWPE (ultra high molecular weight polyethylene) as he believed in the metal on polymer combination for reducing the friction of the articulating surfaces. Although it is now believed that osteolysis induced by polyethylene wear debris is the main cause of joint failure and not frictional torque, Charnley's first intuition on the material combination for total joint replacement remains valid.

2.2.2 Methods of measuring the *in vitro* wear

Two methods are generally used for the simulator wear measurement of polyethylene:

→ gravimetric method;
→ volumetric method.

Gravimetric measurement is generally restricted to measuring wear in component worn *in vitro*. Due to the hydrophilic nature of PE (polyethylene) which induces a mass gain of the polymer with time (Clarke et al., 1985), the amount of mass gain must be taken into account and be compensated for in order to calculate the true amount of wear.

In hip joint studies, two main gravimetric techniques have been used to measure the wear of polyethylene: weight loss measurement and collection of wear debris. Weight loss is a particularly useful method, although it requires the test to be interrupted periodically and a cleaning and drying protocol to be followed. It also requires accurate weighing facilities as weight changes due to wear are generally of the order of micrograms. Furthermore a soak control must be maintained in the same lubricant as the tested prostheses to compensate for moisture absorption. It

has been suggested (Saikko et al., 1992) that the amount of mass gained by UHMWPE can be different under loaded and unloaded conditions, and this would imply that the soak control should be subjected to the same loading cycle as the tested prostheses. Taking into account moisture absorption is important not only in lubricated wear testing, but also in dry conditions when the humidity of the atmosphere might change.

Finally the amount of wear can be estimated simply by collecting wear debris. A study has been reported where the acetabular cup wear rate had been determined by weighing the wear debris after its collection, following filtering from the lubricant and desiccation (Greer, 1979). This technique is, however, not as reliable nor simple as it might seem as the wear particles might contain contaminants from the machine or the atmosphere. Furthermore, with polymeric materials, not all the debris can be easily collected as some may adhere to different surfaces or float or become trapped within any sediment.

Volumetric measurement is generally used for polymeric components worn both in vitro and ex vivo and it can be obtained using direct or indirect methods. The indirect methods include a shadowgraph technique and an indirect CMM (co-ordinate measuring machine) technique. In both cases the initial part of the method requires taking a cast of the worn component generally using dental cement. Following the shadowgraph technique Atkinson et al. (1985a) then machined the cast in 1-mm thick section tracing the magnified image of the cast and measuring the trace to calculate the volumetric wear. Burgess (1996), however, measured the cast using a CMM with an accuracy of ±0.01mm. Furthermore, the use of a CMM for a direct measurement of in vitro volumetric wear has been used by different groups (Bigsby et al., 1998a, Goldsmith and Dowson, 1999).

Volumetric measurement becomes even more complicated as they require taking into account the creep of the polymer. Creep is a deformation process which depends on the material, the loading, the geometry and the temperature (Clarke, 1981). Using a "creep" control, which is subjected to the same loading conditions of the tested components, a creep curve can be obtained. Combining both creep and wear curves allows true dimensional changes to be measured.

Results from all the wear measurement techniques previously explained, can be expressed using the wear curve where the volumetric wear is plotted against the sliding distance (fig. 2.11).

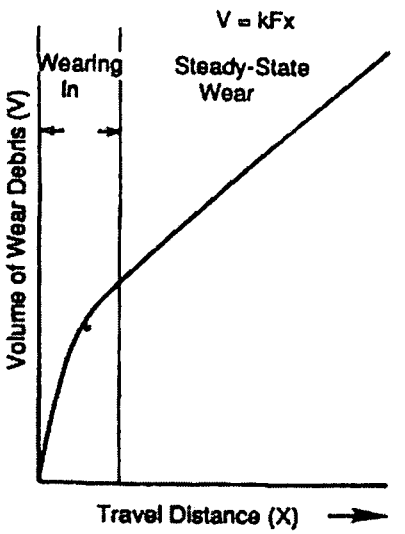

Fig.2.11 The form of the curve of volumetric wear against sliding distance for a stable wear situation

The volumetric wear V, has been shown to be:

$$V = k \cdot F \cdot x$$

when F is the force applied, x is the sliding distance and k is the wear factor of the material (mm^3/Nm) (Archard, 1953).

The curve in fig. 2.11 can be divided in two parts: an initial part where the wear rate is high and changing. This is generally known as "the wearing-in portion" and it depends upon the topography of the surfaces in contact. It is generally believed that the wearing-in period represents mutual topographical modification of the two sliding surfaces. Under stable conditions the wearing-in region is short and followed by "the steady state wear regime". In the steady state wear region, the wear tends to increase linearly with the sliding distance.

2.2.3 Factors affecting the wear behaviour of polymers

Factors affecting the wear behaviour of UHMWPE are complex and they include the surface finish, the material combination, the contact stress and the method of sterilization.

It has been reported (Ratner et al,1967, Lancaster,1969) that the abrasive wear rates of different polymers is inversely proportional to the product of ultimate tensile strength and elongation to failure. A similar correlation was found testing UHMWPE using a reciprocating wear tester under serum-lubricated conditions (Wang et al., 1995). However, recent studies on multi-axial hip joint simulators (Wroblewski et al., 1996, Wang et al., 1996) have indicated otherwise.

In *in vitro* wear testing, the surface roughness of the opposite counterface has been shown to have an important role in the wear rate of UHMWPE. For reciprocating tests, the wear factor k has been found to be proportional to the surface roughness $Ra^{1.2}$ while testing stainless steel pins against UHMWPE in distilled water (Dowson et al., 1985). According to this relationship, increasing the surface roughness from 0.01μm to 0.10μm gave an approximately 60-fold increase in wear rate. For hip simulator tests however, the wear factor k has been reported to be proportional to the surface roughness $Ra^{0.4}$ (Wang et al., 1998). Similar results have been found from explanted hip joints (Hall et al., 1996a, 1997b). Thus, increasing the surface roughness from 0.01μm to 0.10μm resulted now in an increase in the wear rate of the UHMWPE by a factor of only 2.5 in the hip simulator. This might indicate that high clinical wear rates can result from both rough and smooth surfaces, which means that both adhesive and abrasive wear can induce high UHMWPE wear rates.

Another important factor affecting the wear behaviour of polymers is the motion as it can induce molecular orientation. It has been reported that while the coefficient of friction between a linear polymer such as PTFE (polytetrafluoroethylene) or HDPE (high density polyethylene) and a smooth hard counterface depends on the relative motion of the two surfaces, this motion-

dependent behaviour is absent for branched polymers like XLPE (Pooley and Tabor, 1972). This occurs because linear polymers can orientate at the sliding interface while the steric hindrance that characterises the branched polymers doesn't allow it. Also the wear behaviour of PTFE and HDPE has been found to be motion-dependent (Briscoe and Stolarski, 1985). A study conducted on both the materials under dry sliding motion against smooth steel counterfaces has shown higher wear rates associated with linear motion and lower wear rates during non-linear motion. However, recent studies on non-crosslinked linear UHMWPE under lubricated conditions have indicated otherwise: linear motion results in very low wear rate while multidirectional motion results in very high wear rates (Bragdon et al., 1996). The importance of molecular orientation has been recognised by both Jasty et al. (1994) and Wang et al. (1996). Jasty et al. reported that scratches by third-body particles induce a chain-extended fibrillar structure, which is brittle and can therefore increase the wear rate. However, Wang et al. believed that the fibrillar structure exists even without third-body abrasion as surface traction forces induce it. This oriented structure is stronger in the orientation direction, but weaker in the transverse direction.

The method of sterilizing UHMWPE has also been found to affect its wear properties. Until 1995, UHMWPE was normally sterilised using 25-40 kGy of gamma radiation in the presence of air, but different studies (Rimnac et al., 1994; Besong et al., 1998, Chiesa et al., 2000) revealed that gamma sterilisation in air induces oxidative chain scission with subsequent degradation of the mechanical properties of the material which could affect the wear behaviour. Thus, nowadays, UHMWPE is sterilised using gamma radiation, but in a reduced oxygen environment or using ethylene oxide (EtO) or gas plasma.

EtO neutralises viruses and bacteria and although it is highly toxic, it can be used for sterilising UHMWPE because it contains no constituents that will react with the toxic gas. Recently Ries et al., (1996) validated a protocol for EtO sterilising UHMWPE which included: 18 h of preconditioning at 65% relative humidity and 46°C temperature followed by 5 h of exposure to 100% ethylene oxide gas at 0.04 MPa where the gas diffuses into the material, and then 18 h of forced air aeration at 46°C temperature. The entire cycle taking a total of 41h. Furthermore, it can

be stated that the short clinical experience with EtO-sterilised UHMWPE has been favourable so far Sutula et al., 1995; White et al., 1996).

Gas plasma is a surface sterilization method that uses ionized gas for deactivation of biological organisms (Bruck and Mueller, 1988). Two gas plasma sterilization methods commercially available are: Plazlyte (Abtox Inc., Mundelein, IL), which requires 3-4 h cycle time and uses low-temperature paracetic acid gas plasma, and Sterrad (Johnson & Johnson Medical Inc., Irvine, CA), which requires 75 minutes per cycle and uses low-temperature hydrogen peroxide gas plasma. In both cases, temperatures are lower than 50°C (Feldman and Hui, 1997). This method of sterilisation is quite interesting as it does not leave toxic residues and it might offer time and cost savings over EtO sterilisation (Feldman and Hui, 1997). No clinical trials have been reported, while theoretical and experimental studies show that low-temperature gas plasma does not affect the mechanical properties of UHMWPE (Goldman and Pruitt, 1998; Collier et al., 1996).

As the main lubricant used in *in vitro* wear simulator studies is bovine serum, a hip simulator test has been reported (Wang et al., 1998), which investigated the role of lubricant proteins in the wear of UHMWPE acetabular cups. Non-irradiated UHMWPE cups were tested against 32 mm CoCr heads using eight different lubricants ranging from pure water to 100% bovine serum containing 0, 5, 10, 22, 30, 44, 66 and 75 mg/ml of proteins respectively. The wear rate was found to present a peak at a protein concentration between 15 and 40 mg/ml, while either below or above these values, the wear rate decreased. Surprisingly, the protein concentration in synovial fluid of both normal and diseased joints falls within 15-55 mg/ml (Liao et al., 1999). Therefore it can be stated that soluble proteins do not act as an effective boundary lubricant for polyethylene joints. The lower wear rates observed at higher protein concentration can be explained with the fact that serum has been found to degrade more quickly for the lubricants with higher initial protein concentrations. The degradation products were insoluble gel-like precipitates, which could be very effective solid lubricant and therefore shield the polyethylene surface from direct contact with the femoral head surface. Then, the lower wear rates observed at lower protein concentration could be

explained with the observation of a transfer film, which was most severe with pure water as a lubricant.

2.2.4 Wear Debris

It is now widely accepted that UHMWPE generates, at the bearing surface, wear particles which may cause an adverse biological tissue reaction leading to osteolysis and eventual loosening of the artificial joint. Although the precise mechanisms of osteolysis induced by UHMWPE wear debris are still obscure, osteolysis has been identified as a major factor limiting the life of prostheses. It has also been suggested that it is not the wear volume in itself that determines the biological response to the debris, but rather the concentration of the wear volume that is within a critical size range for macrophage activation (Ingham and Fisher, 2000). Therefore the size of the wear debris could make the difference in a new prosthetic design and extend its life if the size of the debris can induce a less serious biological reaction. Furthermore, in *in vitro* wear studies it becomes very important to compare with *in vivo* results, not only the wear rate, but also the quantity, the size and morphology of the wear debris.

Different studies investigated methods to isolate in vitro and in vivo wear debris (Campbell et al., 1994, Fisher et al., 1997, Elfick et al., 1999), and the main problem remains the small number of particles counted. Using a SEM followed by a graphical analysis software allows only around a hundred particles to be studied (Campbell et al., 1996), while only one study has been reported where the number of particles analysed was over a thousand (Besong et al., 1998). These numbers are just a fraction of the total number of particles produced during a joint life, therefore these studies might not be effectively indicative of the main size and shape of the wear debris. However, an alternative method called Low Angle Laser Light Scattering (LALLS) has recently been introduced, which can count around one hundred thousand particles per sample with a size range between 0.05 μm and 1000 μm. The quantity of wear debris contained in a portion of fluid can be counted without the need of filtration or drying and this is very useful as it

eliminates the problem of agglomeration of particles. Thus, although the application of the LALLS technique to artificial joints is very recent, it might show significant improvements over the other methods used (Elfick et al., 1999).

Many studies have also been reported which describe the morphology of the wear debris. McKellop et al. (1995) defined four types of particles, while Wirth et al. (1999) used shape descriptors. It is therefore very important for the different researchers to fix definitions that could be universally accepted and used in order to compare the various studies. Wear debris morphology changes in different joints. In retrieved hip joints for example wear debris has been found to be globular in shape and about 0.5 μm in mean size, while in retrieved shoulder joints the wear paticles observed were of a fibrillar shape and about 1 μm in mean size (Wirth et al., 1999). For knee joints however, the particles were found to be mainly spherical with occasional fibrillar attachments and with a main size of 1.5 μm. Since, as it has been seen, the size of the wear debris influences the magnitude of the biological response, it is possible that in vivo larger knee replacement debris results in a diminished mediator release, which may account for the lower incidence of osteolysis and aseptic loosening in some design of knee arthroplasty (Shanbhag et al., 2000).

Other than the design of the prosthesis, the method of sterilizing, the loading conditions and the coupling materials, also counterface roughness and the lubricant can have an effect on the size and morphology of the wear debris (Hayley et al., 1996). Wang et al. (1996) investigated the effect of lubricant on the size and morphology of UHMWPE wear debris using a hip simulator and they found that when water was used as lubricant, 2-3 mm flakes of UHMWPE were observed as they probably comprised numerous smaller particles compacted together. However, the wear particles produced with bovine serum were submicron sized and were similar to those observed in clinical studies. The same result has been reported in a more recent study by Besong et al. (1999).

2.3 XLPE

UHMWPE has been used in prosthetic devices for nearly 40 years as it is considered a biocompatible, low-friction and low-wear material. However, the recognition that conditions in some joints like the ankle may be much more severe, together with the need to implant artificial joints in younger patients, has pushed the research towards modifications of UHMWPE or to alternative materials. Many studies reported the suggestion to improve the wear behaviour of UHMWPE by crosslinking of the material (Chiesa et al., 2000; Kurtz et al., 1999; Baker et al., 1999).

2.3.1 Clinical trials

Cross-linking of UHMWPE is generally obtained by ionising radiation, peroxide chemistry, or silane chemistry (Dave, 1988). However, only three types of highly cross-linked polyethylene for prosthetic devices have been reported in the clinical literature. In 1971, Oonishi (1995) implanted UHMWPE acetabular components that were cross-linked with 1000 kGy of gamma radiation in air.

In the 1970s, another study (Grobbelaar et al., 1978) investigated the effects of cross-linking UHMWPE using up to 800 kGy of gamma radiation in the presence of nitrogen, acetylene, and chlorotrifluoroethylene. It has in fact been reported (Klein et al., 1991) that the use of a sensitising atmosphere, such as acetylene, leads to a higher ratio of cross-linking when compared with irradiation in air or inert atmosphere.

Most recently, Wroblewski et al. (1996) reported on the clinical performance of 22-mm diameter, silane cross-linked XLPE acetabular components. The base material used was HDPE, which was injection moulded into acetabular cups prior to silane cross-linking. This is the same material that has been used to manufacture both pieces of the MCP Durham prosthesis. Wroblewski's clinical follow-up was 8 years and 3 months with a total of 19 patients. The results showed that after an initial "bedding-in" penetration of 0.2-0.4 mm with an average penetration rate of 0.29 mm/year presumably representing creep, the

subsequent average penetration rate decreased by an order of magnitude to 0.022 mm/year presumably representing wear. Recently the same author reported invariant results for the 10 year follow-up (Wroblewski et al., 1999).

2.3.2 The chemistry of silane cross-linking

This cross-linking procedure has been developed by Dow Corning, modified under licence by the British Steel Corporation (Bloor and Summers, 1982) and it is currently used by the BSC subsidiary, Stewarts and Lloyds Plastics, to produce "Pesalex", a form of polyethylene suitable for hot water piping.

Atkinson and Cicek (1983) stated: "A silane compound containing a vinyl group and hydrolysable groups is grafted onto the polyethylene chain. Vinyl trimethoxysilane is usually used and the grafting achieved with a peroxide such as dicumyl peroxide in an extruder at a temperature of about 220°C. Antioxidants, stabilisers and colouring pigments are added before extrusion" (Fig. 2.11).

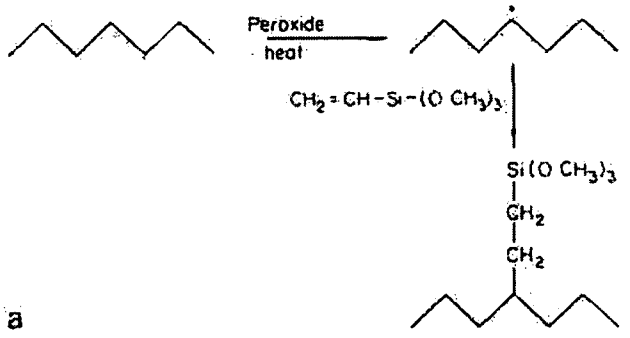

Fig. 2.12 (The peroxide heating into an extruder)

The grafted granules produced from the extruded rod are then injection moulded. Next is the cross-linking stage, which involves steam autoclaving the product at 120°C for several hours when the methoxy groups are hydrolysed to hydroxyl groups (Fig. 2.13).

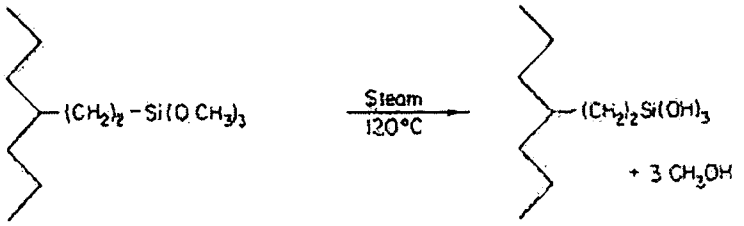

Fig. 2.13 (The steam autoclaving process)

The hydroxyl groups on neighbouring chains condense together to form cross-links (Fig. 2.14).

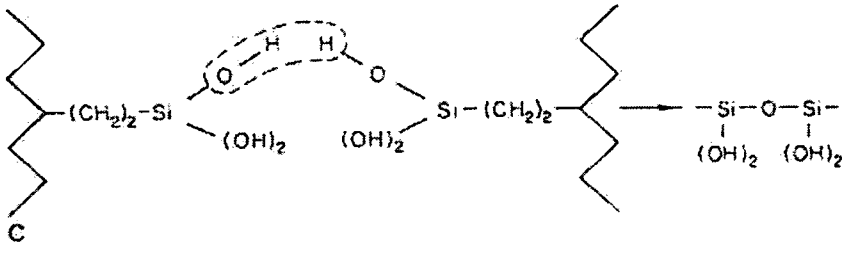

Fig. 2.14 (The cross-linking process)

Each silicon atom is connected to three hydroxyl groups so this single cross-linking site is capable of linking two, three or more chains together (Fig. 2.15).

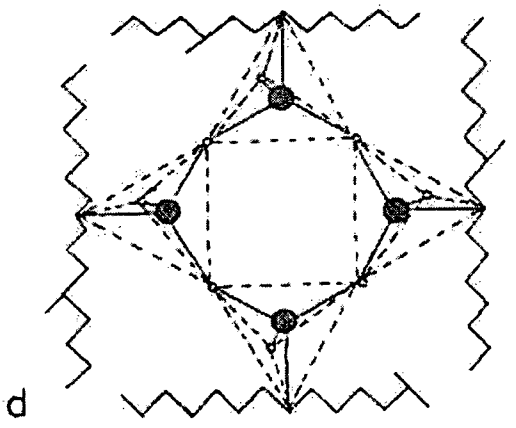

Fig. 2.15 (The compless final cross-linking)

This type of cross-linked polyethylene should have different mechanical properties from polyethylene cross-linked by a single covalent bond, because the network is less tightly bound. The material should have the same wear resistance that the non cross-linked polyethylenes, but an improved behaviour to cold flow, an advantage for prosthetic applications (Atkinson and Cicek, 1983).

2.3.3 Mechanical properties and wear of XLPE

The use of polyethylene cross-linked by silane chemistry in total hip arthroplasty was first reported in 1980 (Atkinson et al., 1980) in an *in vitro* study on creep occurring to an acetabular cup. The authors reported a slightly improved creep resistance as well as improved wear resistance at high sliding velocities under unidirectional motion in XLPE compared with non cross-linked UHMWPE (RCH 1000). Other physical and mechanical properties such as creep and wear behaviour of this material have been discussed in detail by Atkinson and Cicek (1983, 1984). The XLPE showed a crystallinity of about 70% and a density of 0.960 g/dm^3 compared with 58% and 0.941 g/dm^3 respectively exhibited by UHMWPE. The tensile mechanical properties of the XLPE were very similar to those of the UHMWPE showing strong promise for the XLPE to be an alternative material for total joint replacements. Atkinson and Cicek (1983) also investigated the impact fracture behaviour of XLPE and they concluded that compared with non cross-linked UHMWPE, XLPE has a lower resistance to crack propagation, but higher resistance to crack initiation. Other mechanical properties of XLPE are summarised in table 2.3.

	PERCENTAGE GEL CONTENT					
	37	67	73	79	80	88
MOLECULAR WEIGHT BETWEEN CROSS-LINKS	29363	-	11658	6632	-	-
DENSITY AT 23 °C/ kgm^{-3}	954.0	952.5	950.5	948.0	948.5	-
SOFTENING TEMPERATURE / °C	-	135	139	142	-	142
SOFTENING RANGE / °C	-	128-145	128-148	133-148	-	121-149
CRISTALLINITY / %	-	70	68	65	-	62
YIELD STRESS / MPa (STRAIN RATE = 0.0033 s^{-1})	-	-	-	-	-	27.6
YOUNG MODULUS, at 2% STRAIN / MPa	-	-	-	-	-	632.5
VICKERS HARDNESS / $kgmm^{-2}$	5.05	5.74	5.85	-	6.03	-
IMPACT STRENGTH /kJm^{-2}	-	-	-	-	40	-

Tab. 2.3 Properties of Silane XLPE (measurements undertaken at 20 °C except when differently stated)

In an XLPE against stainless steel dry test carried out using a reciprocating wear testing machine, Atkinson and Cicek (1984) reported no significant difference between the wear rate of non cross-linked UHMWPE and XLPE except at 140N which was the highest load applied. During this extreme loading condition, XLPE showed some 10 times higher wear resistance, reporting a wear rate of 0.17×10^{-7} mm^3/Nm compared with the 1.6×10^{-7} mm^3/Nm wear rate of the non cross-linked UHMWPE. However, these wear studies were restricted to dry lubricating conditions using a unidirectional pin-on-disc machine; therefore, their validity in determining the wear behaviour of bearing materials for total joint replacements is questionable.

Most recent tribological studies at body temperature, using 30% bovine serum, and performed on modern pin-on-plate wear testers have suggested that silane XLPE when sliding against stainless steel, has a comparable wear rate to conventional UHMWPE (Joyce et al., 1998). This study also shows that both UHMWPE and XLPE wear 10 times more under multidirectional motion than unidirectional motion while tested in bovine serum. The wear rate of the XLPE under unidirectional motion has been found to be equal to 0.12×10^{-6} mm^3/Nm. This dependence on the direction of motion confirms the results obtained by Bragdon et al. (1996).

However, as the Durham MCP prosthesis is a two piece all XLPE prosthesis, the wear behaviour of XLPE sliding against itself has been investigated. In a first study, a number of tests of gamma irradiated XLPE against itself has been carried out on both reciprocating pin-on–plate wear testers and a finger wear simulator (Joyce et al., 1996). The pin-on-plate study reported wear factors for the XLPE against itself around 0.5×10^{-6} mm^3/Nm which are comparable with those of UHMWPE rubbing against a metallic counterface. In the finger simulator study however, also the influence of gel content was investigated as components with 36%, 66% and 87% of gel content were tested. After 368 km, the prostheses with the highest gel content had a mean wear factor of 0.41×10^{-6} mm^3/Nm, showing about 20 times less wear than the prostheses with the lowest gel content.

A following study performed on a reciprocating pin-on-plate wear tester investigated the influence of the lubricant on the wear of XLPE against itself (Joyce et al., 2000c). Distilled water, Ringers solution, bovine serum and no lubricant were used. The lowest wear rate was found with the bovine serum and was 0.54×10^{-6} mm^3/Nm, while the highest wear rate occurred with Ringers solution and was some 20 times more.

Another study was undertaken in order to investigate the lubricant absorption of loaded and unloaded XLPE prostheses (Joyce and Unsworth, 2000b) and lasted 160 days. The fluid absorption curve was biphasic, remaining almost constant after 40 days. The highest rate of lubricant absorption occurred for unloaded prostheses, showing a mean value of 120×10^{-7} kg, while the loaded prostheses absorbed 95×10^{-7} kg. These results suggested keeping the control prostheses

under the same loading conditions of the tested prostheses in order to take into account the amount of fluid absorption and then measure a true wear rate. The friction of XLPE against itself was measured using a reciprocating pin-on-plate rig and gave a coefficient of friction of 0.14 (Sibly et al., 1991).

2.4 Friction

Leonardo Da Vinci (circa 1400) considered friction to be mainly due to the interaction of surface asperities on the sliding surfaces. However, in this century friction is believed to be influenced other than by the true area of contact, also by the strength of the bond formed at the interface and by the shearing of the materials in contact for unlubricated conditions. Obviously, in lubricated contacts also the shearing of the lubricant trapped between the surfaces influences the friction (Unsworth, 1978).

As has been said before, Charnley's work tried to minimise the frictional torque transmitted to the surrounding bone as he believed it to be the cause of loosening of artificial joints. Although it has never been demonstrated whether or not the reduced frictional torque is a significant factor in prostheses longevity, it has often been asserted that it may, in some part, be responsible for the loosening of prosthetic components. Furthermore Dowson remarked that "(friction measurement) is likely to be particularly valuable in view of the growing appreciation of the importance of surface tractions on sub-surface strains and wear mechanisms". The surface traction affects the orientation of the polymeric molecules and therefore the type of wear encountered. Finally, whenever new designs of replacement joints are developed, friction testing of the prostheses should be undertaken as they give an understanding of the lubrication mechanism likely to be prevalent in *in vivo* conditions.

Two main properties of the frictional force F are:

$F \neq f(A)$

$F = \mu L$

Where A is the apparent area of contact, L the normal load and μ is a constant of proportionality generally called coefficient of friction. However, this second law is not completely true for polymeric surfaces because deformation of the asperities in contact involves an elasto-plastic component (Hall et al., 1997). Furthermore, in MCP prostheses, it is not possible to define the precise pressure distribution on the contact area. Therefore it is not possible to determine the coefficient of friction μ. In order to overcome this problem, a friction factor has been introduced (Unsworth., 1978):

$$f = \frac{T}{RL}$$

where T is the frictional torque generated between the articulating surfaces and R is the radius of the metacarpal component.

In order to understand how friction measurement can predict the lubrication mechanism present in artificial joints, it is necessary to introduce the definition of lubrication. Lubrication is defined as the process of adding a substance (solid, liquid or gas) to reduce friction and/or wear at the interface between two surfaces in relative motion. When a fluid is placed between the sliding surfaces, either fluid or boundary lubrication or both, may occur (Radin and Paul, 1972).

In **fluid-film lubrication** the sliding surfaces are completely separated by a film of lubricant and the resistance to motion only depends on the viscosity of the lubricant.

When the bearing is loaded, the fluid film can be sustained in different ways:

- in ***hydrostatic lubrication*** the fluid is generally maintained under pressure by a pump;

- in ***squeeze film lubrication*** the surfaces by coming together generate a pressure field in the fluid trapped between them;
- in ***hydrodynamic lubrication*** continuous relative motion of the surfaces and a physical a wedge of lubricant between them keeps them apart.

The coefficient of friction in fluid-film lubrication is very low, in the range of 0.001 to 0.01. When the bearing surfaces are elastic the fluid film is more easily maintained because the lubricant pressure generated by motion under a given load can deform the bearing surfaces, producing what is called ***elastohydrodynamic lubrication***.

In **boundary lubrication** each bearing surface is coated with a thin layer of molecules which slide on the opposing surface.

The transition from boundary to fluid-film lubrication does not take place instantaneously as the load increases, but the two regimes can coexist in what is called **mixed lubrication**. In this regime the load is carried partly by the fluid pressure and partly by the contact of asperities on the two articulating surfaces, therefore both the physical properties of the bulk lubricant and the chemical properties of the boundary lubricant are important.

For investigating the lubrication regime acting on two bearing surfaces, a very useful tool is the Stribeck curve which plots friction factor versus an non-dimensional Sommerfeld parameter Z.

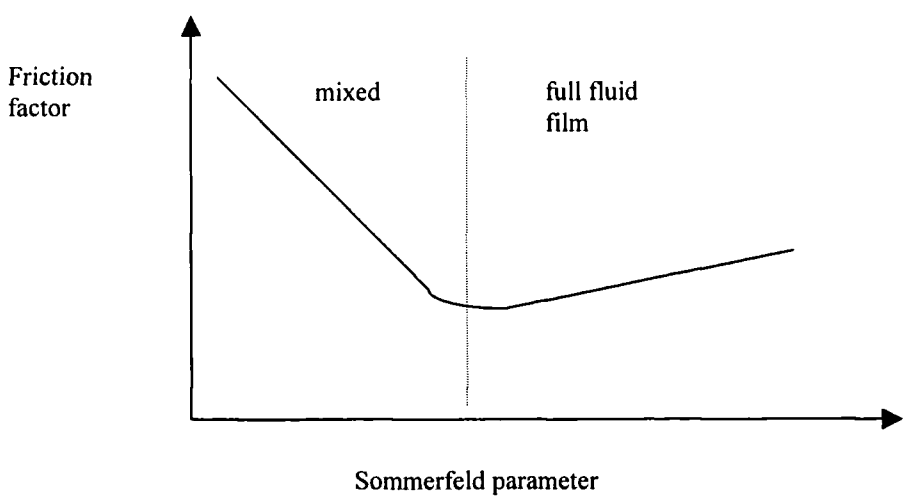

Figure 2.16 Stribeck curve

The Sommerfeld parameter is defined as:

$$Z = \frac{\eta u r}{L}$$

where η is the lubricant viscosity, u is the entraining velocity, r is generally the radius of the component and L is the applied load.

A decreasing coefficient of friction with increasing Sommerfeld parameter is indicative of a mixed lubrication regime, while a rising trend and low coefficient of friction indicate a fluid film regime. The lubrication regime is very important because the type of lubrication influences the wear rates on the prostheses and consequently the prosthetic life as osteolysis, generated by wear debris, leads to failure of the implant as we have seen.

2.5 Lubrication of natural joints

The natural synovial joint can be described as a self-contained plain bearing, which consisting of articulating surfaces and lubricant. The end of each bone is covered with a protective layer of articular cartilage, which reduces contact stresses in the joint, protects bone surfaces from impact stresses, and minimises friction and wear. The natural lubricant, called synovial fluid, is a clear and viscous fluid which lubricates the articulating surfaces, transports waste products away from the cartilage and carries nutrients to the cartilage cells. A normal joint is expected to function for about eighty years whilst transmitting dynamic loads of large magnitude and yet accommodating a wide range of movements. The tribological performance of synovial joints has intrigued physicians and engineers for at least a century, and researchers have proposed dozens of different theories on joint lubrication, most based on friction measurements.

It is now known that the healthy synovial joints experience fluid-film lubrication (Unsworth, 1991). At high rates of relative motion the cartilage surfaces are separated by a fluid film in the hydrodynamic lubrication regime, while at lower

sliding speeds the surfaces are expected to come into contact in the boundary lubrication regime, but this does not seem to happen in the human joints. Many theories have been proposed to explain this unique behaviour. McCutchen (1967) believed that the application of load to the joint caused the fluid within the porous cartilage to be pressurised and that the sponge-like material created a self-pressurised hydrostatic bearing. This mechanism was called weeping lubrication. However, other studies (Dintenfass, 1963; Tanner, 1966; Dowson 1966-67) suggested that the elastic nature of the articular cartilage might form the basis for an elasthohydrodynamic action in synovial joints. Dowson (1966-67) pointed out the importance of squeeze film lubrication in dynamically loaded joints as a way of increasing the values of film thickness, which could be calculated on the basis of elasthohydrodynamic theory.

Digestion experiments on synovial fluid were carried out using static (Linn and Radin, 1968) and dynamic loading (O'Kelly et al., 1978; Roberts et al., 1982). These studies showed that under normal dynamic loading cycles, the fluid film lubrication dominated while under static heavy loads mixed lubrication prevails, with boundary lubrication dominating. Earlier studies also reported that friction increased with time under constant load in presence of sliding motion (McCutchen, 1967; Walker et al., 1968).

2.6 Lubrication of artificial joints

The frictional resistance to motion in an artificial joint depends on the nature of the materials, the mode of lubrication, the geometrical form of the prosthesis and the load.

The materials used for the bearing surfaces should present low wear, low coefficient of friction and also be dimensionally stable and durable, since an increasing number of prostheses being implanted in young patients. In an attempt to meet these demanding specifications, a number of different materials have been used in artificial joints over the last three decades. Highly polished pairs of metal on metal surfaces have shown low wear (Goldsmith et al., 2000), but some concern has been expressed about the high coefficient of friction (Cabitza and Percudani, 1979). Pairs of ceramic (alumina and zirconia) bearings surfaces have also been used due to their extremely low wear and low coefficient of friction, but they require complex manufacturing processes to achieve the required surface finish and they can fracture (Skinner, 1999). However, the most used pair of materials for artificial joints remains metal on polymer.

Since UHMWPE is used in the majority of prostheses currently implanted, many studies have been carried out to calculate the coefficient of friction of this polymer when sliding on metal or ceramic surfaces. Unsworth et al. (1974) showed that hip prostheses operate with boundary or mixed lubrication in simulator studies. An explanation for this lubricating regime is that a lubricating film thickness of 0.1μm has been predicted using elasthoydrodynamic lubrication theory for Charnley prostheses. Since the surface roughness of the plastic component can be much greater than this value, the fluid film may not be able to separate the two bearing surfaces. Therefore the resulting boundary or mixed lubrication produces a value of friction higher of that found in natural joints. However, the frictional torques produced in artificial joints with UHMWPE components are considered to be sufficiently low not to contribute to loosening.

2.7 Frictional studies

2.7.1 Introduction

Tribological studies of joint replacement materials can be divided into three categories:

- *In vitro*: studies of components with joint simulators or with screening apparatus;
- *In vivo*: studies of components that have been implanted in patients;
- *Ex vivo*: studies of components that have been removed from patients.

It is common to compare *in vitro* wear with *in vivo* and *ex vivo* observations, to verify whether test machine results are reliable.

In vitro studies can be carried out using materials screening apparatus or joint simulator machines. Materials screening testers are simple configuration machines which can test simplified geometry specimens as a preliminary step in evaluating the material performances. All of these machines consist of a moving component, usually a plate or a disc, that is loaded statically by means of a second fixed component, typically a pin or a cylinder. The motion can be reciprocating or rotating. These machines are very useful, as they are inexpensive to manufacture, use simple geometry components and are also easy and accurate in measuring friction and wear. Joint simulators however, are quite sophisticated machines which can simulate physiological conditions, including loading and motion patterns. In simulators half of the joint oscillates and the other is still; usually the stationary half is loaded with a cycle that simulates the physiological load.

In the past, the frictional properties of human joints were determined by a pendulum test which measured the rate of decay of oscillations, using the intact joint as the pivot of the pendulum. Linear decay of successive amplitudes of the swing of the pendulum indicates Coulomb friction, while exponential decay

indicates viscous drag at the pivot. However, as these effects are small, a more sensitive measuring technique was required. A successful method for measuring friction in synovial joints has been the pendulum test described by Unsworth et al. (1975). The authors measured the frictional torque using a direct method. The pendulum consisted of a support frame which held the frictional torque-measuring carriage supported by extremely low-friction hydrostatic bearings with $\mu = 10^{-5}$ at least, so as to be two orders of magnitude lower than that for the joint. The pendulum could be loaded with variable weights and the length altered for different frequencies of oscillation. This technique works on the principle that as the femoral head in hip joints swings back and forth, the frictional torque at the joint interface tries to rock the carriage in its bearings. Restraining this movement with a transducer enables the frictional torque T to be determined. The load L acting across the joint surface can also be measured directly using a load cell (fig. 2.17).

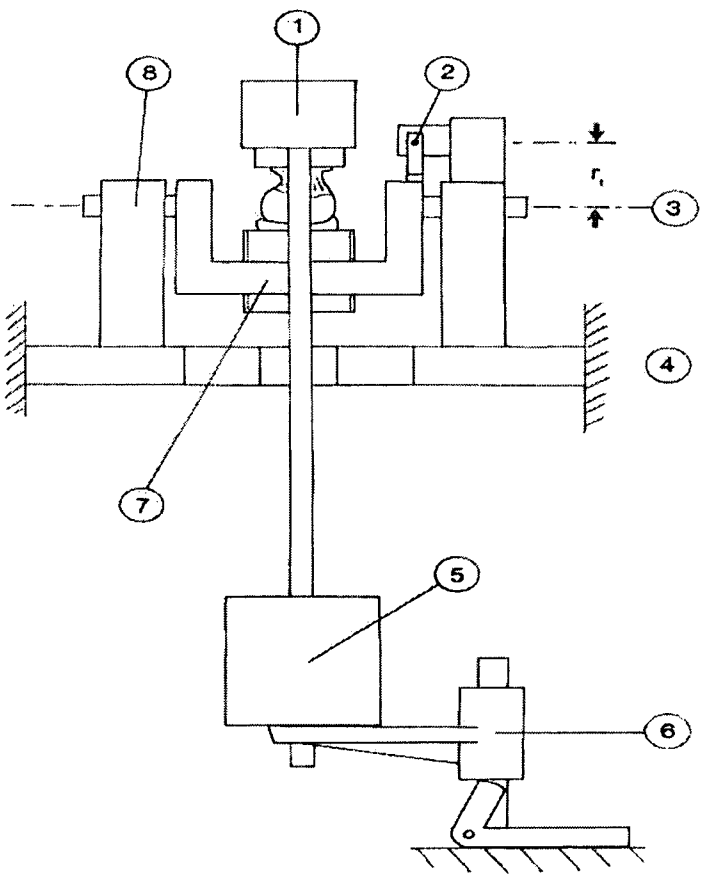

Fig. 2.17 Pendulum apparatus for measuring joint friction: 1. Crosshead; 2. Force transducer; 3. Carriage bearing axis; 4. Frame; 5. Pendulum weights; 6. Weight lifter and quick release; 7. Cradle with adjustable height specimen holder and load cell; 8. Externally pressurized hydrostatic bearings $\mu < 10^{-5}$. r_t is the length of radius arm to transducer.

The friction finger simulator has been designed using the same principle as also the MCP joint swings back and forth during the flexion-extension movement.

2.7.2 Friction measurements using pin-on-plate machine

The standards literature on friction measurements in orthopaedic devices is still very minimal. ASTM F732-82 (1989) states that it is "recommended that machine include...transducers capable of providing a continuous readout of the friction force", while the British Standard 7251 (1990) suggests recording mean and range of friction together with any temporal variations. Therefore the results of frictional studies reported in literature are difficult to compare mainly because of the different testing parameters.

A study using a reciprocating pin-on-plate rig, investigated the effects of different lubricants on the frictional resistance between UHMWPE and 316L stainless steel (McKellop, 1981). The friction produced between the two surfaces was less with bovine serum (μ = 0.12) than with either distilled water (μ = 0.18) or Ringer's solution (μ = 0.27). The presence of a polymeric transfer film on the metallic surface in distilled water and Ringer's solution has been reported. Probably the same transfer film is not present in bovine serum because of attachment of serum proteins to the metal.

Another study evaluated the effects of motion, lubricant and counterface material on friction while sliding against UHMWPE (Kumar et al., 1991). The friction measured in the reciprocating tests was less than in the unidirectional ones and an explanation for this result could be the disruption of the adhesive friction component on the reversal of the motion as suggested by the authors. As regards

the counterface materials, the friction coefficient was found to be less with ceramic than with 316L stainless steel, and lower with zirconia than with alumina. The highest values of μ were found in the saline lubricated environment and this may be explained by the increased roughness of the counterface. However, little difference in the value of the friction coefficient was observed for UHMWPE-316L stainless steel pairings in either bovine serum or distilled water and this might indicate that other effects, as well as transfer film formation, probably played an important role in determining the frictional resistance. A study has also been carried out for investigating the effects of irradiation and load on the coefficient of friction for 316L stainless steel/UHMWPE combinations, in a dry environment (Shen and Dumbleton, 1974). The non-irradiated specimens showed the lowest values of friction at all loads and a deposition of transfer film on the metallic surface, which might explain the result. However, Jones et al. (1981) observed that the cross-linking induced by the sterilisation seemed to be not sufficient to prevent transfer film formation under dry conditions. Furthermore, in the same study, no significant difference was found between the coefficient of friction for different levels of irradiation. A study by McKellop et al. (1983) pointed out that the friction between irradiated and non-irradiated UHMWPE on stainless steel under dry environment was lower for the non-irradiated samples at loads of 225 N, but no significant difference was reported for higher loads (445 N) and in lubricated conditions.

2.7.3 Friction measurements using hip simulators

Friction hip simulators are generally single station machines with a single flexion-extension axis of rotation and a loading vector representing the major component of the joint reaction force (Paul, 1997).

The Leeds and Durham friction simulators measure the frictional torque created by resisting the rotational motion due to the friction, using a piezo-electric transducer and have been used in various studies (Auger et al., 1993; 1995; Stewart et al., 1997; Hall et al., 1997; Elfick et al., 1998).

Initial frictional studies were carried out to compare metal on metal and metal on polymer pairings. An early study (Scales et al., 1969) reported for metal on polymer prostheses approximately up to one-half of the frictional torque produced in the metal on metal prostheses. Subsequent studies confirmed this finding, although the difference was found to be less marked (Weightman et al., 1972). Saikko (1992) studied the frictional behaviour of different head and UHMWPE cup dimensions and combinations with a hip joint simulator and reported the 22-mm joint to produce the lowest frictional torque. The author pointed out that the frictional torque was dependent not only on the head diameter, but also on the surface finish, material combination, clearance ratio, thickness of the cup and stiffness of the swinging. More recent studies (Hall et al., 1994; Scholes and Unsworth, 2000) demonstrated again that metal-on-plastic prostheses function under a mixed lubrication regime. Scholes and Unsworth however, also reported that the ceramic on ceramic pairs exhibited mixed lubrication with synovial fluid and bovine serum, but full fluid film lubrication with synthetic lubricants such as carboxymethyl cellulose (CMC) fluids or silicone.

3 Apparatus

3.1 Introduction

A number of different types of apparatus have been used in order to perform the various tests described. A particle analyser (Malvern Mastersizer 2000s) was used to quantify and characterise the wear debris collected from the lubricant, while a digital microscope (JVD) was used for observing the worn surface of the prostheses after testing.

The aim of this research has been to investigate further the wear behaviour of XLPE rubbing against itself using the finger wear simulator and to design, develop, validate and use a new finger friction simulator for measuring the friction of different possible combination of materials for finger joints. This has obviously required familiarisation with existing friction simulators.

3.2 Finger Friction Simulator

The finger friction simulator has been designed applying the principle of a direct measurement of friction as first described by Unsworth et al. in 1975. Therefore the machine consisted of a support frame which held the frictional torque-measuring carriage supported by extremely low-friction bearings. This technique works on the principle that as the metacarpal head in the MCP joints swing back and forth during the flexion-extension movement, the frictional torque at the joint interface tries to rotate the carriage in its bearings. Restraining this movement with a transducer enables the frictional torque T to be determined. The load L acting across the joint surface was applied by a pneumatic cylinder and was measured directly using a load cell.

The new finger friction simulator is a single station machine designed for investigating the frictional behaviour of different pairs of biomaterials for two-

piece artificial finger joints. The central part of the machine is the lubricant bath where the test prosthesis is mounted in two holders which represent the metacarpal bone and the proximal phalanx. The lubricant bath has been designed such that different sizes of finger prostheses can be tested (Fig. 3.1).

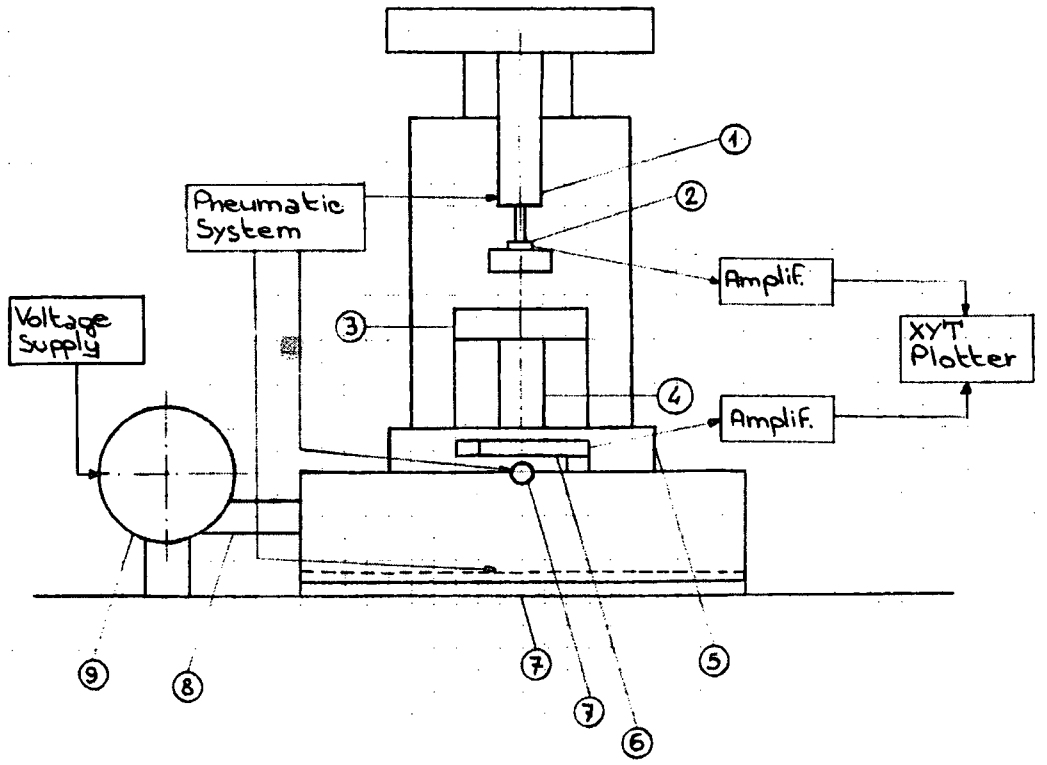

Fig. 3.1 Finger Friction Simulator: 1. Pneumatic cylinder; 2. Load cell; 3. Swinging block; 4. Metacarpal holder; 5. Lubricant bath; 6. Piezoelectric force transducer; 7. Externally pressurized hydrostatic bearings $\mu < 10^{-5}$; 8. Conrod; 9. Electric motor.

The phalangeal holder at the bottom is held stationary, while the metacarpal holder swings against it over a 90 degrees range of motion and this simulates the flexion-extension movement. Lubrication of the bearing is possible by means of a lubricant bath and the lubricant can be varied. The swinging block is driven by a 40W DC motor and the movement is transmitted by a connecting rod. The frequency of swinging can be varied using a variable voltage supply. An 8mm diameter pneumatic cylinder mounted on the top of the machine is used to supply

a static load during flexion-extension and the load can be varied according to the air pressure supplied to the cylinder. This load is constrained to act vertically. A load cell, which is attached at the base of the pneumatic cylinder, measures the dynamic load applied to the metacarpal component and its signal is amplified by a strain gauge amplifier. A piezoelectic quartz force transducer fixed on the phalangeal bath and on the friction carriage measures the friction between the two components. The output signal of the transducer is amplified by a charge amplifier and connected to a X-Y plotter for the final reading. Both the lubricant bath and the friction carriage are mounted on low friction air bearings. The pressure to the cylinder and to the air bearings is supplied by a compressor and is controlled by means of regulators.
A full description of this is given in Chapter 4.

3.3 Finger Function Wear Simulator

The first Durham finger function wear simulator was commissioned and described by Stokoe et al. in 1990 and it combined the rapid movement and the light load of the flexion-extension motion, with the static, high load that characterises the "pinch", dual cycle. This loading cycle accurately reproduced the *in vivo* conditions and this was demonstrated by the fact that it led to failure of a Swanson prosthesis in a time and a manner comparable with surgical experience (Stokoe et al., 1990).

However, in order to solve some problem of reliability encountered with the use of this first simulator, a second finger function wear simulator was commissioned, designed and described by Joyce and Unsworth (2000) and this machine was the one which was used in all the wear simulator experiments undertaken during this research. As this machine has been described extensively elsewhere (Joyce and Unsworth, 2000), only a brief description of its operation has been provided here.

The new wear simulator is a single station machine which essentially differs from the "Stokoe" one by using a different method of load actuation. The central part

of the machine is the lubricant bath (Fig. 3.2) where the test prosthesis was mounted in two holders which represent the metacarpal bone and the proximal phalanx.

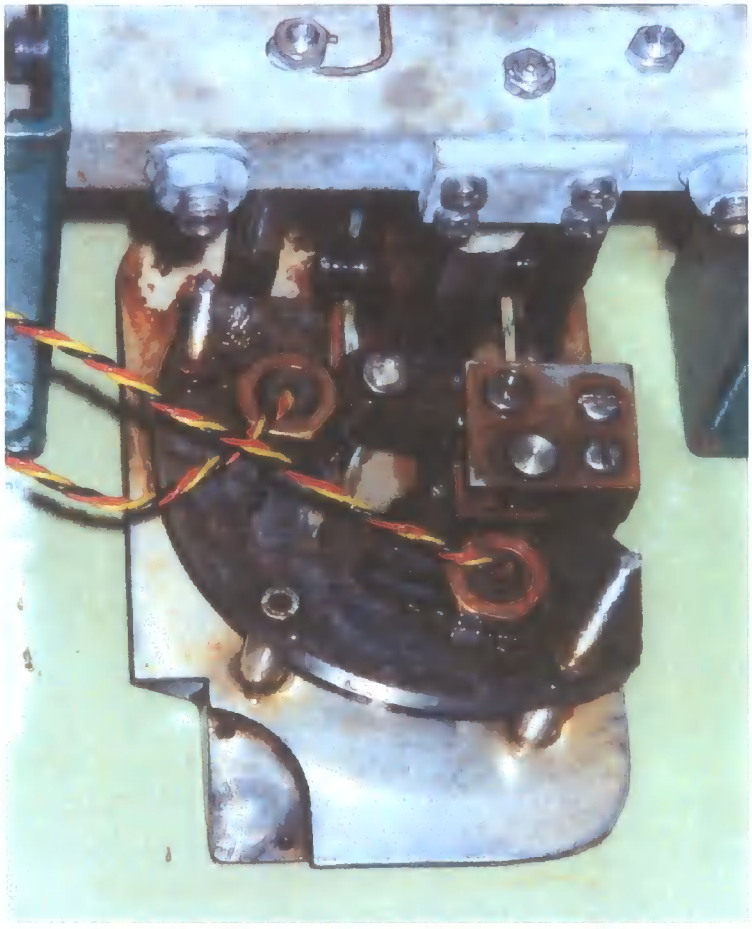

Fig. 3.2 Lubricant Bath of the Finger Wear Simulator

Figure 3.2 shows clearly the square section cantilever whose end held the metacarpal holder. Also visible on this cantilever is the white sealant that protects the 8 strain gauges which allowed the prosthetic load to be measured in two planes. The phalangeal holder was held in a phalangeal clamp positioned between the stainless steel base plate and the polymeric arc piece shown. The two sensors allowed the phalangeal clamp to rotate through a 90° arc of motion under the action of the "tendons", while the metacarpal holder was held stationary. This simulated the flexion-extension movement. A heavy, static load was also applied using a 32mm bore pneumatic "thumb" cylinder with a stainless steel rod attached

to simulate the "pinch". The stainless steel rod acted as a "thumb" against which the "pinch" load was applied. At "pinch" time, the rod passed into a hole drilled in the base plate at a position equivalent to 30° of MCP joint flexion. Then the extensor tendon relaxed, while the flexor tendon transmitted a compressive force together with a subluxing force to the test prosthesis. The figure also shows a free moving pulley which represented the volar plate and the metacarpoglenoidal ligaments.

Figure 3.3 gives a general view of the simulator including the pneumatic components, the heating unit and the computer screen. The "thumb" pneumatic cylinder can be observed mounted on the lid of the test bath.

Fig. 3.3 General view of the Finger Wear Simulator

3.3.1 Application and measurement of load and motion

The dual cycle load is transmitted by pneumatic cylinders which have been chosen as they are a reliable, cheap and clean way of running the new finger function wear simulator continuously, and sometimes unattended, for several weeks. The use of pneumatics would also possibly eliminate the problem of stretching of the "tendons" leading to a gradual reduction in the transmitted load as reported using the "Stokoe" simulator where the load was mechanically transmitted. Therefore using the pneumatics and controlling the air pressure would ensure that the load remained constant.

Two 10 mm diameter pneumatic cylinders were used to supply the 10-15N load which characterises the flexion-extension movement (Tamai et al., 1988), while a 32mm bore pneumatic cylinder provides the 106N load necessary for simulating the static "pinch" load in a rheumatoid hand.
The load was then measured in two directions using 8 strain gauges. A `PC-Alpha G` combined strain gauge amplifier/A-D card is used to amplify the signal from the strain gauges and convert it to a digital signal. A Quick C program constantly measured the numerical value of load and also activated the pneumatic valves in order to create a load cycle of 3000 counts of flexion-extension followed by 45 seconds of "pinch" grip. Figure 3.4 shows the dual cycle load applied on the finger wear simulator.

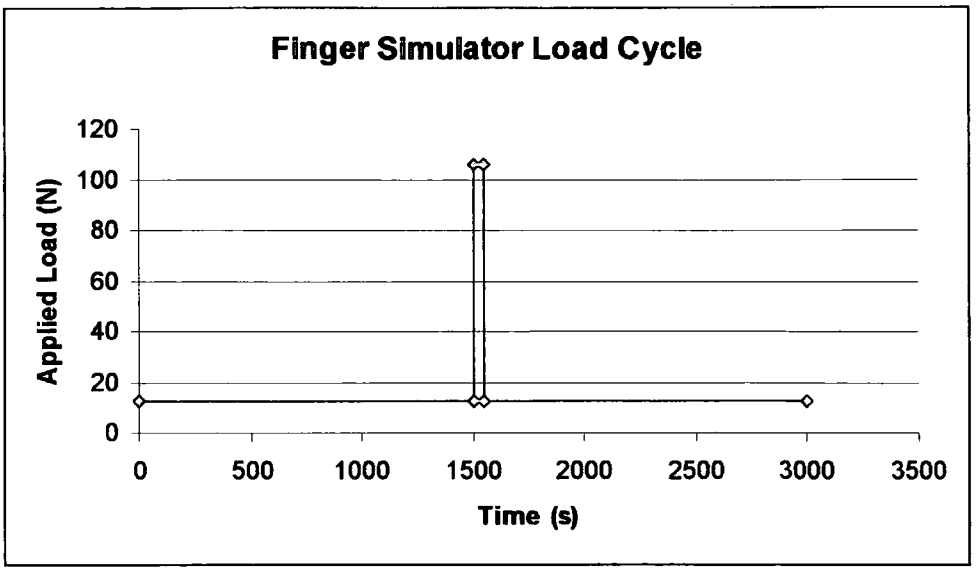

Figure 3.4 Finger wear simulator dual cycle load

The motion on the new finger function simulator is uniplanar as flexion-extension is the predominant movement of the finger. However a little clearance between the phalangeal clamp, the arc and the base plate allows some passive "abduction-adduction". One flexion-extension cycle is the sliding of the phalangeal test component on the metacarpal test component from 0° to 90° and back to 0°, under a constant load of 12.5N.

A computer controls the force application measurement and motion and it is possible to read a direct value of load across the prosthesis on the screen, if required.

3.4 Malvern Mastersizer 2000s

The Mastersizer 2000s is used to ascertain the size of particles held in suspension. It is capable of sizing particles over the size range 0.02μm to 2000μm in 100 discrete size bands. Particles diffract light as it passes them, the size of the particle can then be resolved using Mei theory and the size distribution is reported in terms of either volume or number.

The primary advantages of this technique lie in the simplification of the processing route prior to particle measurement and the ability for the instrument to size the entire population of particles rather than just a sample of the cohort. This results in the reduction of the incorporated errors inherent within alternative techniques such as SEM sizing in 2D.

3.5 JVD Digital Microscope

The JVD Digital Microscope is characterised by a JVD CCD camera connected to a PC via a frame grabber card. The resolution of the images is 640 x 480.

4. Finger Friction Simulator

4.1 Introduction

In the past, the frictional properties of human joints were determined by a pendulum test which measured the rate of decay of oscillations, using the intact joint as the pivot of the pendulum. Linear decay of successive amplitudes of the swing of the pendulum indicates Coulomb friction, while exponential decay indicates viscous drag at the pivot. However, as these effects are small, it is better to measure the frictional force directly, especially if the nature of the lubricating regime is to be determined. A successful method for measuring friction in synovial joints has been the test described by Unsworth et al. (1975). The authors measured the frictional torque using a direct method, instead of the traditional method of calculating it from the miniscule rate of decay of an oscillating pendulum. The machine consisted of a support frame which held the frictional torque-measuring carriage supported by extremely low-friction bearings. It could be loaded with variable weights and the length altered for different frequencies of oscillation. This technique works on the principle that as the femoral head in hip joints swings back and forth, the frictional torque at the joint interface tries to rock the carriage in its bearings. Restraining this movement with a transducer enables the frictional torque T to be determined. The load L acting across the joint surface can also be measured directly using a load cell. Friction hip simulators are generally single station machines with a single flexion-extension axis of rotation and a loading vector representing the major component of the joint reaction force (Paul, 1997).

The friction finger simulator has been designed using the same principle and so the MCP joint swings back and forth during the flexion-extension movement.

4.2 Design of the finger friction simulator

Detailed design of this new simulator can be divided into four parts which are the frictional-torque measuring carriage, the pneumatic load mechanism, the flexion-extension movement control and the XYT plotter for recording the output signal (Fig. 4.1).

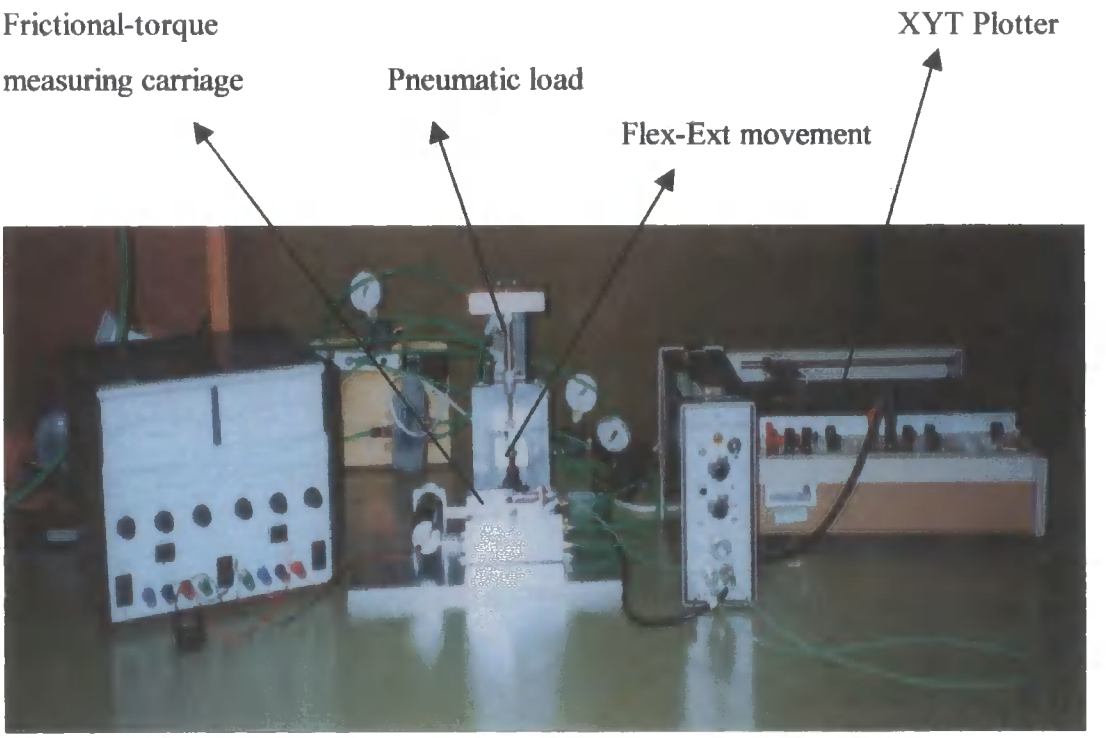

Fig. 4.1 General view of the Finger Friction Simulator

4.2.1 Frictional-torque measuring carriage

The frictional-torque measuring carriage containing the two pairs of externally pressurised bearing pads and holding the lubricant bath was all manufactured from an aluminium block of 120 x 120 mm and a thickness of 50 mm (Fig. 4.2). The two pairs of air bearings were designed parallel to the base plane and orthogonal to each other in order to accommodate the movements of the phalangeal component on the metacarpal component during swinging.

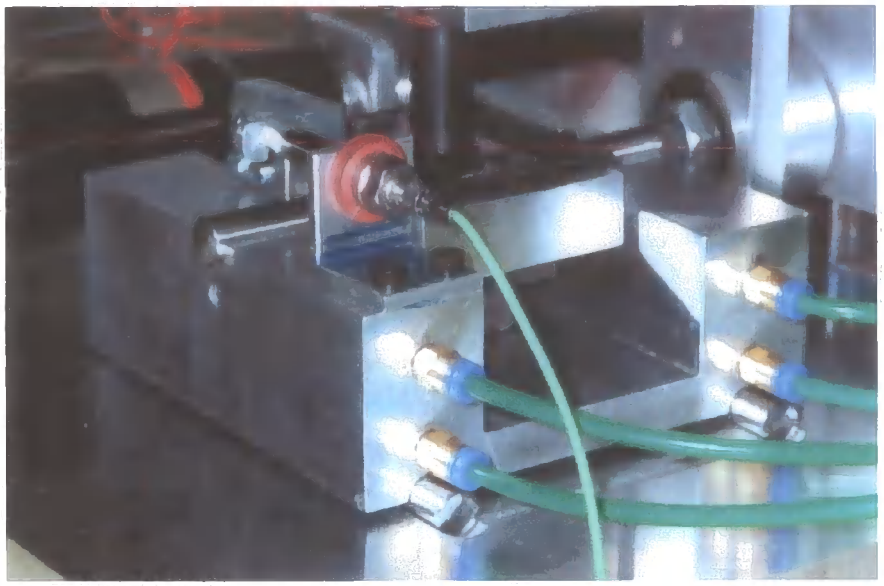

Fig. 4.2 Frictional torque measuring carriage

A hydrostatic air bearing arrangement was chosen for its excellent low friction properties ($\mu < 10^{-5}$), its cleanliness and its stiffness which allowed support of the reactive force of the load. The bearing orifice and pad dimensions required to support the reactive force using the available system pressure were calculated including a safety factor.

The two upper pads were designed to support the lubricant bath with the test prosthesis mounted on it and the reactive force of the load applied through it. They were obtained drilling a ∅ 10.00 mm hole through the aluminium block, then cutting the upper half off. The two upper pads measured ∅ 10.00 mm wide and 28 mm long. The two lower pads were machined the same way, but they were designed to support the additional weight of the frictional-torque measuring carriage, therefore they measured ∅ 10.00 mm wide and 110 mm long. The two upper pads included three 0.41 mm diameter orifices each, while the lower pads included six 0.41 mm diameter orifices each. These orifices were machined along the centre of the pad's width spaced at regular intervals along its length and were bored to a depth of 3 mm to meet the 4.20 mm bore running centrally through the length of the bearing supplying the bearing pressure. In each of the four bearing

pads, one end of the central bore was closed off and the other threaded to a M5 thread to fit suitable pneumatic connections.

All the four bearing pads were coupled with stainless steel rods (precision linear shafting). On the lower arrangement the rods were bolted on the base plate, while on the upper arrangement the rods were bolted on to the lubricant bath support. The surface finish of the rods was $R_a < 0.32$ μm so that it could allow the clearance needed for the air bearings to work.

The lubricant bath was manufactured from a nylon cube of 60 x 60 x 60mm and was rigidly bolted on to its support by means of four screws. The lubricant bath was carefully designed to hold phalangeal components of different sizes, to allow the 90° swinging motion and to match the centre of rotation of the joint. Adjustment was incorporated to ensure centralisation. A 3mm square section hole was drilled through the centre of the lubricant bath in order to accommodate the phalangeal stem without any risk of rotation of the component during the test. The lubricant bath support was manufactured from an aluminium block of 60 x 60 mm and a thickness of 25 mm.

The lubricant bath represented the central part of the machine, where the test took place. The prosthesis was mounted in two holders which were carefully designed for the type and size of prosthesis tested. The phalangeal holder at the bottom was held stationary, while the metacarpal holder oscillated against it over a 90° range of motion and this simulated the flexion-extension movement. The lubrication of the bearing was possible by topping up the lubricant bath and the lubricant could be varied.

The lubricant bath was restrained in its swinging by a piezoelectric force transducer (Kistler 9203) which was rigidly attached to the frame of the frictional-torque measuring carriage. The output from the piezoelectric force transducer was fed to a charge amplifier (Kistler M05-100) which amplified the signal before feeding it to an XYT plotter (RDK RW Series Model 83) which recorded the signal.

4.2.2 Pneumatic load mechanism

A static load of 15N was applied across the test prosthesis pneumatically. A pneumatic cylinder was attached vertically to the upper part of the rig by means of a M8 thread as shown in figure 4.3.

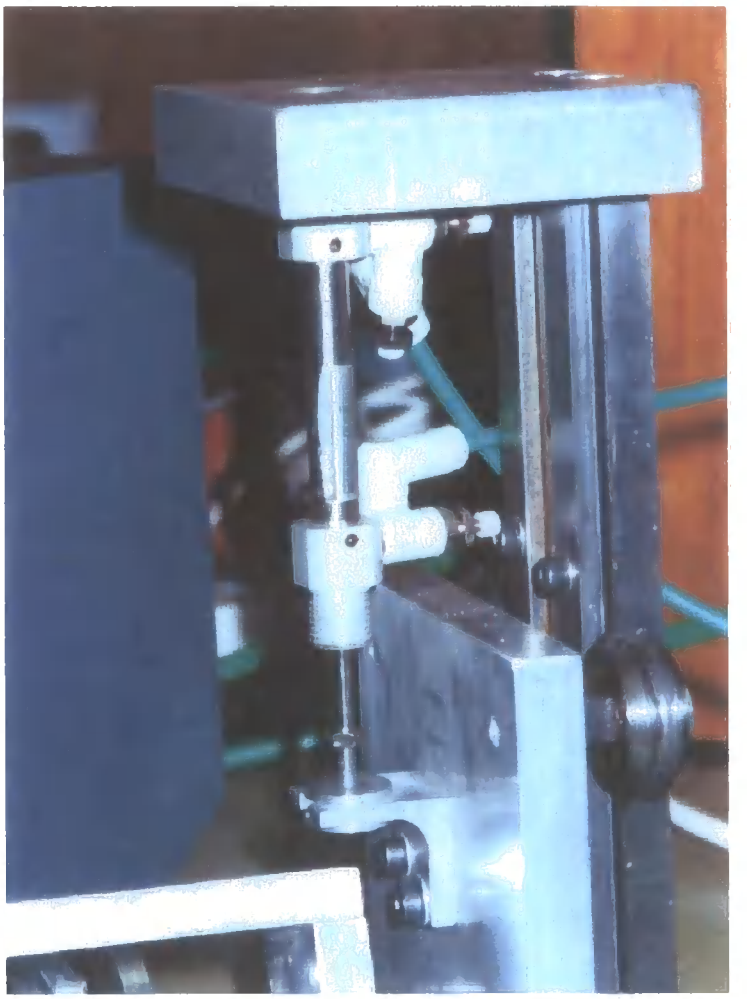

Fig. 4.3 Pneumatic load mechanism

The rod of the pneumatic cylinder was screwed into a spacer which in turn attached to a sub-miniature load cell (RDP Precision Miniature Load Cell Model 34). The load cell was attached to a charge amplifier (RDP Type S7DC) which amplified the signal before sending it to the XYT plotter so that the load applied by the cylinder to the bearings could be measured.

During the calibration process, a load cell was mounted on a special metacarpal holder in order to be sure to measure a load of 15N across the bearings (Fig. 4.4). Both the results obtained using dead weights and the pneumatic cylinder were combined in the calibration relationship. The load applied by the pneumatic cylinder was chosen to give the required one in the bearings. The configuration of the pneumatic cylinder acting on a vertical aluminium plate solidly linked with the roller bearing of the swinging block and free to slide vertically, assured a constant load to be transmitted to the bearings at any angle of flexion-extension.

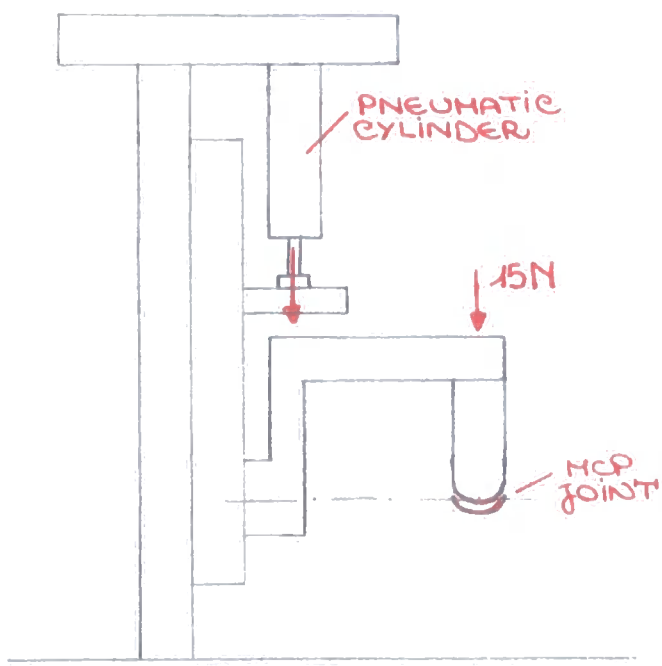

Fig. 4.4 Load-applied mechanism

A cylinder with a short stroke (25mm) was chosen as little vertical motion was required. The bore of the cylinder was chosen by calculating the cylinder area which would be required to give the necessary load under the system pressure available whilst considering the minimum operating pressure of the cylinder and so the load which it could apply:

$$\text{Cylinder.area} = \frac{\text{Required.load}}{\text{Available.pressure}},$$

where the area is given by Cylinder.area = $\pi\left(\frac{\text{bore}}{2}\right)^2$

The required load acting on the prostheses is L = 15 N and the maximum available system pressure offered by the compressor was to approx. P = 5 bar where 1 bar = 10^5 N m^{-2}

Therefore Cylinder.area = $\frac{15}{5 \cdot 10^5} = 3 \cdot 10^{-5}$ $m^2 = 3 \cdot 10^{-5} \cdot 10^6 mm^2 = 30$ mm^2

$1m^2 = 10^6$ mm^2

The cylinder area is also equal to:

$A = \pi r^2 = 30mm^2 \Rightarrow r = \sqrt{\frac{A}{\pi}} = \sqrt{\frac{30}{\pi}} = 3.09$ mm

Therefore the bore of the cylinder should be:
d = 2r = 6.18 mm

A 6 mm bore cylinder was first considered, with a minimum operating pressure of 2 bar, which provided loads in the range of 5.6 N (2 bar) to 14.1 N (5 bar).

1. ∅ 6 mm cylinder

$P = P_{min} = 2$ bar $\Rightarrow$ F = P A = 2 105 28.3 10-6 = 5.6 N

$P = P_{max} = 5$ bar $\Rightarrow$ F = P A = 5 105 28.3 10-6 = 14.1N

A 8 mm bore cylinder (SMC Pneumatics, series C858-25) was chosen, which had a minimum operating pressure of 1 bar and providing loads in the range of 5 to 25.1N.

2. ∅ 8mm cylinder

$P = P_{min} = 1$ bar $\Rightarrow$ F = P A = 1 105 50.3 10-6 = 5N

$P = P_{max} = 5$ bar $\Rightarrow F = P A = 5\ 105\ 50.3\ 10\text{-}6 = 25.1N$

The pressure to the cylinders was controlled by means of a combined filter regulator (Bosch Model 0821 300 700).

Initially the vertical movement of the cylinder was designed by means of two stainless steel rods (precision linear shafting) screwed vertically on the base plate on which two linear bearings (RS, type 311-3468) were sliding. Subsequently the arrangement was changed because the significant losses inside the linear bearings did not allow the pneumatic cylinder to give the load required on the joint.

4.2.3 Flexion-extension movement control

The swinging part of the rig was manufactured from an aluminium block of 40 x 80 x 25mm (Fig. 4.5) and was screwed into the vertical aluminium plate.

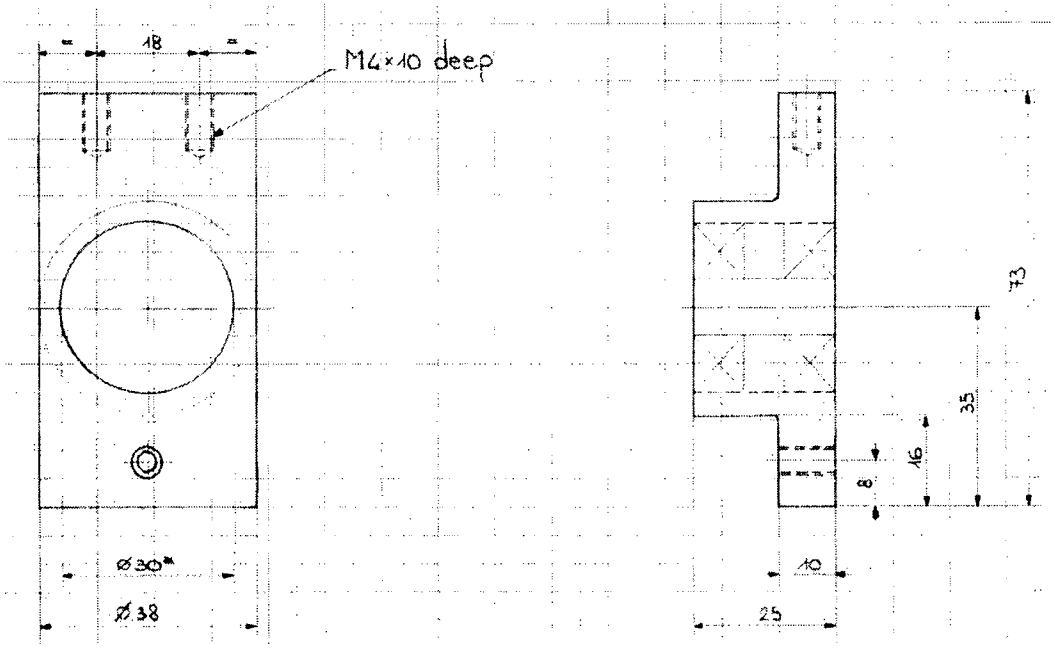

Fig. 4.5 Drawing of the swinging part

The central part of the swinging block was designed to accommodate the roller bearing (RS, type 243-8053) which transmitted the swinging movement to the metacarpal component. The lower part of the block was then screwed to a connecting rod which in turn was attached to the 40W DC motor. The length of the connecting rod was carefully designed (Fig. 4.6) to allow the ± 45° range of movement, being completely horizontal at 0°, when the swinging block was perfectly vertical.

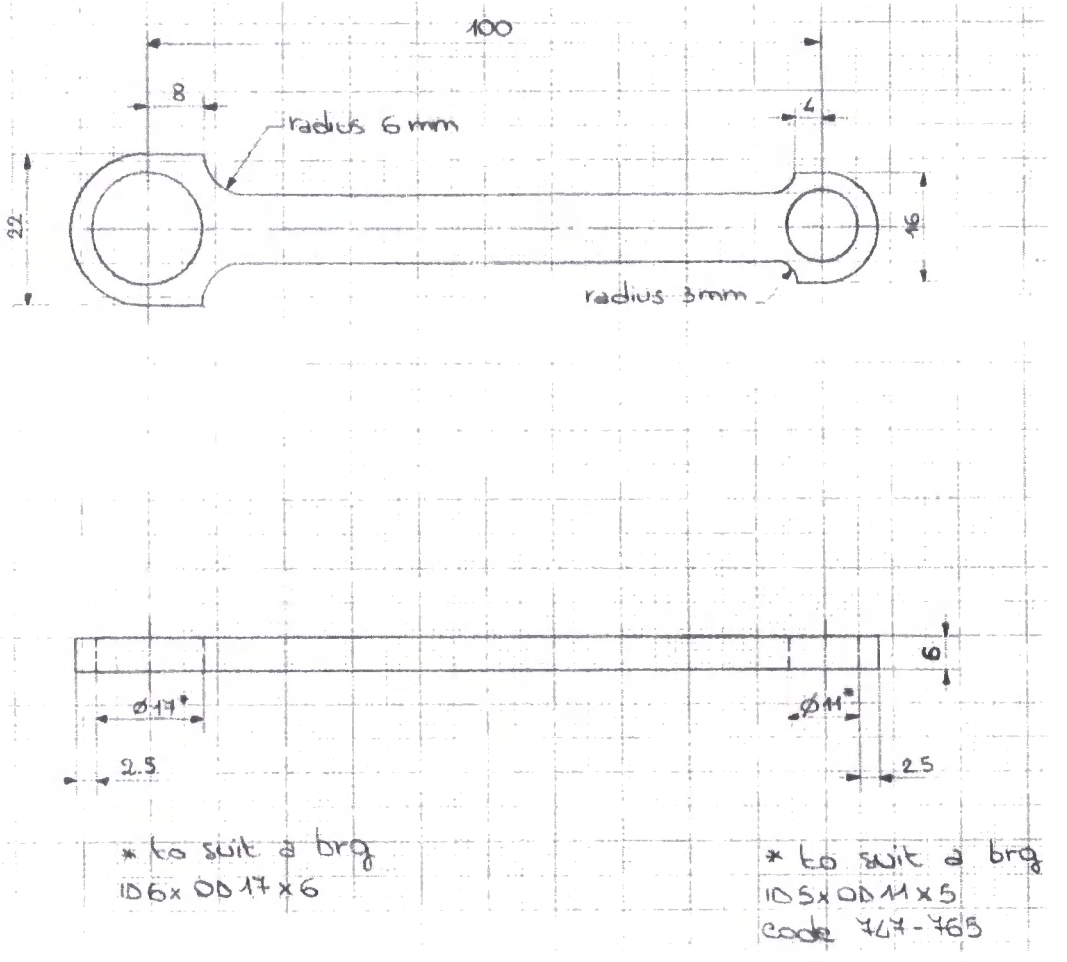

Fig. 4.6 Drawing of the conrod

4.2.4 The XYT plotter for recording the output signal

The XYT plotter attached to the piezoelectric force transducer and to the charge amplifier, was used to record the output signal from the transducer under the required load.

5 Materials and Methods

5.1 Introduction

During all the tests undertaken on both the finger function wear simulator and the friction simulator, standard testing methods and protocols were used to ensure consistency. The work on wear applied a proven test protocol used successfully for several years, while in the case of the friction simulator initial studies allowed a protocol to be designed so that repeatable results could be achieved. The materials and lubricants used were also standardised.

5.2 Materials for the wear experimentation

The wear tests were undertaken on the two piece all XLPE Durham MCP joint. Initially two non-irradiated prostheses of different sizes were tested in distilled water for over 14 million cycles. A 9.4mm radius, γ-irradiated Durham prosthesis was then tested in Ringers solution to have a comparison with the Swanson's prosthesis wear behaviour under the same conditions. For this reason, the metacarpoglenoidal arm was removed in order to simulate removal of the metacarpoglenoidal ligaments which often happens during the surgical implantation of the Swanson prosthesis.

Two other tests were undertaken using 9.4mm radius, γ-irradiated prostheses with the aim of investigating the influence of adding a second degree of motion on the wear behaviour of the XLPE prostheses. One test was run on the finger wear simulator, while the other one was run using a new finger wear simulator to which a rotational movement of ± 20° was added to the flexion-extension movement.

Four other tests were run using ethylene oxide sterilised prostheses of various sizes in order to investigate the influence of a different method of sterilisation. Two tests were run in distilled water and two in bovine serum.

All the production samples employed had square section stems, were of 1.5 mm thickness and also had a percentage gel content of 74% minimum. De Puy International, who manufactured the prostheses, consider a gel content greater than 70% to be acceptable for XLPE for use in a load bearing situation *in vivo*. The density of XLPE was taken to be 949 kg/m^3.

Detailed descriptions of the nine tests are given in Table 5.1.

Size (mm)	Number of cycles	Lubricant	Gel content (%)	Method of sterilisation	Motion
7.5R	14,506,707	D. Water	74-84	Non-irradiated	Flex-Ext
8.5R	14,042,768	D. Water	76-84	Non-irradiated	Flex-Ext
9.4R	8,485,886	Ringers	87	γ-irradiated	Flex-Ext
9.4R	3,181,511	Dry	76-84	γ-irradiated	Flex-Ext
9.4R	2,923,585	Dry	87	γ-irradiated	Flex-Ext + Rot
7.5R	5,000,000	D. Water		EtO sterilised	Flex-Ext
8.5R	5,000,000	B. Serum		EtO sterilised	Flex-Ext
7.5R	5,000,000	D. Water		EtO sterilised	Flex-Ext
8.5R	5,000,000	B. Serum		EtO sterilised	Flex-Ext

Table 5.1 Description of the wear tests undertaken on the MCP Durham prostheses.

The Ringer solution was made up as follows (for one litre):

Sodium chloride 7.5 gm

Potassium chloride 0.075 gm

Calcium chloride 0.1 gm

Sodium hydrogen carbonate 0.1 gm

Distilled water to 1 litre

The "bovine serum" lubricant was a solution of 1/3 of bovine calf serum and 2/3 of Ringer solution, to which 1mg of sodium azide per litre was added in order to reduce the growth of bacteria.

5.3 Materials for friction experimentation

In order to validate the finger friction simulator, various pairs of materials were tested and the results compared with previous work. The phalangeal component was manufactured as a 6.5-mm radius cup, while the metacarpal component was machined as a pin with a 6.5-mm radius hemispherical end. Both the metacarpal and the phalangeal samples incorporated square section stems in order to fix them in place and avoid rotation of the components during testing. The samples were also marked with a pencil so that to be able to replace them in the same position after every test. During the experiment, two UHMWPE cups, one titanium cup, two titanium heads and one stainless steel head were employed. Three differently sterilised Durham XLPE prostheses were also tested (Fig. 5.2). The form and size of the metacarpal and phalangeal samples were carefully designed to match the centre of rotation of the flexion-extension movement with the centre of the swinging motion.

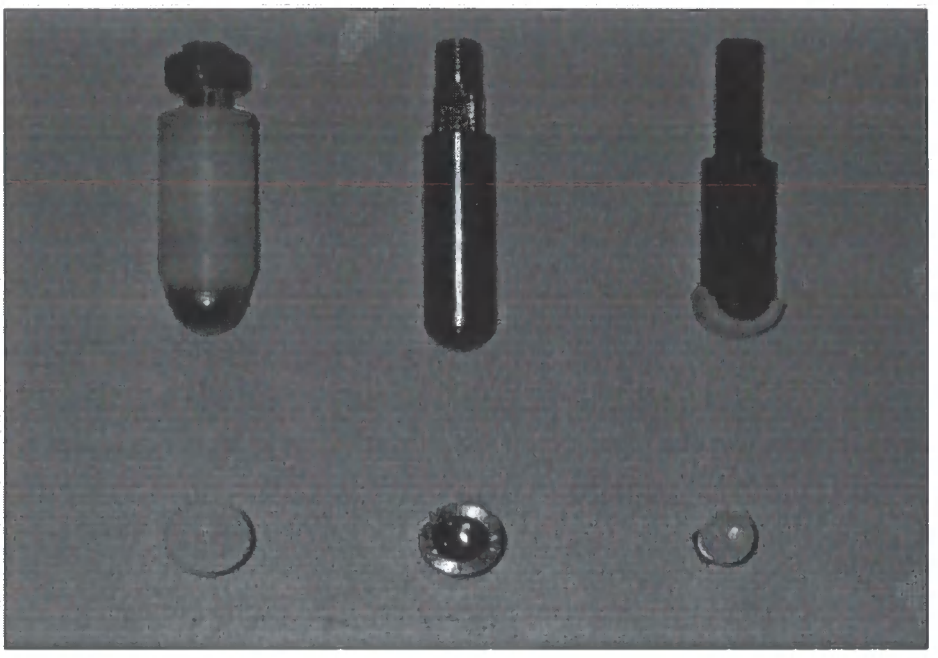

Fig. 5.1 Materials used in the friction tests

During the friction tests, three types of lubricants were used: distilled water, aqueous solutions of CMC (carboxymethylcellulose) fluids and silicone fluids. The CMC fluids and the silicone fluids were used in order to obtain a Stribeck curve and thereby allowing investigation of the lubrication regime present in the joint. CMC solutions are non-Newtonian fluids, with rheological behaviour similar to that of synovial fluid. Their range of viscosity however, is limited as it varied from 0.00303 Pa s to 0.1007 Pa s. All the CMC solutions tested had a shear rate with viscosity equal to 3000 s^{-1}. Silicone fluids present a wider range of viscosity (0.0046-29.250 Pa s), but they are Newtonian fluids and hydrophobic.

5.4 Wear experimentation methods

Extensive testing over its two years of use by Joyce (1997) and then during the course of this research, has allowed a standard testing procedure to be devised. This included steps to mount the component and use of a standard experimental protocol.

Prior to the commencement of a test, two XLPE prostheses were cleaned in acetone and weighed. The test prosthesis was then mounted on the phalangeal and metacarpal holder respectively, while the control prosthesis was placed in a small cage inside the lubricant bath and was loaded with a dead weight corresponding to 12.5N load. The heaters were switched on and the lubricant allowed to reach 37°C, before starting the test. At regular intervals, normally equivalent to 500,000 cycles, the test was stopped, the prosthetic components were removed, cleaned and weighed following Protocol A. Test and control samples were weighed to the nearest 0.1mg using a Mettler AE200 balance. Wear of the test components was defined as the weight loss with respect to the initial weight, to which any gain of the control components was added.

5.5 Friction experimentation methods

5.5.1 Mounting and elimination of misalignment errors

An experimental protocol was carefully devised to minimise misalignment of the bearing components in the simulator and the frictional torque errors that misalignments incur. In order to ensure that the centre of the metacarpal head (i.e. the centre of rotation of the prosthesis) was aligned with the centre of rotation of the motion mechanism, the assembled height of the metacarpal component was designed and set precisely. Furthermore the top end of the metacarpal component was manufactured with a square section in order to prevent rotation of the

component during the test and it was also marked with a pencil to ensure the same position to be maintained after every stop. The metacarpal holder was also mounted on the end of the swinging block slot so as to ensure the same position was maintained. Similarly, the position of the phalangeal cup was set to ensure alignment of the centre of rotation of the phalangeal component with the centre of rotation of motion.

5.5.2 Calibration of the load cell

Before starting the tests, it was necessary to calibrate both the load cell and the piezoelectric force transducer.
The load cell calibration consisted of two phases, a calibration with dead weights and a calibration using the pneumatic cylinder.

5.5.2.1 Calibration with dead weights

The pneumatic cylinder was removed from its position. The load cell was mounted on a special metacarpal holder in order to measure the load acting on the bearing surfaces and then attached to a strain gauge amplifier, which was connected to a XYT plotter. The plotter was calibrated to measure voltage by drawing reference lines at known voltages. The motor was switched off. Masses, that corresponded to an applied force from 0 N to 20 N, were put directly on the metacarpal holder. Each time another mass was added, the corresponding displacement was measured by the plotter. All the measurements were repeated at least five times. With these data it was possible to find a linear relationship (Fig. 5.3) between the applied load (N) and the measured displacement (mm):

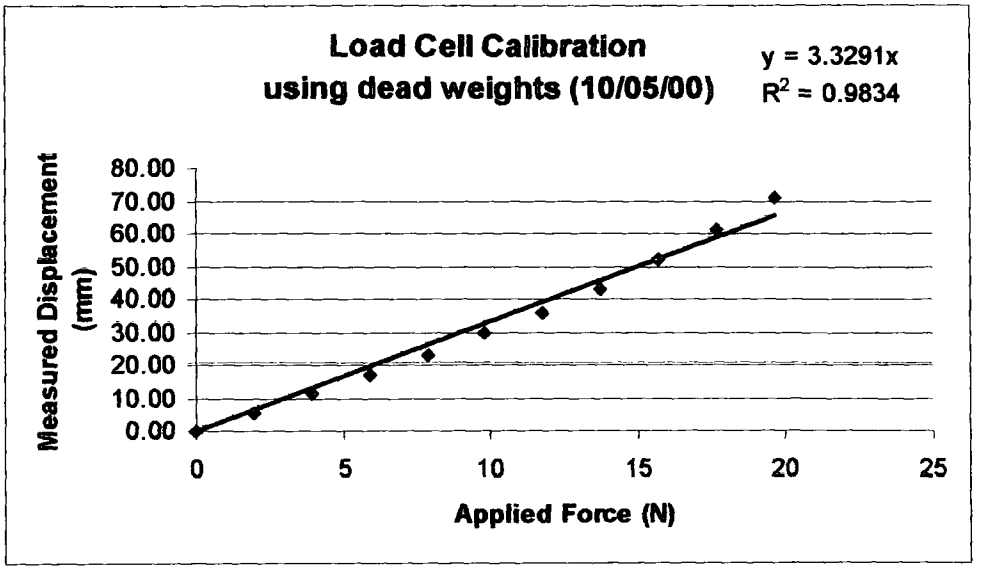

Fig. 5.2 Load Cell Calibration result (using dead weights)

Measured displacement (mm) = 3.3291 Applied load (N)

The correlation coefficient being R^2=0.9834.

The calibration protocol that was developed during this study is called "Protocol B" and is reported at the end of the chapter.

5.5.2.2 Calibration with the pneumatic cylinder

The pressure supply to the air bearings was switched on (upper bearings = 2 bar and lower bearings = 3 bar) and the strain gauge amplifier was connected to the XYT plotter. The motor was switched off and different pressures (from 0 to 4 bar) were applied to the pneumatic cylinder. For each pressure a trace was taken with the plotter. With the obtained values a graph was drawn (Fig. 5.4) to relate the applied pressure to the measured displacement:

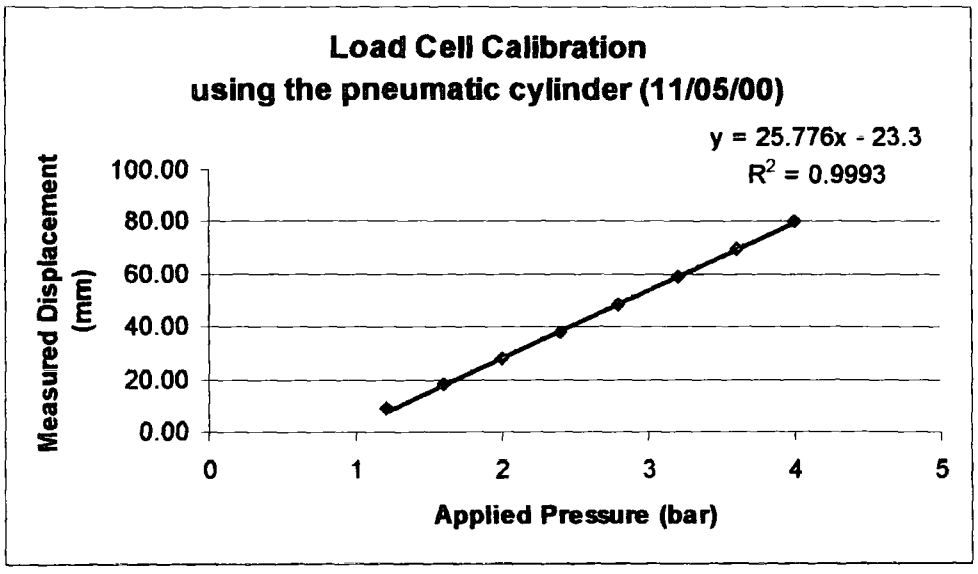

Fig. 5.3 Load Cell Calibration result (using the pneumatic cylinder)

Measured displacement (mm) = 25.776 Applied pressure (bar) – 23.3

It showed a linear characteristic with a very good correlation coefficient: R^2 = 0.9993.

After the two phases of the calibration it was possible to find the relations between the pressure (bar) and the load (N) that was applied on the metacarpal component:

Pressure (bar) = 0.1291 Load (N) + 0.9039
Load (N) = 7.7426 Pressure (bar) – 6.9988

The calibration protocol that was developed during this study is called "Protocol B" and is reported at the end of this chapter.

5.5.2.3 Piezoelectric force transducer calibration

A piezoelectric force transducer was attached to the lubricant bath and to the frictional-torque measuring carriage. It was used to measure the frictional torque that tried to rock the carriage when the metacarpal component swung on the phalangeal one. It was necessary to calibrate this before starting the experimentation.

For this purpose, a special plastic arm was manufactured and attached at the lubricant bath after having removed the metacarpal holder. Both the opposite ends of the plastic arm had a thread at the same distance (80mm) for hanging the dead weights. After having hung known masses to this thread, the corresponding traces were taken with the XYT plotter. In fact, the output signal of the transducer was amplified by a charge amplifier, which was connected to the plotter. After each trace, the masses were removed and the amplifier grounded before hanging a heavier mass. The piezoelectric transducer measures the forces by means of a crystal of quartz: when a force is applied, charges are created on the surfaces of the quartz crystal; if the transducer is not grounded, the charges accumulate and the next measurements are not accurate. The displacement of each trace from the traces at zero grams (i.e. zero Newton tangential force) was measured. By plotting the average displacement (mm) versus the force (N), a good linear relation was obtained (R^2 =0.9991):

Measured displacement (mm) = 1.3327 Applied torque (N mm) for the right part
Measured displacement (mm) = 1.4167 Applied torque (N mm) for the left part

which gave an average linear relation to use:

Measured displacement (mm) = 1.3747 Applied torque (N mm)

The setting data on the charge amplifier were:

Pressure: - upper bearings = 2 bar

- Lower bearings = 3 bar

Charge amplifier: filter = 300 kc/s

multipl. = 10

time constant = 1s

range = 1k

The calibration protocol that was developed during this study is called "Protocol C" and is reported at the end of this chapter.

In order to work out the magnitude of the masses to use in the calibration procedure, the torque acting on the 7.5mm radius size Durham prosthesis was calculated:

$M = L\ r\ f_f = 15N\ 7.5mm\ 0.4 = 45\ N\ mm = F\ b$

Where L is the applied load

R the radius of the prosthesis

f_f is the frictional torque

Thus, the torque on the bearing has to be equal to the torque measured from the piezoelectric transducer:

$M = = 45\ N\ mm = F\ b$

Where F is the gram-force required

b is distance between the centre of the bearing and the thread on the plastic arm

$$F = \frac{M}{b} = \frac{45N \cdot mm}{80mm} = 0.56N = 56g$$

5.5.3 Experimental protocol

During the design of the finger friction simulator, different modifications were made both in the lubricant bath and in the load transmission, therefore the calibration procedure was repeated each time. The lubricant bath was modified in order to be able to allow the 90° motion of swinging without the metacarpal holder impinging on it. The load transmission however, was changed because the first bearing arrangement had too many losses resulting in the incapability of the pneumatic cylinder to transmit the required load. Following the completion of all modifications, tests were started in order to establish the number of cycles of warm-up and testing which were necessary to reach a steady state friction value. A warm up of the friction simulator was recommended for 600 cycles prior to start testing. Then every 40 cycles, a trace was recorded with the XYT plotter and this procedure was repeated for at least three times to give consistency to the results.

Initial friction tests were run using a "standard" pair of biomaterials in order to compare the results with those reported in literature. Lubricants of different viscosities were used to obtain a Stribeck curve.

During these tests the phalangeal component was fixed in its mounting, paying attention that it was in the correct orientation. The metacarpal component was fixed in its holder and the holder carefully screwed to the swinging block adjusting its position and its height. The position was adjusted in order to precisely fit the phalangeal surface, while the height was adjusted to match the right centre of rotation. Then lubricant was added to the lubricant bath. The pressure to the air bearings and pneumatic cylinder was turned on and adjusted to give the appropriate applied load and pressure to each of the components. The position of the piezoelectric transducer was carefully checked and adjusted, allowing half a millimetre of clearance between each of the two screws which fixed it. The charge amplifier, the strain gauge amplifier and the XYT plotter were then switched on as well as the power on the DC motor. Then the simulator was run for 600 cycles and three traces, one every 40 cycles, were recorded with

the XYT plotter. The power to the motor, the plotter, the charge amplifier and the strain gauge amplifier were switched off as well as the pressure at the main filter regulator. The metacarpal and phalangeal component were then removed from their mounting and cleaned. The samples were cleaned in soap and water when water-based lubricants were used, and in isopropanol for oil-based lubricants. At this point a new test could be started, taking care to ground both the charge amplifier and the XYT plotter. The procedure was then repeated at least for a further two times for each viscosity lubricant. It was decided to conduct each series of tests under any set of conditions for at least three times to ensure the consistency of the results. The procedure applied during the friction tests is summarised in Protocol D.

5.6 Analysis of the wear results

Test and control samples were weighed to the nearest 0.1mg using a Mettler AE200 balance. Wear of the test components was defined as the weight loss with respect to the initial weight, to which any gain of the control components was added. The weight loss was calculated with this simple relationship:

$$\Delta w = w_o - w_i + \Delta w_c$$

where :

Δw = change in weight of the sample ($\Delta w>0$ for weight loss);

Δw_c = change in weight of the control sample ($\Delta w_c>0$ for weight gained);

w_o = initial weight of the sample;

w_i = actual weight of the sample (during the control).

The graphics obtained show the volume loss versus the number of cycles. The volume loss was calculated in this way:

$$V = \frac{\Delta w}{\rho}$$

$[V] = [mm^3]$

where:

Δw is the weight loss;

ρ is the density of cross-linked polyethylene

$$\rho = 949 kg/m^3 = 949 \cdot 10^3 g/10^9 mm^3 = 949 \cdot 10^{-6} g/mm^3$$

5.7 Analysis of the friction results

During the friction tests the outputs of the piezoelectric transducer which were recorded on the XYT plotter had the typical trace shown in figure 5.5. The horizontal central line was drawn when the swinging block was perfectly vertical, at 0°. The amplitude of the movement was ± 45°. For each cycle, the full displacement was measured to an accuracy of ± 0.5 mm. The data were then entered into an Excel spreadsheet and using the recorded calibration coefficients, the measured displacement of the load cell and force transducer converted into values of friction factor f.

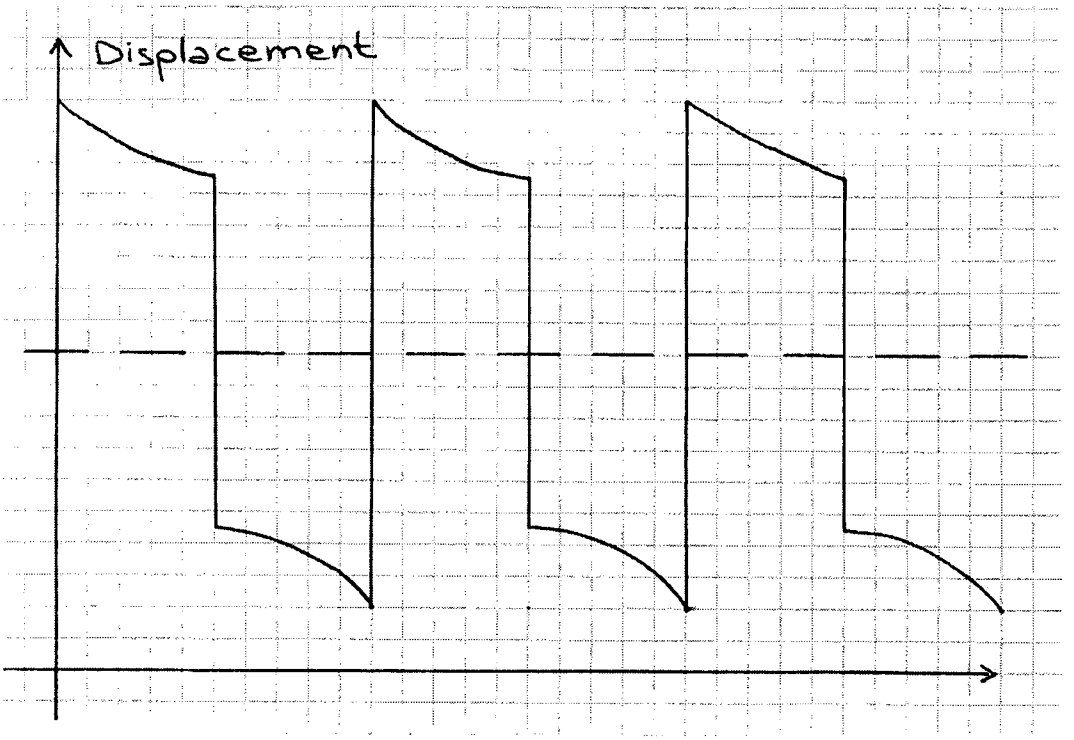

Fig. 5.4 Typical friction trace recorded on the XYT plotter

The output of the piezoelectric transducer which is recorded on the XYT plotter represents twice the measured displacement. Therefore the piezoelectric calibration equation gives a measure of the applied torque:

Measured displacement (mm) = 1.3747 Applied torque (N mm)

Thus it is very easy to calculate the friction factor as it is defined as:

$$f = \frac{T}{r \cdot L}$$

where T is the applied torque, r is the radius of the metacarpal head and L is the load applied to the prostheses which is calculated by the calibration equation of the load cell using the pneumatic cylinder. The importance of using the friction factor instead of the coefficient of friction was underlined by Unsworth (1978).

The study clarified that the pressure distribution in hip joints is unknown and therefore the coefficient of friction is not the best parameter to characterise their frictional properties.

In order to determine which mode of lubrication is present during testing, a useful tool is the Stribeck curve. This curve is defined as the graph where the friction factor, f, is plotted against an non dimensional parameter, the Sommerfeld parameter, Z, defined as:

$$Z = \frac{\eta \cdot u \cdot r}{L}$$

where η is the lubricant viscosity, u is the entraining velocity and L is the applied load.

A definition of entraining velocity is given. When two bodies slide with relative velocities v_1 and v_2, respectively, the entraining velocity is defined as:

$$u = \frac{v_1 + v_2}{2}$$

Since the phalangeal component was still, the entraining velocity used to calculate the Sommerfeld parameter was half the velocity of the metacarpal, i.e. $u = \frac{v_{max}}{2}$.

The entraining velocity, u, was not constant, but it changed while the metacarpal component was sliding on the phalangeal one. The sliding velocity was zero when the metacarpal was at ± 45°, reached its maximum value in the middle of the stroke, and then dropped to zero again. The maximum value of the sliding velocity, v_{max}, was considered in the calculation of the entraining velocity. This is given by the formula:

$$u = \frac{\pi \cdot r \cdot v}{2}$$

where r is the radius of the metacarpal head and ν is the frequency of oscillation (0.5 Hz).

For each test at different viscosity, the Sommerfeld parameter, Z, was calculated. The measured friction factor, f, was then plotted against the Sommerfeld number to obtain a Stribeck curve which was used to define the operating lubrication regime of the bearing. As the viscosity varies with the shear rate, all the experiment done in this thesis were tested at a shear rate value of 3000 s^{-1}.

PROTOCOL A

Weighing Procedure for the wear simulator

Remove the test and control prostheses from the rig by the following procedure, wearing gloves and a lab coat to minimise health risks from the lubricant (if bovine serum):

1. Stop the test, by switching off the electrical supply, heating supply and compressed air supply.
2. Record the relevant test information on the test data record sheet.
3. Remove the thermocouple.
4. Disconnect the two blue heating wires at the ceramic block.
5. Disconnect the two air pipes to the "thumb" cylinder.
6. Release and remove the two M4 wing nuts.
7. Carefully remove the "black" lid on the test bath, sliding it along the heating wires.
8. Slide the entire simulator forward, holding the test bath, until the test bath is clear of the table. The test bath, still being held, can then be removed by guiding it vertically downwards clear of the table.
9. Remove the two split pins from the phalangeal clamp, therefore permitting access to and the removal of the test phalangeal component.
10. Remove the metacarpal test component. If additional access is required then remove the arc piece.

11. Remove the control prosthesis from the hole in the "moon piece" spacer.

Now, with the two prostheses removed:

12. Rinse the prostheses under tap water, being careful not to mix test and control components.
13. Separately, place each prosthesis in the ultrasonic bath and wash for five minutes.
14. Remove the prosthesis and dry with lint free tissue.
15. Wash prosthetic components in acetone.
16. Allow 2 minutes to dry in air, then weigh to the nearest 0.1mg, using the Mettler AE200 balance, taking three readings for each component. Record the results on the test data record sheet.

The prostheses having been weighed, proceed as follows:

17. Replace the control prosthesis.
18. Replace the test prosthesis. Ensure that the phalangeal component is inserted in the correct orientation (moulding mark on extensor side).
19. Reassemble the test bath assembly in the reverse order given above. Check that the lid is correctly fitted and that motion of the test prosthesis on the bath is "free".
20. Switch on the compressed air, 24V supply and 5V supply.
21. Recommence testing. Not forgetting to refit the thermocouple.

PROTOCOL B

B.1 Calibration of the load cell using dead weights

1. Remove the pneumatic cylinder and its mounting.
2. Fix the phalangeal component in the phalangeal holder.
3. Screw the load cell on the special metacarpal holder, taking care not to damage it.
4. Mount the metacarpal component in its holder.
5. Connect the load cell to the strain gauge amplifier and the amplifier to the XYT plotter.

6. Switch the strain gauge amplifier on and let it warm up for about 20 minutes.
7. Switch on the XYT plotter.
8. Record, on the plotter, the Y-displacement correspondent to no weight.
9. Add known masses directly on the metacarpal holder, recording the Y-displacement after each adding.
10. After having reached a displacement correspondent to 2 kg (19.62N load), remove the masses one by one, recording the displacement each time.
11. Repeat the last two steps at least five times.
12. Plot the measured displacement (mm) versus the applied load (N) and find their linear relation.

B.2 Calibration of the load cell using the pneumatic cylinder

1. Replace the pneumatic cylinder, screwing its lower end to the load cell.
2. Connect the pneumatic cylinder with the air supply.
3. Turn the main air supply on and let the pressure stabilise at 4 bar.
4. Adjust the air bearings pressure knob to reach 2 bar in the upper bearings and 3 bar in the side bearings.
5. Switch on the XYT plotter and adjust its sensitivity (0.2 V).
6. Connect the load cell to the strain gauge amplifier and the amplifier to the plotter.
7. Record, on the plotter, the Y-displacement correspondent to no pressure.
8. Apply a known pressure to the cylinder and record a trace on the plotter.
9. Increase the pressure and repeat the previous step.
10. Repeat the last two steps until you reach the maximum pressure that the load cell can support without damaging (4 bar)
11. Repeat steps 8 to 5 five times to assure consistency of the measurements.
12. Plot the measured displacement (mm) versus the applied pressure (bar) and find their linear relation.

Combine the two equations found in the previous phases to relate the pressure in the pneumatic cylinder to the load applied to the joint.

PROTOCOL C

Calibration of the piezoelectric force transducer

1. Mount the piezoelectric force transducer on the frictional-torque measuring carriage and screw its other end to the lubricant bath taking care of leaving half mm of clearance in each side.
2. Attach the piezoelectric force transducer to the charge amplifier and the amplifier to the XYT plotter.
3. Switch the charge amplifier and the plotter on and let them warm up for approximately 20 minutes.
4. Turn the main air supply on and regulate the knobs to get the following values:
   - upper bearings: 2 bar
   - lower bearings: 3 bar
5. Take the metacarpal holder off.
6. Screw the plastic lever on the lubricant bath, taking care to equally distribute its weight (two arms of the same length from both sides)
7. Choose a plotter sensitivity and adjust the zero of the plotter.
8. Zero the charge amplifier by switching the ground lever on and off.
9. Draw a short trace with the plotter that corresponds to a zero Newton tangential force.
10. Hang a mass on the thread fixed on the right side of the plastic lever and record a trace with the plotter. Then remove the mass.
11. Repeat the last three steps, using increasing masses.
12. Repeat steps 8 to 11 five times to assure the consistency of the measurements.
13. Repeat steps 7 to 12 with different plotter sensitivities.
14. For each sensitivity measure the displacements (mm) and plot them versus the applied tangential force (N).

PROTOCOL D

Finger friction simulator experimental protocol

1. Mount the phalangeal component in the lubricant bath and fix it in place with a grub screw.
2. Mount the metacarpal component in its holder and the holder in the swinging slot, fixing it in place with a nut. Check the vertical height and subsequently the horizontal alignment and adjust if necessary by adding spacers.
3. Try the free sliding and the perfect coupling between the two surfaces. Add lubricant in the lubricant bath.
4. Switch on the pressure at the main filter regulator, the strain gauge amplifier, the charge amplifier and the X-Y plotter. Check the plotter noise and adjust the air bearings pressure to optimise the reading.
5. Fix the pressure to the pneumatic cylinder in order to achieve the load required.
6. Switch on the power on the DC motor and check that the alignment is maintained during the 90° swinging.
7. Run the finger friction simulator for 600 warm-up cycles and take three traces, one every 40 cycles, with the XYT plotter.
8. Remove both components and clean them with soap and water (water-based lubricants) or isopropanol (oil-based lubricants). Dry using a lint-free tissue.
9. Replace the component in position and add new lubricant.
10. Zero the charge amplifier and the XYT plotter.
11. Repeat the test again recording 3 traces, one every 40 cycles, for every viscosity lubricant.

6 Results

6.1 Wear tests results

Several wear tests were undertaken in order to evaluate further the wear behaviour of XLPE when sliding against itself. Two tests were undertaken using non-irradiated Durham XLPE prostheses and were run in distilled water for over 14 million cycles which, at a rate of one million cycles per annum, was equivalent to 14 years in vivo. The tests employed 7.5 mm and 8.5 mm radius production samples of 1.5 mm thickness. These production samples also had square section stems and a percentage of gel content equal to 74% minimum. The density of XLPE was taken to be 949 kg/m^3. Allowing for an error of $\pm$ 1×10^{-4}g in weight measurement, based on the accuracy of the Mettler balance, for each of the control and test samples gave a total error of $\pm$ 2×10^{-4}g for each prosthetic component. Tab. 6.1 summarises the results of the two wear tests.

Test Number	1	2
Material	**XLPE**	**XLPE**
Irradiation Age	**Non-irradiated**	**Non-irradiated**
Dynamic Load (N)	**12.5**	**12.5**
Prosthesis Radius (mm)	**7.5**	**8.5**
Lubricant	**Distilled Water**	**Distilled Water**
Sliding Distance (km)	**342**	**375**
Mean K Metacarpal Component (10^{-6} mm^3/Nm)	**0.316**	**0.318**
Mean K Phalangeal Component (10^{-6} mm^3/Nm)	**0.077**	**0.085**
Mean K (10^{-6} mm^3/Nm)	**0.393**	**0.403**

Tab. 6.1 Wear tests results on non-irradiated XLPE prostheses

The prostheses were of two different sizes:

R=7.5mm

NON-IRRADIATED XLPE rubbing against itself

in DISTILLED WATER

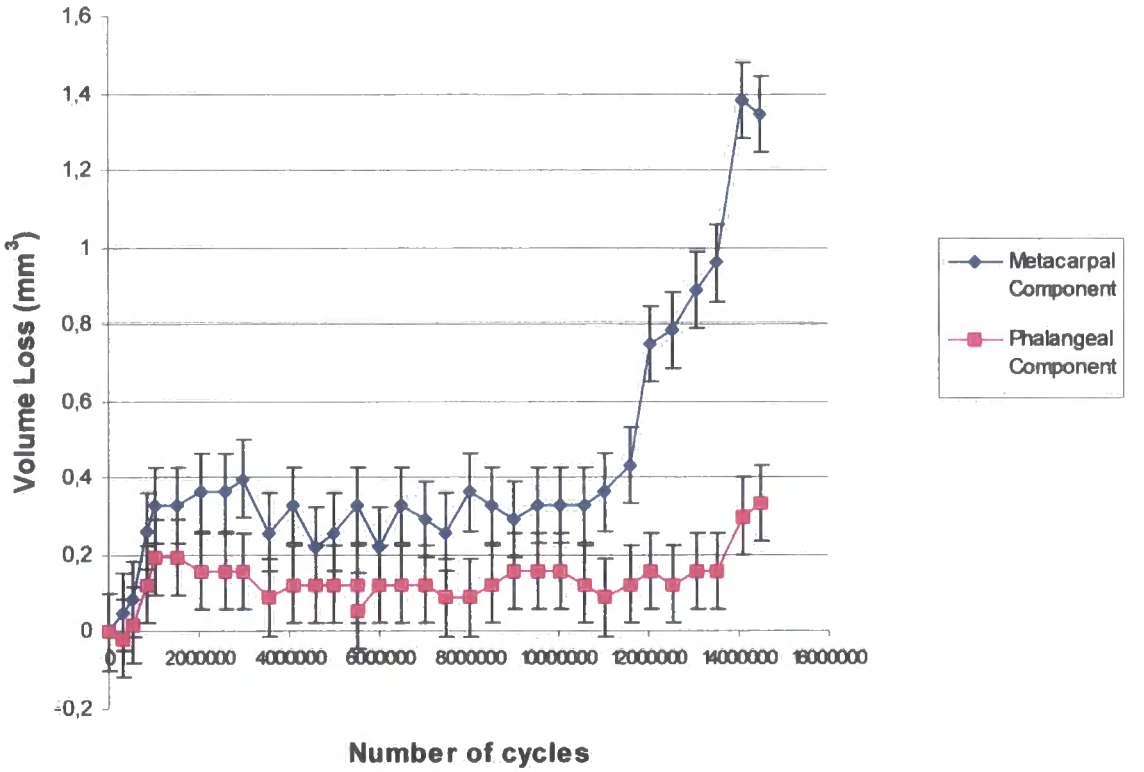

Fig. 6.1

Fig. 6.1 shows that in this test the wear behaviour of both the metacarpal and the phalangeal components can be divided into three regions characterised by different wear factors. For the metacarpal component the wear factors were 1.09 x 10^{-6} mm^3/Nm for the first 24.15 km indicating the wearing-in portion, 0.001 x 10^{-6} mm^3/Nm between 24.15-259.42 km for the steady state region and a rise to 0.96 x 10^{-6} mm^3/Nm between 259.42-341.78 km. For the phalangeal component the wear factors were 0.63 x 10^{-6} mm^3/Nm for the first 24.15 km indicating the

wearing-in portion, -0.008 x 10^{-6} mm^3/Nm between 24.15-318.10 km for the steady state region and a rise to 0.574 x 10^{-6} mm^3/Nm between 318.10-341.78 km. It can clearly be noticed that the metacarpal component wears more than the phalangeal one.

Weight Change (in $n \times 10^{-4}$ g)

XLPE vs XLPE

Load: 12.5 N

Lubricant: Distilled Water

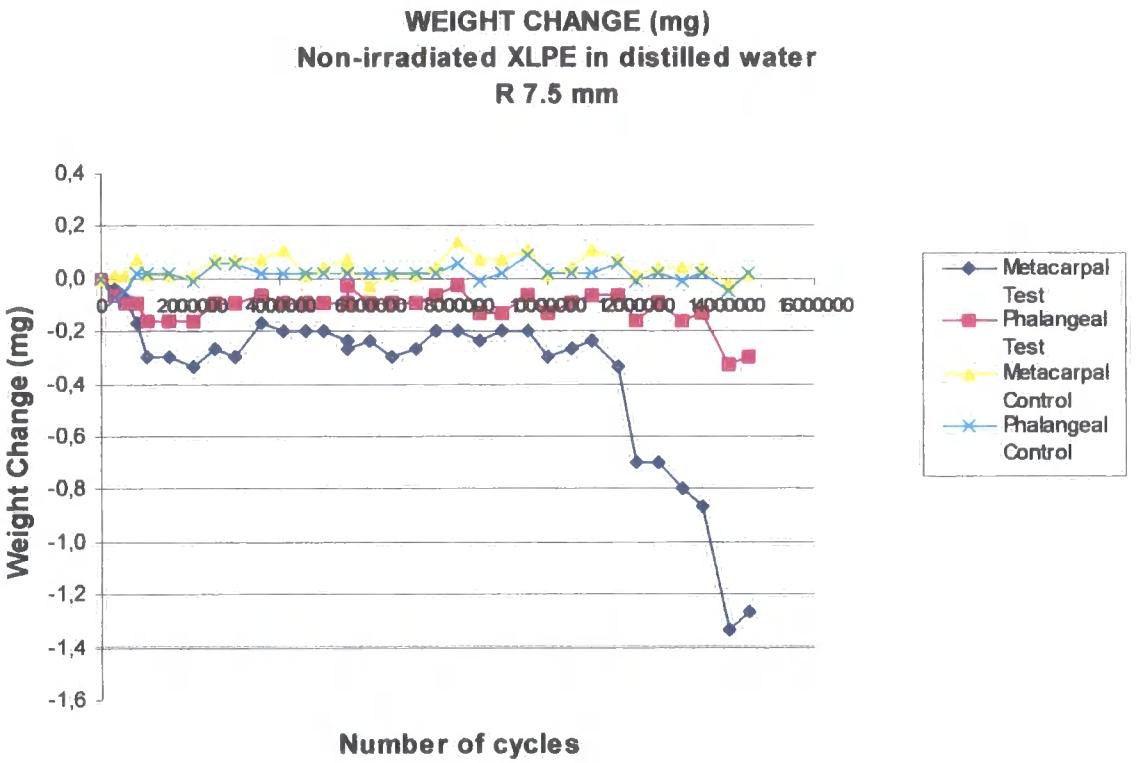

Fig. 6.2

Fig. 6.2 shows the weight change of the samples test and component during the test. The metacarpal test lost only 0.3 mg after 12 million cycles, but the loss reached 1.3 mg at 14.5 million cycles. The % of increasing weight was zero for both the metacarpal and the phalangeal control.

R=8.5mm

NON-IRRADIATED XLPE rubbing against itself

in DISTILLED WATER

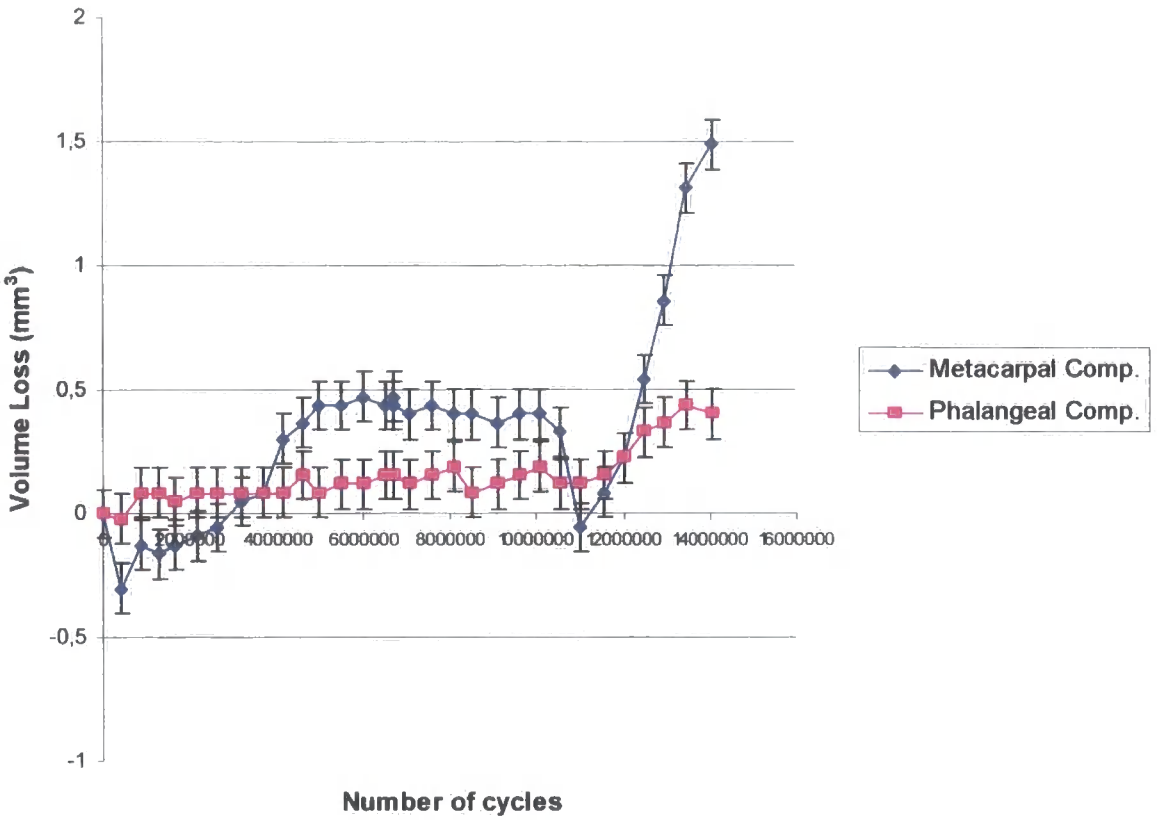

Fig. 6.3

Fig. 6.3 shows that the wear behaviour of the metacarpal component can be divided into three regions characterised by different wear factors: 0.257 x 10^{-6} mm^3/Nm for the first 133.88 km, -0.054 x 10^{-6} mm^3/Nm between 133.88-281.13 km for the steady state region and a rise to 1.533 x 10^{-6} mm^3/Nm between 294.22-374.94 km. For the phalangeal component, only two regions were observed where the wear factors were 0.039 x 10^{-6} mm^3/Nm for the first 308.55 km and an ending rise to 0.301 x 10^{-6} mm^3/Nm between 308.55-374.94 km. The metacarpal component wore more than the phalangeal one, especially after 12 million cycles.

Weight Change (in $n \times 10^{-4}$ g)

XLPE vs XLPE

Load: 12.5 N

Lubricant: Distilled Water

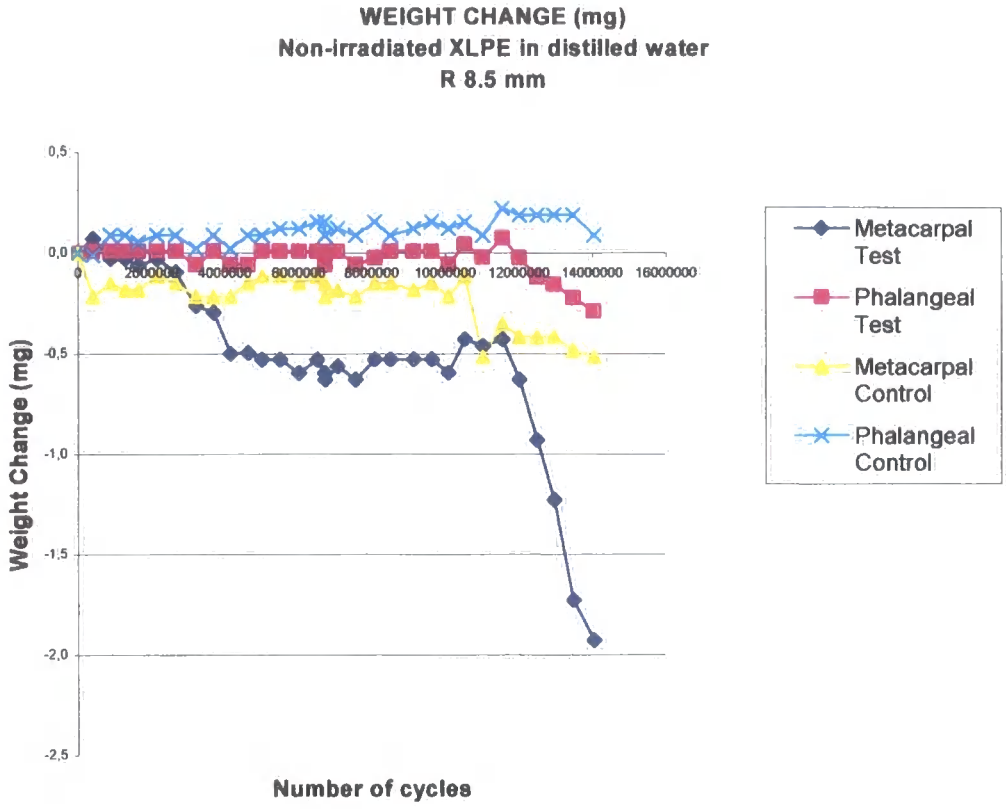

Fig. 6.4

Fig. 6.4 shows the weight change of the samples test and component during the test. The metacarpal and the phalangeal test lost only 0.5 mg and 0.1 mg respectively after 12 million cycles, but the loss reached 1.9 mg and 0.3 mg respectively at 14 million cycles. The % of increasing weight was 4.3 for the phalangeal control, while the metacarpal control lost weight (0.5 mg).

One test was undertaken using gamma-irradiated Durham XLPE prostheses in Ringers solution. The percentage of gel content was equal to 87%. The

One test was undertaken using gamma-irradiated Durham XLPE prostheses in Ringers solution. The percentage of gel content was equal to 87%. The metacarpoglenoidal arm was removed from the rig to simulate what happens during the Swanson's prosthesis implantation. The test employed 9.4 mm radius sample and was run for over 8 million cycles without any fractures or cuts.

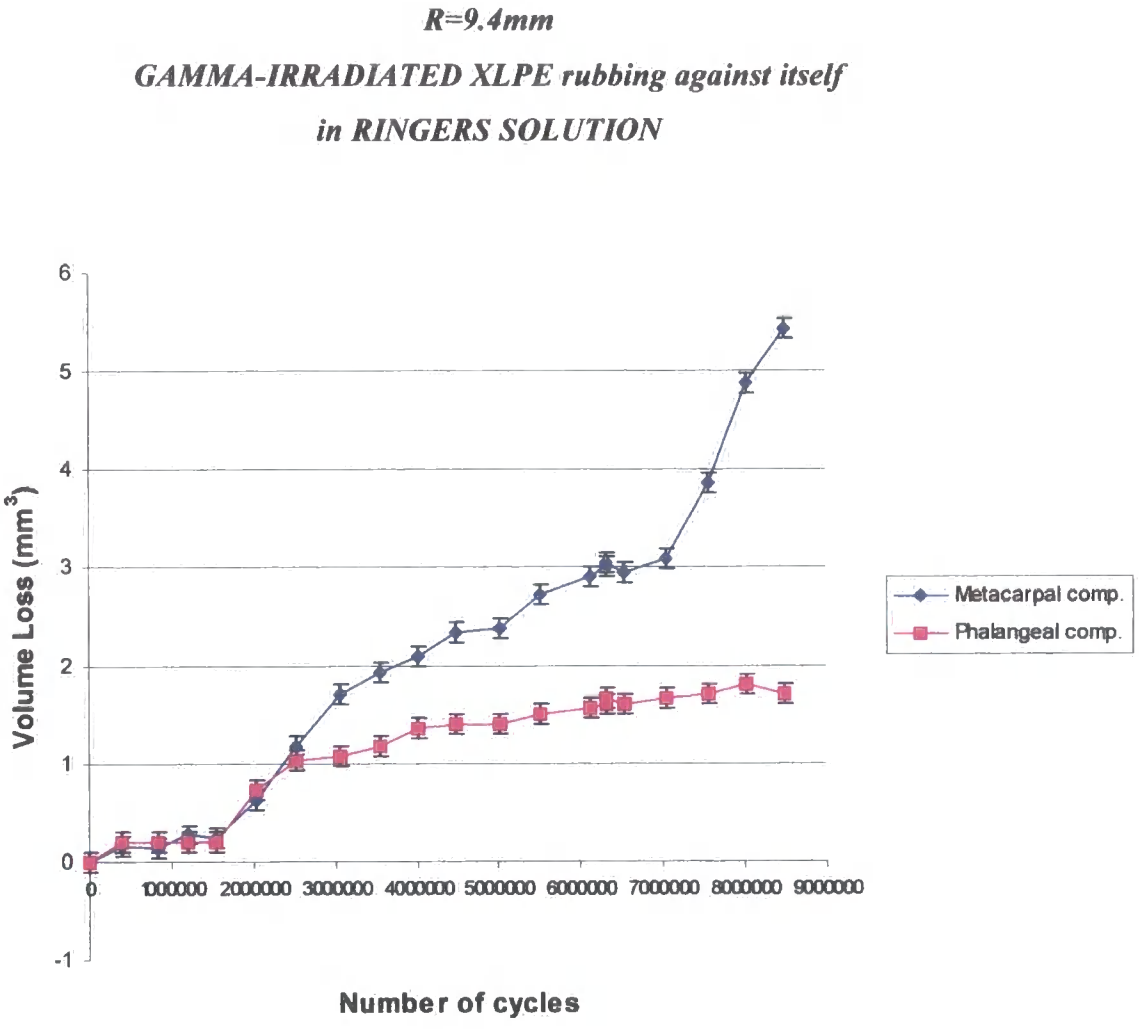

Fig. 6.5

The test result shown in fig. 6.5 shows that the prosthesis worked for the whole length of the test without fracturing even if the metacarpoglenoidal arm was removed. The overall wear factor was equal to 1.74 x 10^{-6} mm^3/Nm for the metacarpal component and 0.55 x 10^{-6} mm^3/Nm for the phalangeal one. Once again the wear behaviour of both the metacarpal and the phalangeal components

can be divided into three regions characterised by different wear factors. For the metacarpal component the wear factors were 0.35 x 10^{-6} mm^3/Nm for the first 45.24 km, 1.41 x 10^{-6} mm^3/Nm between 45.24-208.32 km and a rise to 4.47 x 10^{-6} mm^3/Nm between 208.32-250.59 km. For the phalangeal component the wear factors were 0.35 x 10^{-6} mm^3/Nm for the first 45.24 km, 2.32 x 10^{-6} mm^3/Nm between 45.24-74.21 km and 0.30 x 10^{-6} mm^3/Nm between 74.21-250.59 km. Starting from 2,500,000 cycles until the end, the metacarpal component wore more than the phalangeal one.

Weight Change (in n×10^{-4} g)

XLPE vs XLPE

Load: 12.5 N

Lubricant: Ringers Solution

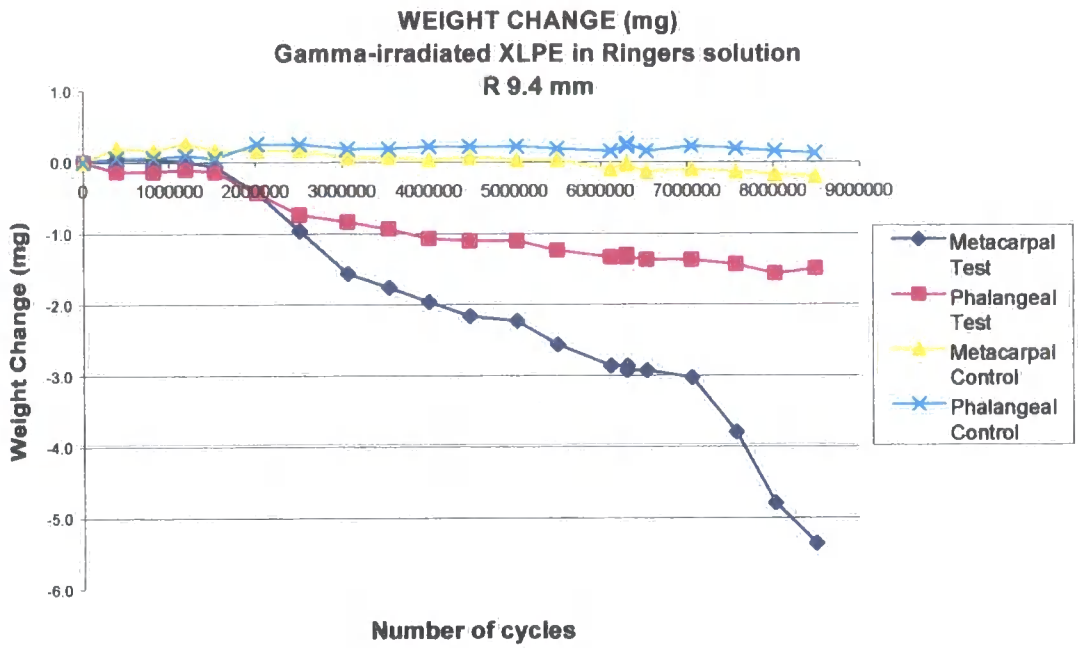

Fig. 6.6

Fig. 6.6 shows the weight change of the samples test and component during the test. The metacarpal and the phalangeal test started loosing weight at 2 million cycles and the loss reached 5.4 mg and 1.5 mg respectively at 8.5 million cycles.

The % of increasing weight was 0.09 for the phalangeal control, while the metacarpal control lost weight (0.2 mg).

In order to evaluate the influence of motion on the wear behaviour of XLPE rubbing against itself, two tests were run dry using 9.4mm radius Durham prostheses with a percentage of gel content of 76% minimum. One test was run using the wear simulator while the other test was run using a special simulator which added a twist of ± 10° to the normal flexion-extension movement. This simulated the rotation movement of the prosthesis around its centre. Table 6.8 summarises the results of the two dry tests.

Test Number	4	5
Material	**XLPE**	**XLPE**
Irradiation Age	**Gamma-irradiated**	**Gamma-irradiated**
Load (N)	**12.5**	**12.5**
Motion	**Flex-Ext**	**Flex-Ext + Rot**
Lubricant	**Dry**	**Dry**
Sliding Distance (km)	**94**	**86**
Mean K Metacarpal Component (10^{-6} mm^3/Nm)	**4.25**	**3.29**
Mean K Phalangeal Component (10^{-6} mm^3/Nm)	**1.70**	**3.25**
Mean K (10^{-6} mm^3/Nm)	**5.95**	**6.54**

Tab. 6.2 Wear tests results on gamma-irradiated XLPE prostheses

R = 9.4 mm

GAMMA-IRRADIATED XLPE rubbing against itself

Tested DRY at FLEX.-EXT. only

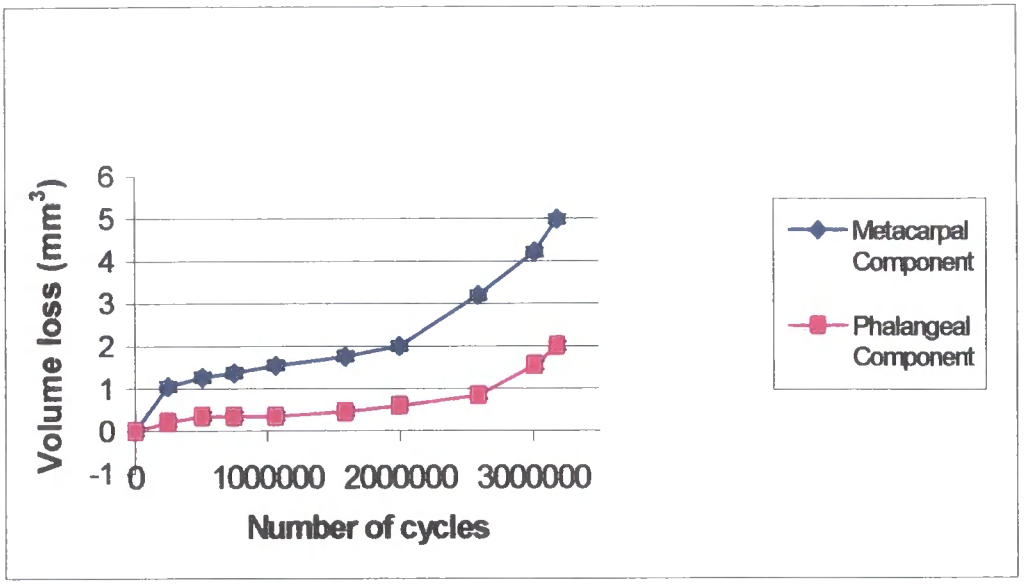

Fig. 6.7

The wear behaviour of the metacarpal component can be divided into three regions characterised by different wear factors: 11.56 x 10^{-6} mm^3/Nm for the first 7.27 km indicating the wearing-in portion, 3.10 x 10^{-6} mm^3/Nm between 7.27-58.87 km for the steady state region and a rise to 11.38 x 10^{-6} mm^3/Nm between 58.87-93.95 km. For the phalangeal component the wear factors were 0.88 x 10^{-6} mm^3/Nm for the first 76.37 km and a rise to 9.10 x 10^{-6} mm^3/Nm between 76.37-93.95 km. At any point during the test, the metacarpal component wore more than the phalangeal one.

R = 9.4 mm

GAMMA-IRRADIATED XLPE rubbing against itself

Tested DRY at FLEX.-EXT. + ROTATION

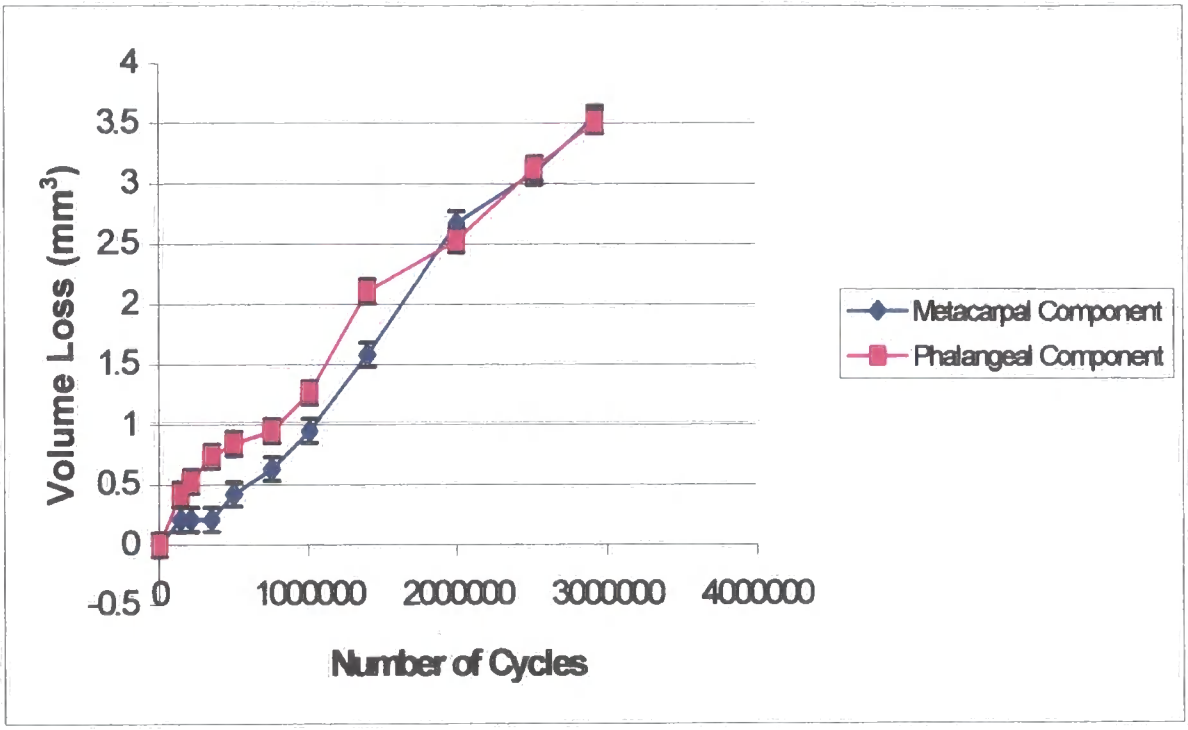

Fig. 6.8

In this case both the metacarpal and the phalangeal components wore at a similar rate during the test. The average wear factors being: 3.29×10^{-6} mm^3/Nm for the metacarpal component and 3.25×10^{-6} mm^3/Nm for the phalangeal one. In contrast to all the other previous tests, the metacarpal component wore less than the phalangeal one for almost all the test.

To evaluate the influence of sterilisation on the wear behaviour of XLPE while sliding against itself, four ethylene-sterilised Durham prostheses were tested: two in bovine serum and two in distilled water. The use of ethylene oxide allows a non-invasive sterilisation process which prevents the re-formation of free radicals (Chiesa et al., 2000). Therefore its influence on the wear behaviour of XLPE rubbing against itself has been investigated. Table 6.13 summarises the results of the four tests.

Test Number	6	7	8	9
Material	**XLPE**	**XLPE**	**XLPE**	**XLPE**
Irradiation Age	**EtO-sterilised**	**EtO-sterilised**	**EtO-sterilised**	**EtO-sterilised**
Load (N)	**12.5**	**12.5**	**12.5**	**12.5**
Radius (mm)	**7.5**	**8.5**	**7.5**	**8.5**
Lubricant	**D. Water**	**D. Water**	**B. Serum**	**B. Serum**
Sliding Distance (km)	**118**	**136**	**88**	**80**
Total K Metacarpal component (10^{-6} mm^3/Nm)	**1.52**	**3.00**	**0.25**	**0.35**
Total K Phalangeal component (10^{-6} mm^3/Nm)	**0.74**	**1.46**	**0.23**	**- 0.32**
Total K (10^{-6} mm^3/Nm)	**2.26**	**4.46**	**0.48**	**0.03**

Tab. 6.3 Wear tests results on EtO-sterilised XLPE prostheses

R=7.5mm

EtO-IRRADIATED XLPE PROSTHESIS rubbing against itself in DISTILLED WATER

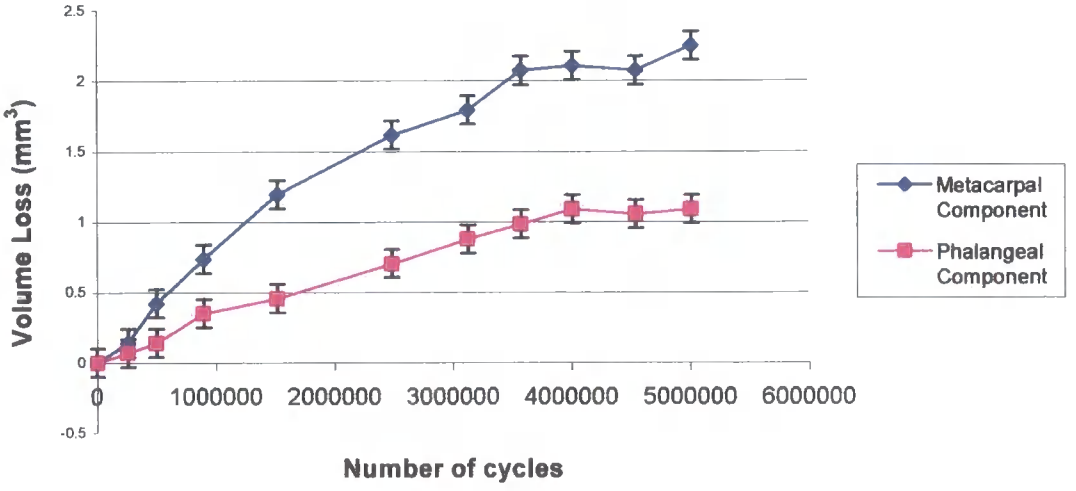

Fig. 6.9

For the 7.5mm radius EtO-sterilised Durham prosthesis, the overall wear factor was 1.52 x 10^{-6} mm^3/Nm for the metacarpal component and 0.74 x 10^{-6} mm^3/Nm for the phalangeal one. Therefore the metacarpal component wore at twice the rate of the phalangeal one. For both the components, the wear curve can be divided in two regions characterised by different wear factors. For the first 84.25 km, the metacarpal wear factor was equal to 1.97 x 10^{-6} mm^3/Nm, while the phalangeal wear factor was 0.93 x 10^{-6} mm^3/Nm, indicating the wearing-in portion. The second region, between 84.25-118.01 km, gives a wear factor of 0.43 x 10^{-6} mm^3/Nm for the metacarpal component and a wear factor of 0.26 x 10^{-6} mm^3/Nm for the phalangeal one.

Weight Change (in $n \times 10^{-4}$ g)

XLPE vs XLPE

Load: 12.5 N

Lubricant: Distilled Water

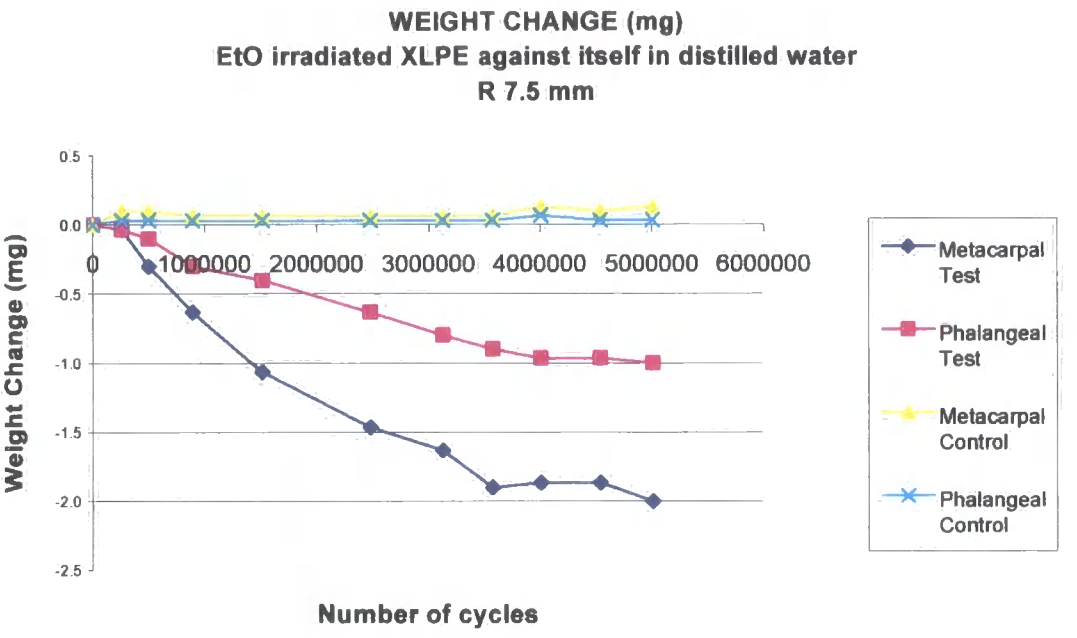

Fig. 6.10

Fig. 6.10 shows the weight change of the samples test and component during the test. The metacarpal and the phalangeal test lost respectively 2.0 mg and 1.0 mg after 5 million cycles. The % of increasing weight was: 0.05 for the metacarpal component and zero for the phalangeal one.

R=8.5mm

EtO-IRRADIATED XLPE PROSTHESIS rubbing against itself in DISTILLED WATER

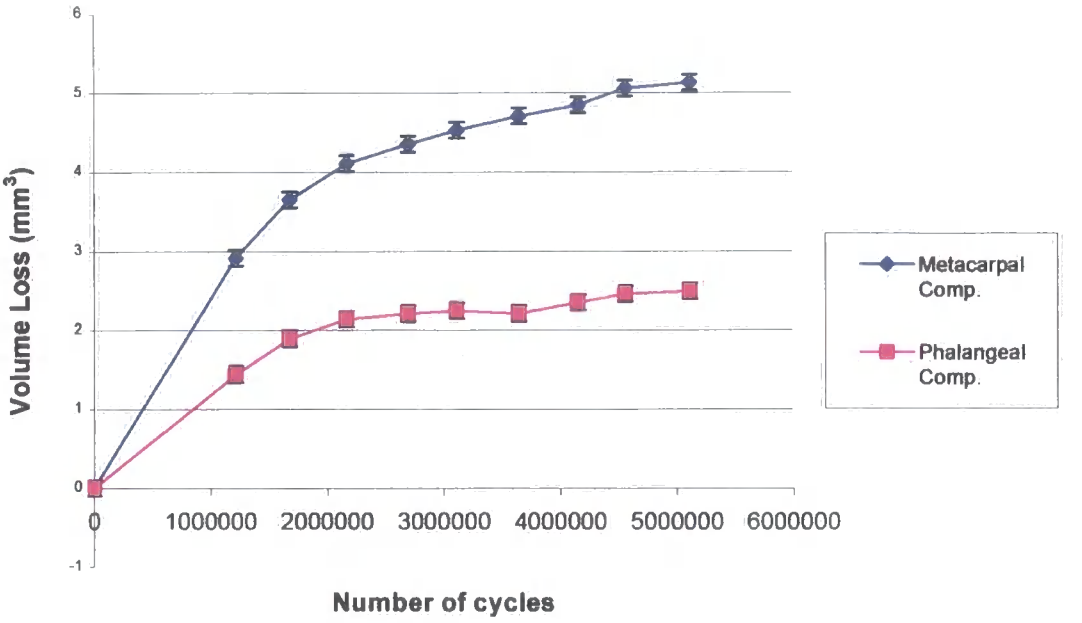

Fig. 6.11

The 8.5mm radius EtO-sterilised Durham prosthesis wore a lot more than the 7.5mm radius one. The overall wear factor was 3.00 x 10^{-6} mm^3/Nm for the metacarpal component and 1.46 x 10^{-6} mm^3/Nm for the phalangeal one. Once again the metacarpal component wore more than twice the phalangeal one. For both components, the wear curve can be divided in two regions characterised by different wear factors. For the first 44.84 km, the metacarpal wear factor was equal to 6.51 x 10^{-6} mm^3/Nm, while the phalangeal wear factor was 3.39 x 10^{-6} mm^3/Nm, indicating the wearing-in portion. The second region, between 44.84-136.46 km, gives a wear factor of 1.29 x 10^{-6} mm^3/Nm for the metacarpal component and a wear factor of 0.51 x 10^{-6} mm^3/Nm for the phalangeal one.

Weight Change (in $n \times 10^{-4}$ g)

XLPE vs XLPE

Load: 12.5 N

Lubricant: Distilled Water

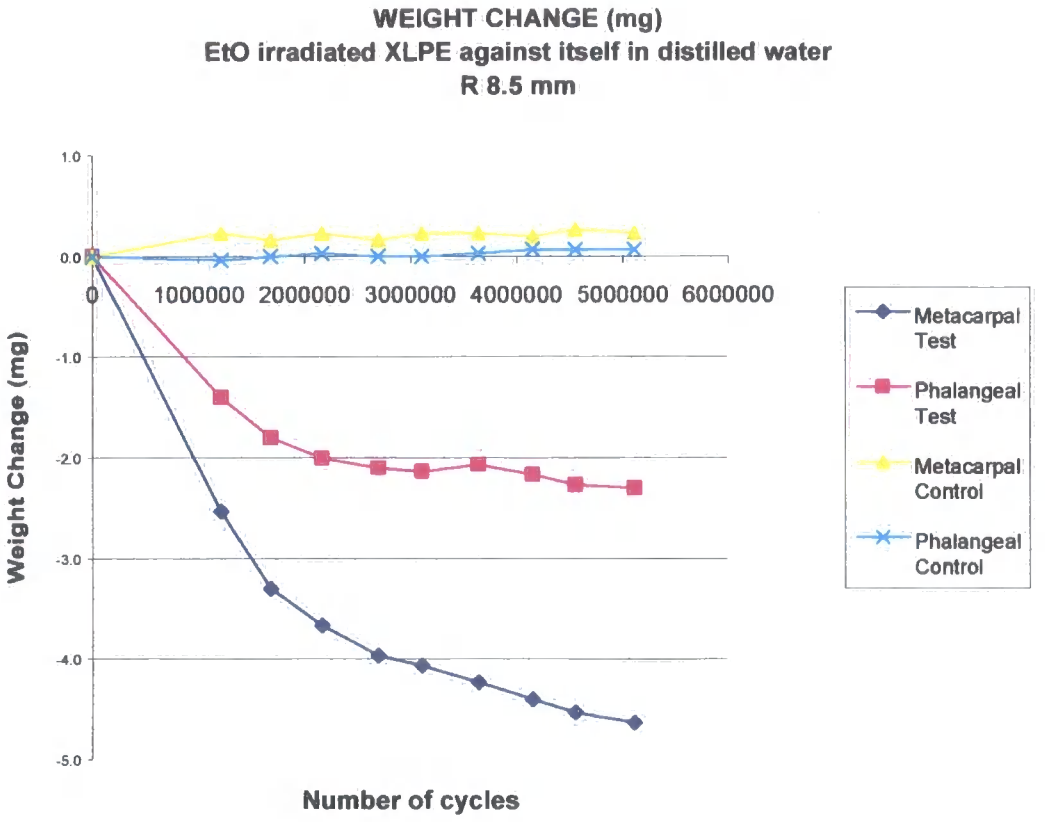

Fig. 6.12

Fig. 6.12 shows the weight change of the samples test and component during the test. The metacarpal and the phalangeal test lost 2.5 mg and 1.4 mg respectively just after 1 million cycles, reaching a loss of 4.6 mg and 2.3 mg respectively at the end of the test (5 million cycles). The % of increasing weight was: 0.06 for the metacarpal control and 0.04 for the phalangeal control.

R=7.5mm

EtO-IRRADIATED XLPE PROSTHESIS rubbing against itself in BOVINE SERUM

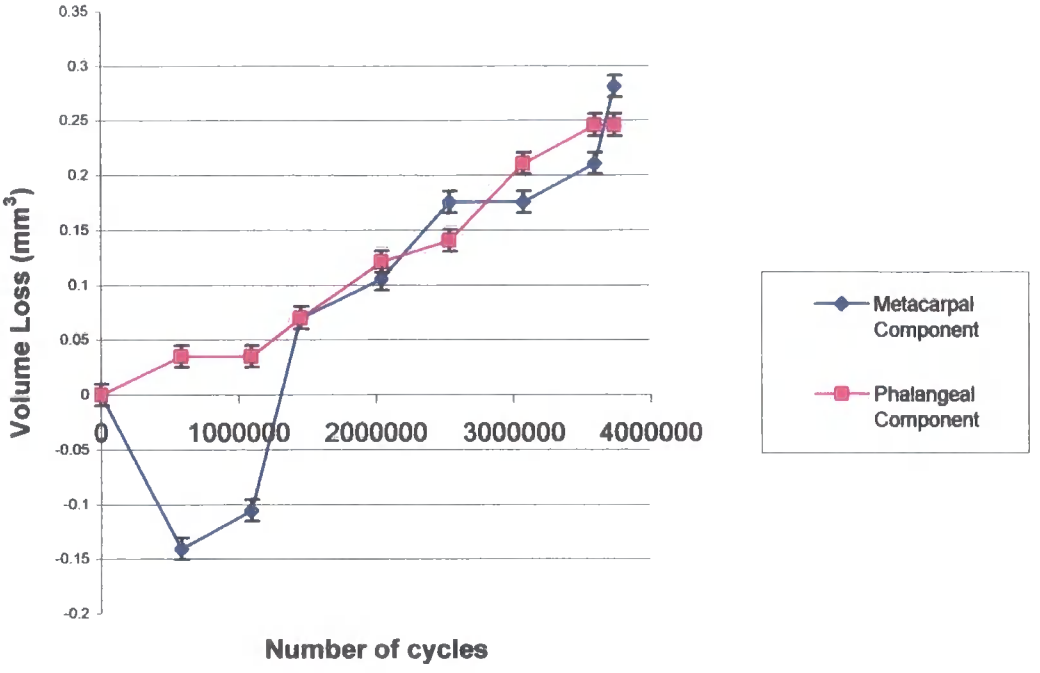

Fig. 6.13

For the 7.5mm radius EtO-sterilised Durham prosthesis tested in bovine serum, the overall wear factor was 0.25 x 10^{-6} mm^3/Nm for the metacarpal component and 0.23 x 10^{-6} mm^3/Nm for the phalangeal one. Therefore the wear rate of both the metacarpal and the phalangeal components were similar. While the phalangeal component started losing weight from the beginning, the metacarpal component gained weight until 1.5 million cycles, when then started loosing weight too.

Weight Change (in $n \times 10^{-4}$ g)

XLPE vs XLPE

Load: 12.5 N

Lubricant: Bovine Serum

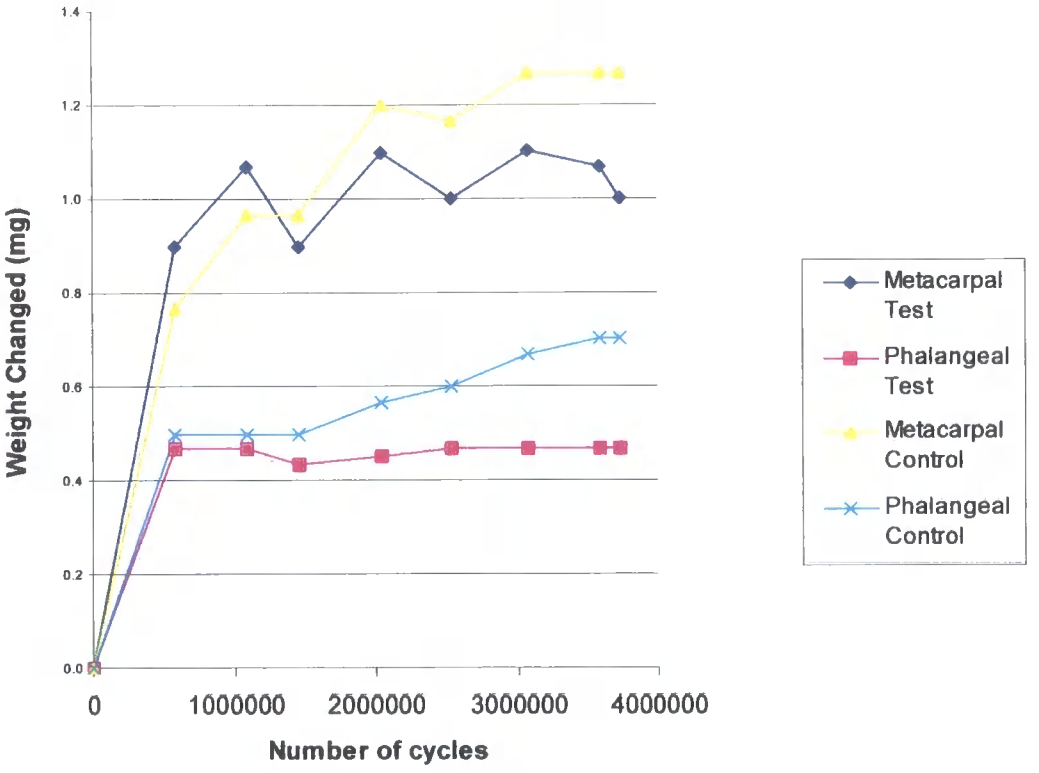

Fig. 6.14

Fig. 6.14 shows the weight change of the samples test and component during the test. Differently from what happened in distilled water, in bovine serum not only the control samples, but also the test samples gained weight. The metacarpal and the phalangeal test gained respectively 1.0 mg and 0.5 mg after 3.5 million cycles. The % of increasing weight was: 0.35 for the metacarpal component and 0.34 for the phalangeal one.

R=8.5mm

EtO-IRRADIATED XLPE PROSTHESIS rubbing against itself in BOVINE SERUM

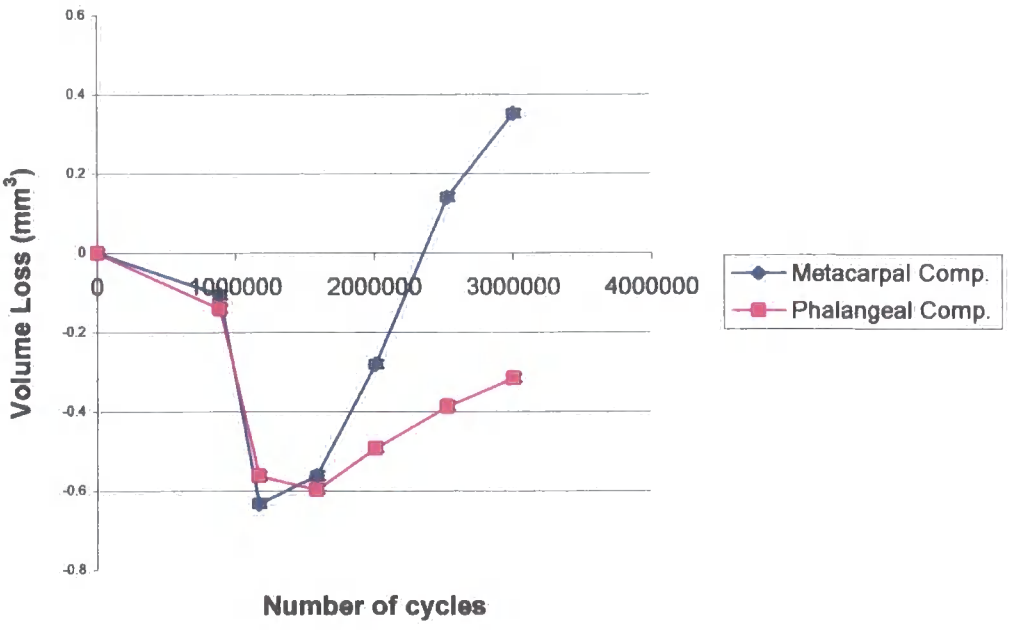

Fig. 6.15

For the 8.5mm radius EtO-sterilised Durham prosthesis tested in bovine serum, the overall wear factor was 0.35 x 10^{-6} mm^3/Nm for the metacarpal component, becoming positive only after 2.5 million cycles, while it was always negative and equal to -0.32 x 10^{-6} mm^3/Nm for the phalangeal one. The 8.5mm radius metacarpal component wore more than the correspondent 7.5mm radius component, while in this test the phalangeal component gained weight. Therefore, for the phalangeal sample, the test gained more weight than the control throughout the experiment.

Weight Change (in $n \times 10^{-4}$ g)

XLPE vs XLPE

Load: 12.5 N

Lubricant: Bovine Serum

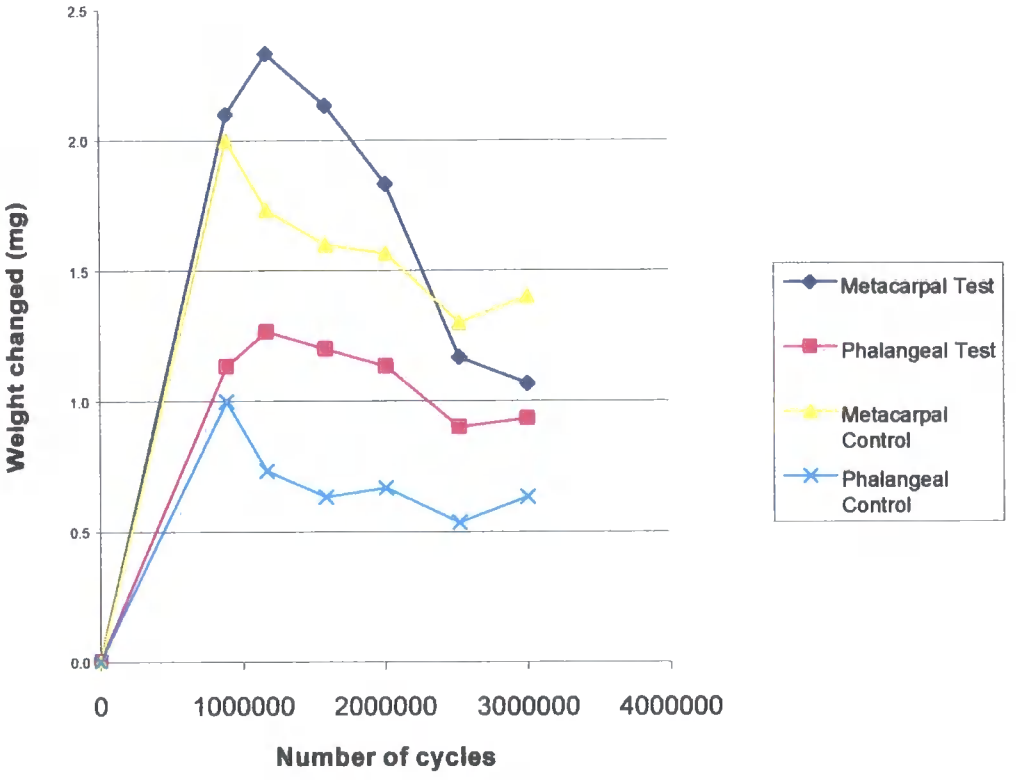

Fig. 6.16

Fig. 6.16 shows the weight change of the samples test and component during the test. Similarly to what happened with the 7.5mm radius prosthesis, both the control and the test samples gained weight. The metacarpal test gained more weight that the correspondent control until 2.5 million cycles, while the phalangeal test weight more than the correspondent control for the all experiment. The metacarpal and the phalangeal test gained respectively 1.1 mg and 0.9 mg after 3 million cycles. The % of increasing weight was: 0.29 for the metacarpal control and 0.25 for the phalangeal one.

6.2 Friction tests results

After having calibrated both the load cell and the piezoelectric force transducer, the tests were started. It was known, from previous experiments that the coefficient of friction changes during the first 700-800 cycles. To verify that, thus assuring the repeatability of the subsequent tests, the machine was let run for 1000 cycles. Every 50 cycles a trace was taken with the plotter; the friction was calculated by converting the displacements into forces, using the results of the transducer calibration. The load applied to the metacarpal component was 14.54 N (2.8 bar); the pressures in the bearings were 2 bar for the upper ones and 3 bar for the lower ones. Three tests were made to get consistent results.

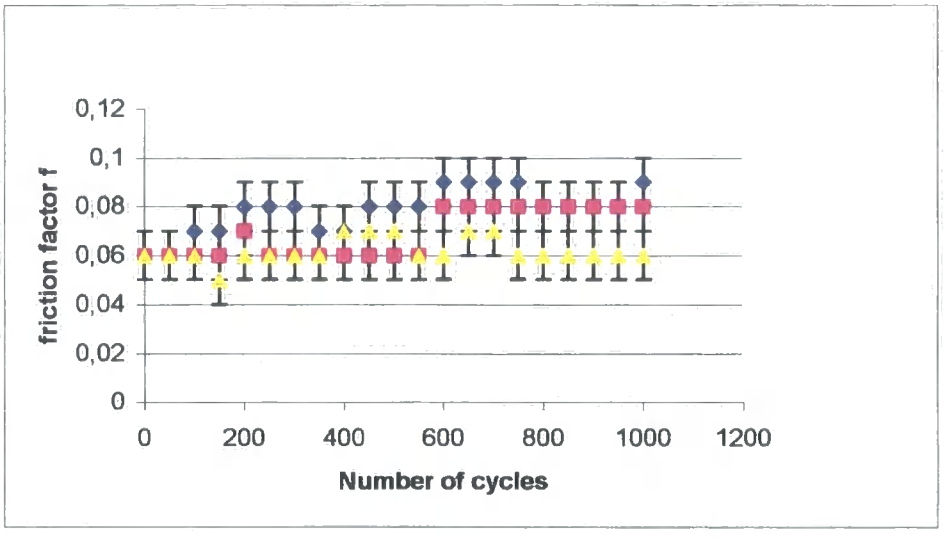

Fig. 6.17 Steady state friction test using UHMWPE cup/Ti head in distilled water

In order to validate the new simulator, different material combinations were then tested using lubricants of various viscosity, as described in section 5.3. The measured friction factors f were plotted versus the Sommerfeld parameter, Z, in order to get a Stribeck curve.

Cooke et al. (1978) showed that CMC fluids were non-Newtonian, as synovial fluid, while silicone fluids showed a Newtonian behaviour. Moreover, silicone fluids are more expensive and difficult to clean, so CMC fluids are generally preferred. However CMC solutions cannot reach very high viscosity, while a wider range of viscosity can be obtained with silicone fluids. In order to see if a complete Stribeck curve could be obtained with the new finger friction simulator, silicone fluids had to be used to get fluid film lubrication. Among the lubricants used, CMC solutions had a range of viscosity from 0.00303 to 0.107 Pa s, while silicone fluids had viscosities between 0.975 and 29.25 Pa s. Water (η=0.001 Pa s) was used as well.

The first test was undertaken using an UHMWPE cup and a titanium head and was repeated three times for each lubricant. The results are the following:

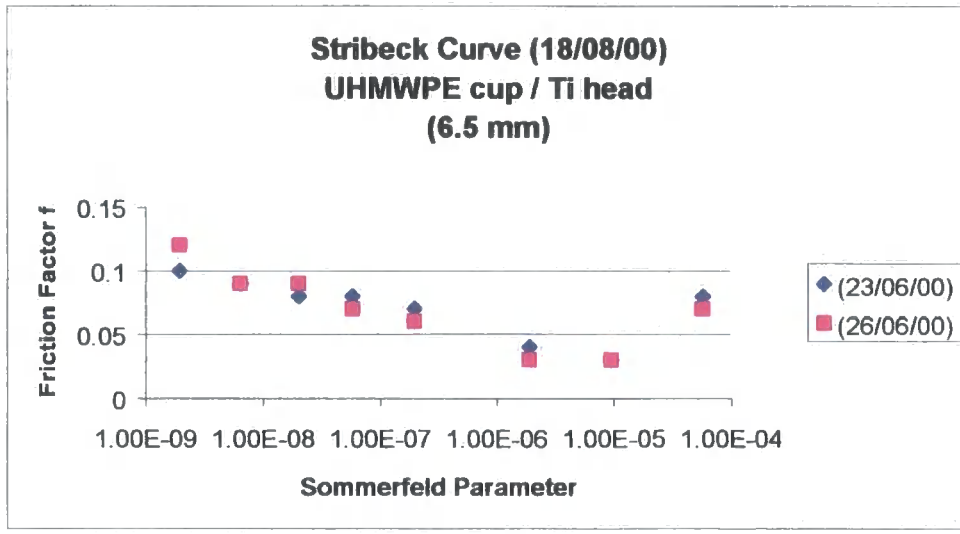

Fig. 6.18 Stribeck curve for UHMWPE/Ti

Another test was run using an UHMWPE cup and a stainless steel and was repeated three times for each lubricant.

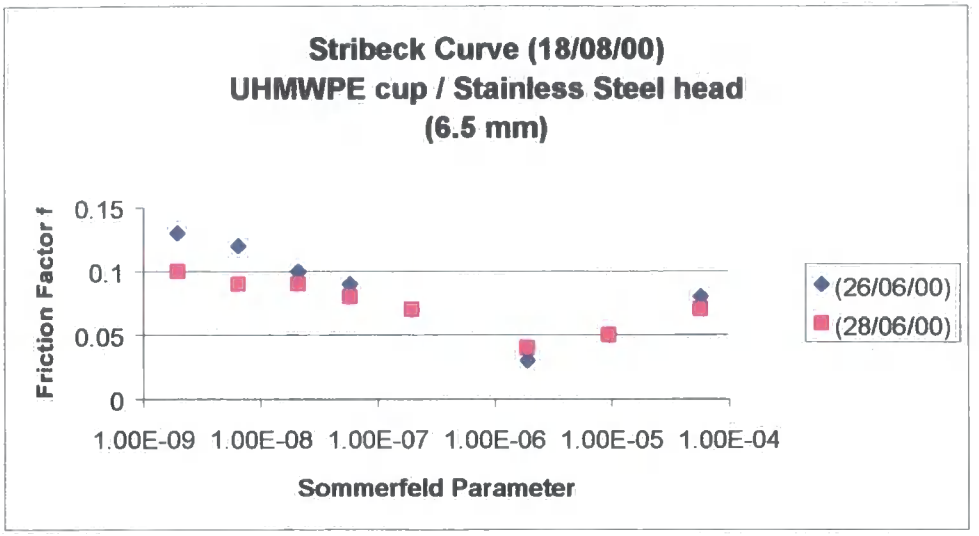

Fig. 6.19 Stribeck curve for UHMWPE/Stainless Steel

In order to obtain a wider range of value for the friction factor and therefore validate the finger friction simulator, a test was run using a titanium cup and a titanium head and was repeated three times for each lubricant.

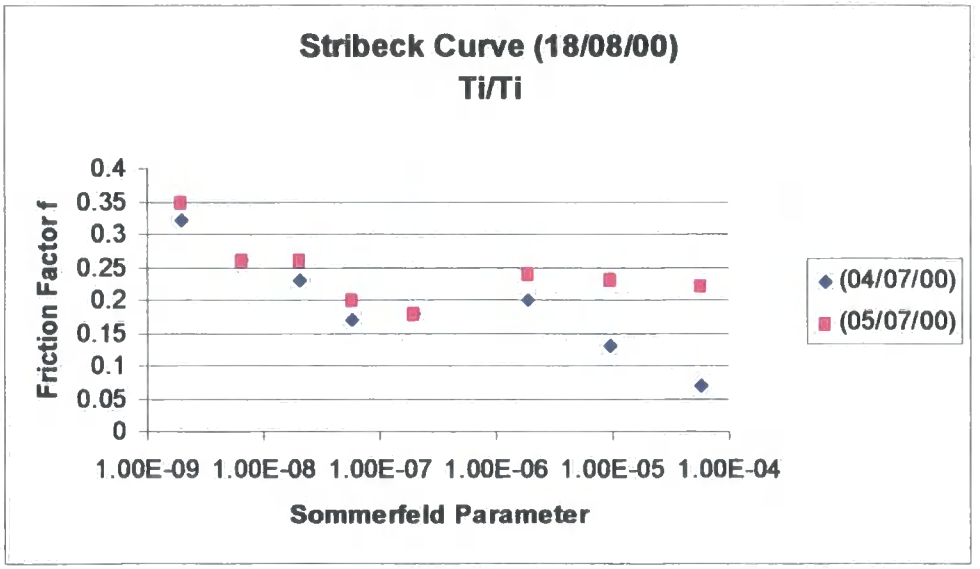

Fig. 6.20 Stribeck curve for Ti/Ti

7 Discussion of the results

7.1 Discussion on the wear tests results

7.1.1 Non-irradiated XLPE tested in distilled water

The first two tests were run in distilled water, using two different sizes of non-irradiated Durham XLPE prostheses. After 14 million cycles (approximately 14 years in vivo), the 7.5mm radius joint (7.5R) showed a total wear factor of 0.316 x 10^{-6} mm^3/Nm for the metacarpal component and a total wear factor of 0.077 x 10^{-6} mm^3/Nm for the phalangeal component while the 8.5mm radius joint (8.5R) showed a total wear factor of 0.318 x 10^{-6} mm^3/Nm for the metacarpal component and a total wear factor of 0.085 x 10^{-6} mm^3/Nm for the phalangeal component. These values correspond to wear volumes of 1.347 mm^3 and of 0.334 mm^3 for the 7.5R metacarpal and phalangeal components respectively, while the wear volumes were 1.489 mm^3 and 0.400 mm^3 for the 8.5R metacarpal and phalangeal components respectively. Thus this total wear volume of 1.681 mm^3 for the 7.5R prosthesis and of 1.889 mm^3 for the 8.5R prosthesis can be considered as a wear rate of 0.12 mm^3 and of 0.13 mm^3 per million cycles or per annum respectively. These values are exactly the same that had been reported in a previous study (Joyce, 1997). For a finger joint, a wear rate of 1.65 mm^3 per annum should be acceptable (Joyce, 1997). Consequently, the 0.12-0.13 mm^3 wear rate per million cycles determined in these two first tests indicate that the all XLPE Durham finger prosthesis is acceptable from a wear point of view.

Furthermore, both the XLPE prostheses tested had a wear curve which had a relatively constant gradient decreasing with time up to 12 million cycles where the gradient showed a sudden increase which might indicate that a period of fatigue wear had occurred. For this reason all the components were inspected using a JVD Digital Microscope (Figg. 7.1-7.2), but no pitting or delamination seemed to have happened. Scratches in the direction of sliding were observed on the sliding surfaces of both components, indicating that the wear was mainly abrasive.

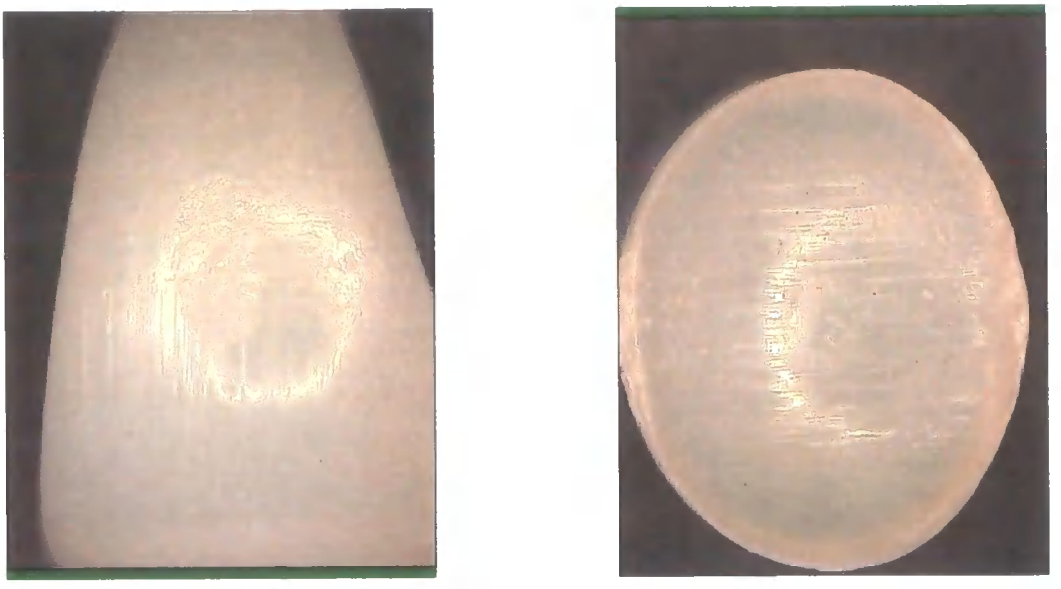

Fig. 7.1 Wear surfaces of the 7.5R non-irradiated XLPE prosthesis at the end of the test

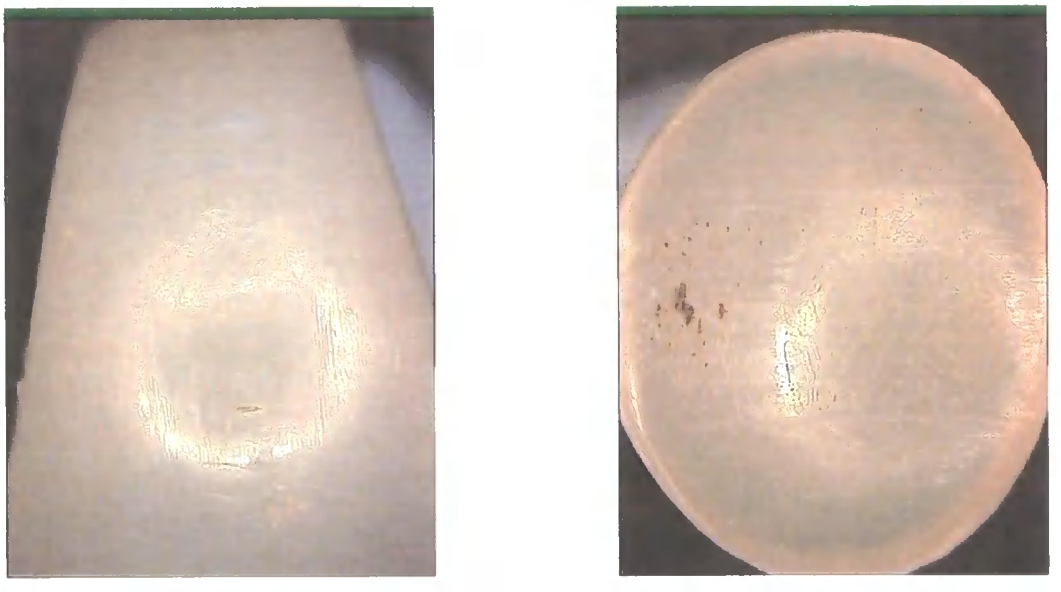

Fig. 7.2 Wear surfaces of the 8.5R non-irradiated XLPE prosthesis at the end of the test

The metacarpal components showed higher wear factors than those of their respective phalangeal components (Fig. 6.1-6.3) and this can be explained by their geometrical differences as convex surfaces tend to wear more than concave surfaces (Sibly and Unsworth, 1991).

Lubricant absorption was not significant in these two tests as at the end of the tests only the 8.5R phalangeal control had actually gained weight. This percentage of increasing weight was found to be equal to 4.3%.

Wear debris from one rig collected over 1.5 million cycles were also analysed using the Malvern Mastersizer. The most numerous particles that were present in a percentage of volume over 3% had a size of 2.5-10μm, but this size tended to increase with the progress of the test. This however might be due to metallic or fibre particles from the rig. However, the majority of wear debris were 0.4-0.7μm in size up to 891,388 cycles while being 0.35-0.63μm in size up to 1,650,973 cycles. Therefore it can be stated that the majority of XLPE particles collected were less than 1μm in size. The same result has been found in a study on retrieved total hip replacement prostheses (Schmalzried et al., 1994) where the majority of polyethylene particles found in the tissues were less than 1μm in size. In the same study a broader size range of polyethylene particles was found in total knee replacement specimens compared with the hips. An *in vitro* study also suggested that polyethylene particles in a size range of 0.3-10μm appears to be the most biologically active in producing mediators to osteolysis which may lead to aseptic implant loosening (Green et al., 1998).

7.1.2 Gamma-irradiated XLPE tested in Ringer solution

The third test undertaken using a gamma-irradiated 9.4mm Durham XLPE prostheses in Ringer solution and run removing the metacarpoglenoidal arm from the rig, was done to compare the result with a previous study (Joyce and Unsworth, 2000a). The metacarpoglenoidal arm was removed to simulate what happens during surgery for the Swanson's prosthesis implantation. In the earlier

study (Joyce and Unsworth, 2000a) a Swanson prosthesis and a Durham prosthesis were tested. The Swanson prosthesis failed at the intersection of the hinge and the distal stem after 936,544 cycles as happens in surgical experience (Weightman et al., 1972). The Durham prosthesis tested in distilled water for 4.8 million cycles showed a total wear factor of 0.36 x 10^{-6} mm^3/Nm for the metacarpal component and of 0.24 x 10^{-6} mm^3/Nm for the phalangeal component. In the test undertaken during this research and run for 8.5 million cycles the Durham prosthesis at the end of the test showed no cuts and fractures and a total wear factor of 1.74 x 10^{-6} mm^3/Nm for the metacarpal component and of 0.55 x 10^{-6} mm^3/Nm for the phalangeal component. The total wear volume was equal to 7.15 mm^3 which corresponded to a wear rate of 0.84 mm^3 per million cycle. Therefore the Durham prosthesis tested under the same conditions of motion as the Swanson prosthesis is acceptable from the wear point of view (Joyce, 1997). An explanation of the higher wear rate measured in this study with the Durham prosthesis compared with the previous relates to the removal of the metacarpoglenoidal arm which forced the prosthesis to work under more severe conditions of motion. Another reason might be found in the different lubricant used. The use of Ringers solution as lubricant in fact might give higher wear factor than distilled water (Joyce, 1997). Furthermore, also in this test the metacarpal component showed higher wear factors than the phalangeal component (Fig. 6.5) and the lubricant absorption was again not significant as it was detectable only for the phalangeal control and it was equal to 0.09%.

7.1.3 Non-irradiated XLPE tested dry (without any lubricant)

Two tests were carried out with no lubricant used (i.e. under dry conditions), and run for over 3,000,000 cycles. The aim of this test was to evaluate the influence of a second degree of motion on the wear of the XLPE using the Durham finger wear simulator. The first test was therefore run using the normal finger wear simulator in a flexion-extension motion while the second test was carried out using a modified finger wear simulator which added rotation to the flexion-extension motion. With rotation added to the flexion-extension movement, the

total wear factor was found to be equal to 6.54 x 10^{-6} mm^3/Nm. However, under only one degree of motion, the total wear factor measured at the end of the test was equal to 5.95 x 10^{-6} mm^3/Nm. Therefore the addition of a second degree of motion increased the wear. The same result was found in a previous study carried out on a pin-on-plate rig using bovine serum as lubricant (Joyce et al., 2000c). Again an explanation does not appear to lie with the roughness as, at an eye-inspection, scratches in the direction of the motion were visible only in the flexion-extension motion test. Perhaps instead the more complex motion was continuously smoothing the contact surfaces leading to an increase in wear. Each point on the surface of both the metacarpal and the phalangeal components were undertaking a variable and complex load cycle. In the same study two tests were also carried out using XLPE specimens run dry on a pin-on-plate rig and the results found are reported in Table 7.1.

Machine used	**Sliding Distance (km)**	**Motion**	**Mean k metacarpal (plate) x 10-6mm3/Nm**	**Mean k phalangeal (pin) x 10-6mm3/Nm**
Finger wear simulator	94	Flexion-Extension	4.25	1.70
Pin-on-plate rig	84	Reciprocation	0	0.66
Finger wear simulator	86	Flexion-Extension + Rotation	3.29	3.25
Pin-on-plate rig	87	Reciprocation + Rotation	0.18	0.45

Tab. 7.1 Dry tests on XLPE specimens carried out using a finger wear simulator and on a pin-on-plate rig

If we compare the two tests through the surface contact, we have that both the phalangeal component and the pin are completely in contact and loaded during

their motion, therefore with both one and two degree of motion each point on their surface undergoes a static load. In both studies the addition of a second degree of motion decreased the wear rate in the metacarpal/plate components while increased it in the phalangeal/pin components. This might be due to the bi-dimensional motion which changes the contact condition of each point in the surface of all the components. This might cause more damage to the material physical properties and consequently lead to more wear.

7.1.4 Eto-sterilized XLPE tested with different lubricants

To evaluate the influence of sterilisation on the wear behaviour of XLPE while sliding against itself, four ethylene-sterilised Durham prostheses were tested: two in bovine serum and two in distilled water.

Cross-linked polyethylene MCP prostheses have only been tested at the University of Durham and so only a few results are available from literature. The results of Joyce are reproduced from his thesis (Joyce, 1997).

Researcher	Dist. (km)	K metacarpal x 10^6 mm^3/Nm	K phalangeal x 10^6 mm^3/Nm
Joyce 1	224	0.72	0.34
Joyce 2	633	0.24	0.12
Joyce 3	252	0.40	0.23
Joyce 4	272	0.03	0.12
Joyce 5	247	0.13	0.10
Vandelli 1	118	1.52	0.74
Vandelli 2	136	1.94	0.92
Vandelli 3	88	0.25	0.23
Vandelli 4	80	0.35	-0.32

Tab. 7.2 XLPE MCP prosthesis wear test results

For the two tests run in distilled water (test Vandelli 1-Vandelli 2), the 7.5R test showed a total wear factor of 1.52 x 10^{-6} mm^3/Nm for the metacarpal component and a total wear factor of 0.74 x 10^{-6} mm^3/Nm for the phalangeal component while the 8.5R test showed a total wear factor of 3.00 x 10^{-6} mm^3/Nm for the metacarpal component and a total wear factor of 1.46 x 10^{-6} mm^3/Nm for the phalangeal component. These values correspond to wear volumes of 2.248 mm^3 and of 1.089 mm^3 for the 7.5R metacarpal and phalangeal components respectively, while the wear volumes were equal to 5.128 mm^3 and of 2.494 mm^3 for the 8.5R metacarpal and phalangeal components respectively. Thus this total wear volume of 3.337 mm^3 for the 7.5R prosthesis and of 7.622 mm^3 for the 8.5R prosthesis can be considered as a wear rate of 0.67 mm^3 and of 1.43 mm^3 per million cycles or per annum respectively. It appears that the 8.5R Durham prosthesis wore more than twice the rate of the 7.5R Durham prosthesis, but it has to be said that the prosthesis was actually damaged during the first million cycle. If we consider the wear curve after that period, we can see that total wear factors drop to 1.94 x 10^{-6} mm^3/Nm and 0.92 x 10^{-6} mm^3/Nm for the metacarpal and the phalangeal components respectively. Therefore the wear factors obtained for the two different sizes EtO irradiated all XLPE Durham prostheses were comparable.

These results however showed a higher wear rate than all of the Joyce's tests which used non-sterilised XLPE Durham prostheses run in distilled water and in Ringer solution. Therefore it could be stated that the use of ethylene oxide gas for sterilizing XLPE might lead to an increase of the wear. A similar result was found in a study by Wang et al. (1998) where EtO-sterilized UHMWPE cups run against both CoCr and alumina ceramic heads showed more wear than with gamma-irradiated/stabilized UHMWPE cups. Another clinical study (Oonishi et al., 1992) also found significantly higher wear rates for EtO-sterilized cups than for gamma irradiated cups against both stainless steel and alumina ceramic heads. However, the two tests run using EtO-sterilized XLPE prostheses in bovine serum (Vandelli 3, Vandelli 4) showed wear factors very similar to Joyce's results and this might indicate that the lubricant more than the method of sterilization caused the higher wear factors measured in the first two tests.

7.2 Discussion on the friction tests results

The steady-state friction test (Fig.6.17) obtained running UHMWPE cup against a titanium head in distilled water showed that the measured friction was not consistent for all the three runs after about 1,000 cycles as it was still variable and slightly increased. This might be due to the fact that the specimens in this simulator were subjected to a fixed and constant load and not a variable load as in the hip simulators. The load cycle applied to the specimens tested on the hip simulator explains however the different trend of the friction factor. Therefore it was decided to let the finger friction simulator run for a few cycles before starting the test.

Three tests (Fig. 6.18, Fig. 6.19 and Fig. 6.20) were then undertaken with the aim of validating the finger friction simulator by comparing the friction results on different couples of material with those found in literature.

Initially each pair of materials was tested using a wide range of lubricant viscosity in order to obtain a Stribeck curve. Both CMC and silicone fluids were used. The use of silicone fluids allowed high values of Z to be reached such that the full fluid film lubrication could be demonstrated on the finger friction simulator. Each lubricant at different viscosity was tested at least three times so that any deviation in measurements during the course of the test could be measured.

All three tests produced full Stribeck curves with initially falling trends indicating mixed lubrication. An increase in lubricant viscosity generated an increased fluid film, greater separation of surfaces, less asperity contact and therefore lower friction. At a certain viscosity an equilibrium point was reached at which the bearing surfaces became completely separated and so further increase in viscosity produced no benefits in terms of frictional performance. At this stage the friction generated was entirely due to the shearing of the lubricant and so further increases in lubricant viscosity would lead to an increase in friction.

In the first friction test (Fig. 6.18) run using an UHMWPE cup against a titanium head, a Stribeck curve was obtained. During this test very little deviation was measured and the highest values were obtained using distilled water as expected. At higher viscosity in fact the greater film thickness establishes a better separation of the surfaces which should stabilise the friction. Furthermore the stronger inter-molecular forces in a high viscosity lubricant would create a more stable fluid film than with lower viscosity lubricant. The average coefficient of friction recorded while using distilled water was 0.11, which compares well with published results of plastic on metal. Hitchmough (1994) used the original Durham pin-on-plate machine to obtain coefficient of friction between 0.14-0.18 for metal on UHMWPE. Saikko (1992a) measured an average value of the coefficient of friction of 0.10 for UHMWPE pins run against CoCrMo plates under 4.8 MPa of contact pressure. In another study (Scholes et al., 1997) carried out on a hip simulator using a Ti head against a polyethylene cup, coefficients of friction very similar to the CoCrMo/polyethylene couple of materials were reported.

In the second test (Fig. 6.19) a UHMWPE cup was tested against a stainless steel head and an average coefficient of friction of 0.12 was found with distilled water. A reported study (McKellop et al., 1977) was conducted on a reciprocating pin-on-plate machine using polyethylene against steel. The friction recorded under a constant pressure of 6.9 MPa was varing between 0.10 and 0.18 while using distilled water. Another study by Caravia et al. (1990) measured the steady state coefficient of friction of UHMWPE against stainless steel under a constant load of 20N to be between 0.05 and 0.2. Shen and Dumbleton (74) measured a coefficient of friction of 0.185 for PE against 316 stainless steel under a constant load of 20N on a thrust washer bearing tester.
The frictional factor measured in the physiological range was of the order of 0.1, therefore higher than the value of 0.06 reported by Scholes et al (2000) in a hip simulator while using biological fluid.

In a third test (Fig. 6.20) a titanium cup was run against a titanium head and an average coefficient of friction of 0.35 was measured while using distilled water.

It is very difficult to find results on metal on metal, in part due to the commercial confidentiality companies feel is required in protecting their interests (Hall and Unsworth, 1997). A study conducted by Cipera and Medley the friction measured in each of three types of CoCrMo alloys articulating against themselves showed no statistical variation. In a hip simulator study (Weightman et al., 1992) the metal on metal prostheses gave a coefficient of friction between 0.12 and 0.25 which is lower than the value found in this study. An explanation for the higher result however might be found in the static and not dynamic load applied with our simulator. Typical values of friction factors with all the metal joints are 0.31 for CMC fluids (Scholes et al., 1997) and this relates quite well with the results obtained in this test.

8 Conclusions

8.1 Conclusions on the wear tests results

Various wear tests were undertaken using the new Durham finger wear simulator and the following results can be summarized:

- Non-irradiated XLPE prostheses gave a wear rate per annum of 0.13 mm^3 which is exactly the same as Joyce found in his study. Furthermore the wear was mainly of the abrasive type and no pitting or delamination seemed to have occurred. This all reaffirms the conclusion that the all XLPE Durham finger prosthesis is acceptable from a wear point of view. The wear debris investigation showed that the majority of the wear debris was less than 1μm in size. This should be further investigated as this size appears to be the most biologically active in producing osteolysis which may lead to implant loosening.

- A gamma-irradiated XLPE prosthesis run under the same conditions of motion as the Swanson prosthesis showed an acceptable behaviour from a wear point of view. After 8.5 million of cycles, the total wear volume was equal to 7.15 mm^3 which corresponds to a wear rate of 0.84 mm^3 per million cycle or per annum.

- In the dry tests the addition of a second degree of motion increased the overall wear. An explanation of this phenomenum might be found in the more complex contact and load conditions of the bearings.

- EtO-sterilized all XLPE Durham prosthesis showed different wear factors depending on the lubricant. The high wear found while using distilled water decreased dramatically becoming very similar to Joyce's results in

the bovine serum tests. This might indicate that EtO sterilization does not influence the wear properties of an all XLPE prosthesis.

8.2 Conclusions on the friction tests results

During this research a finger friction simulator was designed, manufactured and validated. The full Stribeck curves obtained during the three tests run on it demonstrate the possibility of achieving repeatable curves that were consistent with the lubrication theory. Furthermore the form of the curves and the values of the coefficients of friction measured were consistent over the three tests and compared well with published results. Therefore the Durham finger friction simulator was validated and can be used for further friction investigations.

9 Suggestions for further work

9.1 Suggestions on the wear tests

- A complete wear debris analysis on all the wear debris collected during the two tests run with the non-irradiated all XLPE prostheses in distilled water should be carried out using the Malvern Mastersizer 2000s. During this research the wear debris investigation showed that the majority of the wear debris was less than 1μm in size, therefore as this size appears to be the most biologically active in producing ostheolysis which may lead to implant loosening, this aspect should be further investigated.

- Further tests should be carried out on the Durham finger wear simulator using EtO-sterilized all XLPE Durham prostheses in order to improve our understanding of the influence of the lubricant used on this sterilization method used for the Durham finger prostheses. Also further investigation on the wear behaviour of the EtO-sterilized prostheses compared with the wear results obtained from the gamma-irradiated prostheses already tested would be recommended. This could explain which one is the more favorable method of sterilization from a wear point of view.

9.2 Suggestions on the friction tests

- Further friction tests should be carried out on the Durham finger friction simulators with different couples of materials and different lubricants like bovine serum and Ringer solution. The all XLPE Durham finger prosthesis could then be investigated in its frictional properties and also at each wear stops in order to most completely record and understand its tribilogical behavior.

Acknowledgments

First of all I would like to thank Professor Anthony Unsworth for having allowed me to come back to Durham for this year of research within the Centre of Biomedical Engineering and for having supervised my work again. Many thanks also to Dr Tom Joyce for his patience, suggestions and advice. It has been a wonderful experience and I've felt very proud to be part of the ambitious and revolutionary project connected with the new Durham MCP joint prosthesis.
A grateful thanks also to the EPSRC (Engineering and Physics Research Council) and to the Department of Engineering for the financial support. This year of research wouldn't have been possible without them.

A very affectionate thanks to all the people of the Mechanical and Electrical Workshop. Thanks a lot especially to George Turnbull, Colin Wintrip, Brian Blackburn, Roger Little and Alex McGuffie for their help and friendship. A special thanks to Kevan Longley for the daily help and for having manufactured the finger friction simulator.

Thanks to all the people I met during this year. First of all to all the guys who had to share the flat with me: Sachi, Yaron, Simon, Tie, Zianon, Liviu, Lynsey and Mohammed. Thanks for the delicious food, for my birthday party, for our never-ending discussions and for having dried my tears so many times. Thanks to Sachi for having been such a wise friend and to Yaron for his sense of humour and for his special "pasta with pesto". Thanks to all the Italian group: Giancarlo, Silvia, Moira, Giovanna, Marco, Dimitri, Cinzia, Paolo, Giusy, Andrea, Edoardo, Claudia, Renato, Luca e Gabriella. And last but not least thanks to all the International friends I met during this year. I know I won't have another chance to meet so many people from all over the world again in my life. I will carry with me these marvellous memories for the rest of my life.

Thanks to my family and to Roberto for having accepted my choice and for having supported me every day from Italy. Thanks to my beloved country as I've missed it more than everything else.

References

Adams BD, Blair WF and Shurr DG (1990): Schultz metacarpophalangeal arthroplasty: A long-term follow-up study. *J Hand Surg*, 15A: 4: 641-645

Archard J F (1953): Contact and rubbing of flat surfaces *J Appl Phys*, 24, pp. 981-988

ASTM F732-82 (1989): Standard practice for reciprocating pin-on-flat evaluation of friction and wear properties of polymeric matherials for use in total joint prostheses. *In Annual Handbook of ASTM Standards, 13.01, American Society for Testing and Materials, Philadelphia*, 212

Atkinson JR and Cicek RZ (1983): Silane cross-linked polyethylene for prosthetic applications. Part I. Certain physical and mechanical properties related to the nature of the material. *Biomaterials*, 4: 267-275

Atkinson JR and Cicek RZ (1984): Silane cross-linked polyethylene for prosthetic applications. Part II. Creep and wear behaviour and preliminary mouling test. *Biomaterials,* 5: 326-335

Atkinson JR, Dowling JM and Cicek RZ (1980): Materials for internal prostheses: the present position and possible future developments. *Biomaterials,* 1: 89-96

Atkinson JR, Dowson D, Isaac JH, Wroblewski BM (1985a): Laboratory wear tests and clinical observations of the penetration of femoral heads into acetabular cups in total replacement hip joints. III: The measurement of internal volume changes in explanted Charnley sockets after 2-16 years in vivo and the determination of wear factors. *Wear*, 104: 225-244

Auger D D, Dowson D, Fisher J (1995): Cushion form bearings for total knee joint replacement. Part 1: Design,friction and lubrication *Proc Inst Mech Eng [H]*, 209(2): 73-81.

Auger D D, Dowson D, Fisher J, Jin Z M (1993): Friction and lubrication in cushion form bearings for artificial hip joints. *Proc Inst Mech Eng [H],* 207(1): 25-33.

Baker DA, Hastings RS, Pruitt L (1999): Study of fatigue resistance of chemical and radiation crosslinked medical grade ultrahigh molecular weight polyethylene. *J Biomed Mater Res.*, 46(4): 573-81.

Bartel DL, Fisher GW and Flatt AE (1968): Investigation of human finger joint motion using the method of over determined collocation. *Proc Ann Con Eng Med Bio*, 10: 26A8

Beckenbaugh RD (1983): Preliminary experience with a noncemented nonconstrained total joint arthroplasty for the metacarpophalangeal joints. *Orthopedics*, 6: 8: 962-965

Beckenbaugh RD, Dobyns JH, Linscheid RL and Bryan RS (1976): Review and analysis of silicone-rubber metacarpophalangeal implants. *J Bone Jt Surg*, 58A: 4: 483-487

Beevers DJ and Seedhom BB (1993): Metacarpophalangeal joint prostheses: a review of past and current designs. *Proc Inst Mech Eng [H];* 207(4): 195-206

Beevers DJ, Seedhom BB (1995): Metacarpophalangeal joint prostheses. A review of the clinical results of past and current designs. *J Hand Surg [Br].;* 20(2): 125-136

Besong AA, Tipper JL, Ingham E, Stone MH, Wroblewski BM, Fisher J (1998): Quantitative comparison of wear debris from UHMWPE that has and has not been sterilised by gamma irradiation. *J Bone Joint Surg Br.*, 80(2): 340-344.

Besong AA, Tipper JL, Mathews BJ, Ingham E, Stone MH, Fisher J (1999): The influence of lubricant on the morphology of ultra-high molecular weight polyethylene wear debris generated in laboratory tests. *Proc Inst Mech Eng [H],* 213(2): 155-158

Bigsby RJA, Auger DD, Jin ZM, Dowson D, Hardaker CS and Fisher J (1998a): A comparative tribological study of the wear of composite cushion cups in a physiological hip joint simulator. *J Biomechanics*, 31: 363-369

Blair WF, Shurr DG and Buckwalter JA (1984a): Metacarpophalangeal joint arthroplasty with a metallic hinged prosthesis. *Clin Orthop and Related Research*, 184: 156-163

Blair WF, Shurr DG and Buckwalter JA (1984b): Metacarpophalangeal joint arthroplasty with a silastic spacer. *J Bone Jt Surg*, 66A: 3: 365-370

Bloor C and Summers MJ (1982): Creep rupture testing of cross-linked polyethylene pipe. *Plastic and Rubber Institute National Conference.*

Bragdon CR, O`Connor DO, Lowenstein JD, Jasty M and Syniuta WD (1996): The importance of multidirectional motion on the wear of polyethylene. *Proc. Inst. Mech. Engrs, Part H: J. Eng. Med.*, 210: 157-166

Brannon EW and Klein G (1959): Experiences with a finger-joint prosthesis. *J Bon Jt Surg*, 41A: 1: 87-102

Briscoe BJ and Stolarski TA (1985): Transfer wear of polymers during combined linear motion and load axis spinning. *Wear*, 104: 121-137

British Standard, BS 7251, (1990): Orthopaedic Joint Prostheses, Part 8. Guide to laboratory evaluation of change of form of bearing surfaces of hip joint prostheses. *British Standards Institution, London.*

Bruck SD, Mueller EP (1988): Radiation sterilization of polymeric implant materials. *J Biomed Mater Res.*, 22(A2 Suppl): 133-44.

Burgess IC (1996): Tribological and mechanical properties of compliant bearings for total joint replacements. *PhD Thesis.*

Cabitza P, Percudani W (1979): [Long-term results of 2 continuous series of total hip prostheses of the McKee-Farrar metal-metal type and the Charnley metal-plastic type]. *Arch Sci Med (To),* 136(1): 45-50. Italian.

Calnan JS and Reis ND (1968): Artificial finger joints in rheumatoid arthritis: I. Development and experimental assessment. *Annals of Rheumatic Diseases*, 27: 3: 207-217

Campbell P, Forey F and Amstutz HC (1996): Wear and morphology of ultra-high molecular weight polyethylene wear particles from total hip replacements. *Proc. Instn. Mech. Engrs., Part H,* 210(H2): 167-174

Campbell P, Ma S, Schmalzried T and Amstutz HC (1994): Tissue digestion for wear debris particle isolation. *J of Biomedical Materials Research*, 28: 523-526

Caravia L, Dowson S, Fisher J and Jobbins B (1990): The influence of bone and bone cement debris on counterface roughness in sliding wear tests of ultra-high molecular weight polyethylene on stainless steel. *Proc instn Mech Engrs.* 204: 65-70.

Charnley J (1961): Arthroplasty of the hip. A new operation. *The Lancet,* 1129-1132.

Chiesa R, Tanzi MC, Alfonsi S, Paracchini L, Moscatelli M, Cigada A (2000): Enhanced wear performance of highly crosslinked UHMWPE for artificial joints. *J Biomed Mater Res.*, 50(3): 381-387.

Cipera WM and Medley JB (2000): A friction-based study of cobalt-based alloys for metal-metal hip implants. In *Proc. 5th World Biomaterials Congress, Toronto, Canada,* 29 May-2 June, p.781.

Clarke I (1981): Wear of artificial joint materials 4. Hip joint simulator studies. *Eng Med*, 10 (4): 189-198

Clarke IC, Starkebaum W, Hosseinian A, McGuire P, Okuda R, Salovey R, Young R (1985): Fluid-sorption phenomena in sterilized polyethylene acetabular prostheses. *Biomaterials*, 6(3): 184-188.

Collier JP, Sutula LC, Currier BH, Currier JH, Wooding RE, Williams IR, Farber KB, Mayor MB (1996): Overview of polyethylene as a bearing material: comparison of sterilization methods. *Clin Orthop.*, (333): 76-86.

Cook SD, Beckenbaugh R, Weinstein AM and Klawitter JJ (1983): Pyrolite carbon implants in metacarpophalangeal joint of baboons. *Orthopedics*, 6: 8: 952-961

Cook SD, Beckenbaugh RD, Redondo J, Popich LS, Klawitter JJ, Linscheid RL (1999): Long-term follow-up of pyrolytic carbon metacarpophalangeal implants. *J Bone Joint Surg Am*; 81(5): 635-48.

Cooke, A F, Dowson D and Wright, V (1978): The rheology of synovial fluid and some potential synthetic lubricants for degenerate synovial joints *Eng. Med.*, 7(2): pp 66-72

Dave B (1988): Crosslinked polyethylene. In: Bhowmick AK, Stephens HL, editors. Handbook of elastomers. *New York: Marcel Dekker Inc.*

Derkash RS, Niebauer JJ and Lane CS (1986): Long-term follow-up of metacarpal phalangeal arthroplasty with silicon dacron prostheses. *J Hand Surg,* 11A: 4: 553-558

Dintenfass J (1963): Lubrication in synovial joints: a theoretical analysis – a rheological approach to the problem of joint movements and joint lubrication. *J. Bone Jt Surg.,* 45A: 1241

Doi K, Kuwata N and Kaway S (1984): Alumina ceramic finger implants: a preliminary biomaterial and clinical evaluation. *J Hand Surg,* 9A, 740-749

Dowson D (1966-67): Modes of lubrication in human joints. *Proc. Instn. Mech. Engrs.,* 181: 45-54

Dowson D and Wright V (1981): Introduction to the biomechanics of the joints and joint replacement, *Mechanical Engineering Publications LTD, London*

Dowson D, Diab M, Gillis B and Atkinson JR (1985): Influence of counterface topography on the wear of UHMWPE under wet or dry conditions. *American Chemical Society,* 171-187

Elfick A P, Hall R M, Pinder I M, Unsworth A (1998): The frictional behaviour of explanted PCA hip prostheses. *Proc Inst Mech Eng [H],* 212(5): 395-397.

Elfick APD, Green SM, Pinder IM and Unsworth A (1999): A novel technique for the detailed size characterisation of wear debris. *Submitted to Journal of Material Science: Materials in Medicine.*

Feldman LA and Hui HK (1997): Compatibility of medical devices and materials with low-temperature hydrogen peroxide gas plasma. *Med. Dev. Diag. Ind.,* 19: 57-62

Felric DC, Clayton ML and Holloway M (1975): Complications of silicone implant surgery in the metacarpophalangeal joint. *J Bone Jt Surg*, 57A: 7: 991-994

Fisher J, Barbour PSM, King MJ, Besong AA, Hailey J, Tipper JL, Ingham E, Stone M and Wroblewski BE (1997): Wear of ultrahigh molecular weight polyethylene in artificial joints: A new approach to the quantification of wear debris. *5th European Conference on Advanced Material Processes& Application.*

Flatt AE (1961): Restoration of rheumatoid finger-joint function. Interim report on trial of prosthetic replacement. *J Bone Jt Surgery*, 43A: 5: 753-774

Flatt AE (1967): Prosthetic substitution for rheumatoid finger joints. *Plastic and Reconstructive Surgery*, 40: 6: 565-570

Flatt AE (1983): Care of the Arthritic Hand. *4th Edition, St Louis, CV Mosby Co., London*

Flatt AE and Ellison MR (1972): Restoration of rheumatoid finger joint function: 3. A follow-up note after 14 years of experience with a metallic-hinged prosthesis. *J Bone Jt Surg*, 54A: 6: 1317-1322

Flatt AE and Fisher GW (1969): Biomechanical factors in the replacement of rheumatoid finger joints. *Ann Rheum Dis*, 28: 36-41

Fleming SG and Hay EL (1984): Metacarpophalangeal arthroplasty: Eleven year follow-up study. *J Hand Surg*, 9B: 3: 300-302

Fowler S B (1962): Arthroplasty of the metacarpophalangeal joint in rheumatoid arthritis. *J Bone Joint Surg*; 44A: 1037-1038

Gillespie TE, Flatt AE, Youm Y and Sprague BL (1979): Biomecanical evaluation of metacarpophalangeal joint prosthesis designs. *J Hand Surg*, 4: 6: 508-521

Goldman M, Pruitt L (1998): Comparison of the effects of gamma radiation and low temperature hydrogen peroxide gas plasma sterilization on the molecular structure, fatigue resistance, and wear behavior of UHMWPE. *J Biomed Mater Res.*, 40(3): 378-384

Goldsmith A A, Dowson D, Isaac G H, Lancaster J G (2000): A comparative joint simulator study of the wear of metal-on-metal and alternative material combinations in hip replacements. *Proc Inst Mech Eng [H]*, 214(1): 39-47.

Goldsmith AA, Dowson D (1999): A multi-station hip joint simulator study of the performance of 22 mm diameter zirconia-ultra-high molecular weight polyethylene total replacement hip joints. *Proc Inst Mech Eng [H]*, 213(2): 77-90.

Gore T A, Higginson G R, Kornberg R E (1981): Some evidence of squeeze film lubrication in hip prostheses. *Engng. Med.*, 10: 89-94

Greer KW (1979): Four years of wear testing experience on three joint simulators. *Annual meeting of the Society of Biomaterials.*

Griffith RW and Nicolle FV (1975): Three years' experience of metacarpophalangeal joint replacement in the rheumatoid hand. *The Hand*, 7: 3: 275-283

Grobbelaar CJ, Du Plessis TA, Marais F (1978): The radiation improvement of polyethylene prostheses: A preliminary study. *J. Bone Joint Surg. Br.*, 60: 370-374

Hagert CG (1975b): Metacarpophalangeal joint implants. II. Roentgenographic study of the Niebauer-Cutter metacarpophalangeal joint prosthesis. *Scan J Plast and Reconstr Surg,* 9: 2: 158-164

Hagert CG, Branemark P-I, Albrektsson T, Strid K-G and Irstam L (1986): Metacarpophalangeal joint replacement with osseointegrated endoprostheses. *Scan J Plast Recon Surg*, 20: 2: 207-218

Hagert CG, Eiken O, Ohlsson NM, Aschan W and Movin A (1975a): Metacarpophalangeal joint implants: I. Roentgenographic study on the silastic finger joint implant, Swanson design. *Scan J Plast and Reconst Surg*,9: 2: 147-157

Hailey JL, Ingham E, Stone M, Wroblewski BM, Fisher J (1996): Ultra-high molecular weight polyethylene wear debris generated in vivo and in laboratory tests; the influence of counterface roughness. *Proc Inst Mech Eng [H],* 210(1): 3-10

Hall R M, Unsworth A, Wroblewski B M, Burgess I C (1994): Frictional characterisation of explanted Charnley hip prostheses. *Wear*, 175: 159-166

Hall R M, Unsworth A, Wroblewski B M, Siney P, Powell N J (1997): The friction of explanted hip prostheses. *Br J Rheumatol.*, 36(1): 20-26.

Hall RM, Siney P, Unsworth A and Wroblewski BM (1997b): The effect of surface topography of retrieved femoral heads on the wear of UHMWPE sockets. *Med. Eng. Phys.*, 19(8): 711-719

Hall RM, Unsworth A, Siney P and Wroblewski BM (1996a): Wear in retrieved Charnley acetabular sockets. *Proc. Instn. Mech. Engrs.*, H209: 233-241

Hamrock B J and Dowson D (1978): Elastohydrodynamic lubrication of elliptical contacts for materials of low elastic modulus. *J Lubric Technol*, 100: 236-245

Hansraj KK, Ashworth CR, Ebramzadeh E, Todd AO, Griffin MD, Ashley EM and Cardilli AM (1997): Swanson metacarpophalangeal joint arthroplasty in patients with rheumatoid arthritis. *Clin Orthop*, 342: 11-15

Ingham E, Fisher J (2000): Biological reactions to wear debris in total joint replacement. *Proc Inst Mech Eng [H]*, 214(1): 21-37.

Jasty M, James S, Bragdon CR, Goetz D, Lee KR, Hanson AE and Harris WH (1994): Patterns and mechanisms of wear in polyethylene acetabular components retrieved at revision surgery. In: *Transactions of 20th Annual Meeting of the Society for Biomaterials, Minneapolis, MN*, 103

Jensen CM, Boeckstyns MEH and Kristiansen B (1986): Silastic arthroplasty in rheumatoid MCP-joints. *Acta Orthop Scan*, 57: 2: 138-140

Jones W R, Hady W F, Crugnola A (1981): Effect of irradiation on the friction and wear of ultra-high molecular weight polyethylene. *Wear*, 1981, 70: 77-92

Joyce T J (1997): The development of an endoprosthesis for the metacarpophalangeal joint. *Ph.D. Thesis, Durham University*

Joyce T J and Unswoth A (2000a): The design of a finger wear simulator and preliminary results. *Accepted for publication J Engng Med.*

Joyce TJ and Unsworth A (2000b): Comparison of lubricant absorption between loaded and unloaded XLPE prostheses. *Trans. British Orthop. Res. Soc.*, in press

Joyce TJ, Ash HE and Unsworth A (1996): The wear of cross-linked polyethylene against itself. *Proc. Instn. Mech. Engrs.*; 210(1): 11-16

Joyce TJ, Unsworth A, Cartwright TM and Monk D (1998): Preliminary comparison of the wear of silane XLPE with that of UHMWPE, both polymers rubbing against hard interfaces. *Trans British Orthop Res Soc.*, 19.

Joyce TJ, Vandelli C, Cartwright TM, Dalla Mura M and Unsworth A (2000c): Influence of the lubricant on the wear of cross-linked polyethylene against itself. *Trans. British Orthop. Res. Soc., in press*

Kessler I (1974): A new silicone implant for replacement of destroyed metacarpal heads. *The Hand*,6: 3: 308-310

Kirschenbaum D, Schneider LH, Adams DC and Cody RP (1993): Arthroplasty of the metacarpophalangeal joints with use of silicone-rubber implants in patients who have rheumatoid arthritis. *J Bone Jt Surg*, 75A: 1: 3-12

Klein PG, Gonzales-Orozco JA and Ward IM (1991): Structure and morphology of highly oriented radiation crosslinked polyethylene fibres. *Polymer*, 32: 1732-1736

Kumar P, Oka M, Ikeuchi K, Yamamuro T, Okumura H, Kotoura Y (1991): Low wear rate of UHMWPE against zirconia ceramic (y-psz) in comparison to alumina ceramic and sus 31 alloy. *J. Biomed. Mater. Res.*, 25: 813-828

Kurtz SM, Muratoglu OK, Evans M, Edidin AA (1999): Advances in the processing, sterilization, and crosslinking of ultra-high molecular weight polyethylene for total joint arthroplasty. *Biomaterials,* 20(18): 1659-1688

Lancaster JK (1969): Abrasive wear of polymers. *Wear*, 14, pp.223

Lancaster JK (1990): Material-specific wear mechanisms: relevance to wear modelling. *Wear,* 141: 159-183

Levack B, Stewart HD, Flierenga H and Helal B (1987): Metacarpophalangeal joint replacement with a new prosthesis: Description and preliminary results of treatment with the Helal flap joint. *J Hand Surg*, 12B: 3: 377-381

Liao Y-S, Benya PD and McKellop HA (1999): Effect of protein lubrication on the wear properties of materials for prosthetic joints. *J Biomed Mater Res.*, 48(4): 465-473.

Linn F C, Radin E L (1968): Lubrication of animal joints III – The effect of certain alteration of the cartilage and lubricant. *Arth. Rheum.*, 11: 674-682

Linscheid RL and Beckenbaugh RD (1991): Arthroplasty of the Metacarpophalangeal Joint. In: Morrey B. F. (Ed): *Joint Replacement Arthroplasty. New York, Churchill Livingstone*, 159-172

Linscheid RL and Beckenbaugh RD (1993): Arthroplasty in the Hand and Wrist. *In: Green D. P. (Ed): Operative Hand Surgery (3rd Edn). New York, Churchill Livingstone*, 159-172

Mahoney OM and Dimon JH (1990): Unsatisfactory results with a ceramic total hip prosthesis. *J Bon Jt Surg (Am.),* 72, 663-671

Mannerfelt L and Andersson K (1975): Silastic arthroplasty of the metacarpophalangeal joints in rheumatoid arthritis: lomg-term results. *J Bone Jt Surg,* 57A: 4: 484-489

McArthur PA and Milner RH (1998): A prospective randomized comparison of Sutter and Swanson silastic spacers. *J Hand Surg [Br];* 23(5): 574-577

McCutchen C W (1967): Sponge hydrostatic and weeping bearings. *Nature*, 181: 1284-1285

McKellop H (1981): Wear of artificial joint materials II. Twelve-channel wear screening devices: correlation of experimental and clinical results. *Engng. Med.*, 10: 123-126

McKellop H, Campbell P, Park S-H, Schmalzried TP, Grigoris P, Amstutz HC and Sarmiento A (1995): The origin of submicron polyethylene wear debris in total hip arthroplasty. *Clinical Orthopaedics and Related Research*, 311: 3-20

McKellop H, Clarke I C, Markolf K, Amstutz H (1983): Friction and wear properties of polymer, metal and ceramic prosthetic joint materials evaluated an a multichannel screening device. *J. of Biomed. Mater. Res.*, 15: 619-653

McMaster M (1972): The natural history of the rheumatoid metacarpo-phalangeal joint. *J Bone Jt Surg.*, 54B:687-697.

Millender LH and Nalebuff EA (1973): Metacarpophalangeal joint arthroplasty utilizing the silicone rubber prosthesis. *Orthop Clin North Am* 4:349-371.

Millender LH, Nalebuff EA, Hawkins RB and Ennis R (1975): Infection after silicone prosthetic arthroplasty of the hand. *J Bone Jt Surg*, 57A: 6: 825-829

Minami M, Yamazaki J, Kato S and Ishii S (1988): Alumina ceramic prosthesis arthroplasty of the metacarpophalangeal joint in the rheumatoid hand (a 2-4 year follow-up study). *J Arthritis*, 3, 157-166

Nicolle FV and Calnan JS (1972): A new design of finger joint prosthesis for the rheumatoid hand. *The Hand*, 4: 2: 135-146

Nicolle FV and Gilbert S (1979): Assessment of past results and current practice in the treatment of rheumatoid metacarpophalangeal joints: Five years review. *The Hand*, 11: 2: 151-156

Niebauer JJ and Landry RM (1971): Dacron-silicone prosthesis for the metacarpophalangeal and interphalangeal joints. *The Hand*, 3: 1: 55-61

Niebauer JJ, Shaw JL and Doren WW (1969): Silicone-dacron prosthesis: Design, evaluation and application. *Annals of the Rheumatic Diseases*, 28: 5(supplement): 56-58

Niebauer JJ, ShawJL and Doren WW (1968): The silicone-dacron hinge prosthesis: Design, evaluation and application. *J Bone Jt Surg*, 50A: 3: 634

Nordin M and Frankel V H (1989): Basic biomechanics of the muscoloskeletal system. *Lea & Febiger; Philadelphia, London.* pp.300

O'Kelly J, Unsworth A, Dowson D, Hall D A, Wright V (1978): A study of the role of synovial fluid and its constituents in the friction and lubrication of human hip joints. *Engng. Med.*, 7: 73-83

Oonishi H (1995): Long term clinical results of THR. Clinical results of THR of an alumina head with a cross-linked UHMWPE cup. *Orthop. Surg. and Traumatol.*, 38: 1255-1264

Oonishi H, Takayama Y and Tsuji E (1992): Improvement of polyethylene by irradiation in artificial joints. *Radiat. Phys. Chem..*, 39(6): 495-504

Pagowski S and Piekarski K (1977): Biomechanics of metacarpophalangeal joint. *J Biomech*; 10(3): 205-209

Paul J P (1997): Development of standards for orthopaedic implants. *Proc Inst Mech Eng [H]*, 211(1): 119-26.

Pooley CM and Tabor D (1972): Friction and molecular structure: the behaviour of some thermoplastics. *Proc. Royal Soc. London*, 329A: 251-258

Radin, E.L. and Paul, I.L (1972): A consolidated concept of joint lubrication. *J. Bone Jt Surg.*, 54-A(3): 607-616

Ratner SB, Farberova II, Radyukevich OV and Lur'e EG (1967): Connection between wear resistance of plastics and other mechanical properties. In: James DI, editor, *Abrasion of rubber. London: MacLaren and Sons*, pp.145

Rhodes K, Jeffs JV and Scott JT (1972): Experience with silastic prostheses in rheumatoid hands. *Annals of the Rheumatic Diseases*, 31: 2: 103-108

Ries MD, Weaver K, Beals N (1996): Safety and efficacy of ethylene oxide sterilized polyethylene in total knee arthroplasty. *Clin Orthop.*, (331): 159-163.

Rimnac CM, Klein RW, Betts F, Wright TM (1994): Post-irradiation aging of ultra-high molecular weight polyethylene. *J Bone Joint Surg Am.*, 76(7): 1052-1056.

Roberts B J , Unsworth A, Mian (1982): Modes of lubrication in human hip joints. *Ann. Rheum. Dis.*, 41: 221-224

Saikko V (1992a): A simulator study of friction in total replacement hip joints. *Proc Inst Mech Eng [H]*, 206(4): 201-211.

Saikko V, Paavolainen P, Kleimola M, Statis P (1992b): A five-station hip joint simulator for wear rate studies. *Proc Inst Mech Eng [H]*, 206(4): 195-200.

Scales J, Kelly P, Goddard D (1969): Friction torque studies of total hip replacements - the set of a simulator. *In Wright V. (ed): Lubrication and wear in joints, Sector Publishing Ltd,* 88

Schetrumpf J (1975): A new metacarpophalangeal joint prosthesis. *The Hand*, 7, 75-77

Schmidt K, Michlke RK and Witt K (1996): Status of endoprosthesis in rheumatoid metacarpophalangeal joints. Lon-term results of metacarpophalangeal prostheses using Swanson's silastic spacers. *Hanchir Mikrochir Plast Chir*, 28(5): 254-64

Scholes SC, Hall RM, Unsworth A, Scott R (1997): The effects of material combinations and lubricant on the friction of total hip prostheses *JBJS, 79B, 464.*

Scholes S C, Unsworth A (2000): Comparison of friction and lubrication of different hip prostheses" *Proc Inst Mech Eng [H]*, 214(1): 49-57.

Schultz RJ, Johnston AD and Kristhnamurthy S (1987): Thermal effects of polymerisation of methyl-methacrylate on small tubular bones. *International Orthopaedics*, 11: 277-282

Shanbhag AS, Bailey HO, Hwang DS, Cha CW, Eror NG and Rubash HE (2000): Quantitative analysis of ultrahigh molecular weight polyethylene (UHMWPE) wear debris associated with total knee replacements. *J. Biomed. Mater. Res.*, 53(1): 100-110

Shapiro JS, Heigna W, Nasatir S et al. (1971): The relationship of wrist motion to ulnar phalangeal drift in the rheumatoid patient. *Hand,* 3: 68.

Shen C, Dumbleton J H (1974): The friction and wear behaviour of irradiated very high molecular weight polyethylene. *Wear*, 30: 349-364

Sibly T F and Unsworth A (1991): Wear of cross-linked polyethylene against itself: a material suitable for surface replacement of the finger joint. *J. Biomed. Engng*, 13: 217-220

Skinner H B (1999): Ceramic bearing surfaces. *Clin Orthop.*, (369): 83-91

Smith EM, Juvinall C, Bender LF and Pearson JR (1966): Flexor forces and rheumatoid metacarpophalangeal deformity. *J. Am. Med. Ass.* 198, 150

Steffee AD, Beckenbaugh RD, Linscheid RL and Dobyns JH (1981): The development, technique, and early clinical results of total joint replacement for the metacarpophalangeal joint of the fingers. *Orthopedics*, 4: 2: 175-180

Stewart T, Jin Z M, Fisher J (1997): Friction of composite cushion bearings for total knee joint replacements under adverse lubrication conditions. *Proc Inst Mech Eng [H]*, 211(6): 451-465.

Stirrat CR (1996): Metacarpophalangeal joints in rheumatoid arthritis of the hand. *Hand Clin.*, 12:515-529.

Stokoe S M, Unsworth A, Viva C and Haslock I (1990): A finger function simulator and the laboratory testing of joint replacements. *Proc. Instn. Mech. Engrs, Part H*, 204: 233-240

Sutula LC, Collier JP, Saum KA, Currier BH, Currier JH, Sanford WM, Mayor MB, Wooding RE, Sperling DK, Williams IR, et al. (1995): The Otto Aufranc Award. Impact of gamma sterilization on clinical performance of polyethylene in the hip. *Clin Orthop.*, (319): 28-40.

Swanson AB (1968): Silicone rubber implants for replacement of arthritic or destroyed joints in the hand. *Surg Clinics of North America*, 48, 5: 1113-1127

Swanson AB (1969): Finger joint replacement by silicone rubber implants and the concept of implant fixation by encapsulation. *Annals of the Rheumatic Diseases*, 28, 5 (supplement): 47-55.

Swanson AB (1972a): Flexible implant arthroplasty for arthritic finger joints. *J Bone Jt Surg,* 54A: 3: 435-456

Swanson AB (1972b): Flexible implant resection arthroplasty. *The Hand,* 4: 2: 119-132.

Swanson AB, Poitevin LA DeGroot-Swanson G and Kearney J (1986): Bone remodelling phenomena in flexible implant arthroplasty in the metacarpophalangeal joints. Long term study. *Clin. Orthop.Rel. Res.,* 205: 254-262

Taleisnik J (1989): Rheumatoid arthritis of the wrist. *Hand Clin.,* 5: 257-278

Tamai K, Ryu J, An K N, Linscheid R L, Cooney W P and Chao Y S (1988): Three dimensional geometric analysis of the metacarpophalangeal joint. *J Hand Surg.,* 13A: 521-529

Tanner R I (1966): An alternative mechanism for the lubrication of synovial joints. *Phys. Med. Biol.,* 11: 119-127

Tubiana R (1969): Anatomical and phisiopathological features *In the Rheumatoid Hand. Edited by Tubiana R. with the collaboration of Archach P. C. et al. Group d'Etude de le main. Paris, L'Expansion Scientifique Française,* pp 23-31.

Tubiana R (1980): Traite` de Chirurgie de la Main, vol. 1, *Churchill Livingstone, New York,* p. 2.

Unsworth A (1978): The effects of lubrication in hip joint prostheses. *Phys. Med. Biol.,* 23: 253-268

Unsworth A (1991): Tribology of human and artificial joints. *Proc Inst Mech Eng [H],* 205(3): 163-172

Unsworth A and Alexander WJ (1979): Dimensions of the metacarpophalangeal joint with particular reference to joint prostheses. *Engng Med,* 8: 75-80

Unsworth A, Dowson D and Wright V (1971): 'Cracking joints'. A bioengineering study of cavitation in the metacarpophalangeal joint. *Ann Rheum Dis.*, 30(4): 348-358

Unsworth A, Dowson D and Wright V (1975): *Ann. Rheum. Dis.*, 34, 277

Unsworth A, Dowson D, Wright V, Koshal (1974): The frictional behaviour of human synovial joints – Part II: artificial joints. *Jour. Lub. Tech.*

Vainio K (1989): Vainio atrhroplasty of the metacarpophalangeal joints in rheumatoid arthritis. *J Hand Surg*; 14A: 367-368

Walker P.S. *et al.* (1968): 'Boosted lubrication' in synovial joints by fluid entrapment and enrichment. *Ann. Rheum. Dis.*, 27: 512-520

Walker PS and Erkman MJ (1975): Laboratory evaluation of a metal-plastic type of metacarpophalangeal joint prosthesis. *Clin Orthop*, 112: 349-356

Wang A, Essner A, Polineni VK, Stark C and Dumbleton JH (1998): Lubrication and wear of ultra-high molecular weight polyethylene in total joint replacements. *Tribology International*, 31(1-3): 17-33

Wang A, Stark C and Dumbleton JH (1996): Mechanistic and morphological origins of ultra-high molecular weight polyethylene wear debris in total joint replacement prostheses. *Proc. Inst. Mech. Engrs, Part H: J. Eng. Med.*, 210: 141-155

Wang A, Sun DC, Stark C and Dumbleton JH (1995): Wear mechanisms of UHMWPE in total joint replacement. *Wear*, 181-183, pp. 241-249

Weightman B, Simon S, Paul I, Rose R, Radin E (1972a): Lubrication mechanisms of UHMWPE in total joint replacements. *J. Lub.Tech*, 94: 131-135

Weightman B, Simon S, Rose R, Paul I and Radin E (1972b): Enviromental fatigue testing of silastic finger joint prostheses. ***J. Biomed. Mat. Res. Symposium***, 3: 15-24

White SE, Paxson RD, Tanner MG and Whiteside LA (1996): Effects of sterilization on wear in total knee arthroplasty. *Clin. Orthop.*, 331: 164-171

Wilson YG, Sykes PJ and Niranjan NS (1993): Long-term follow-up of Swanson's silastic arthroplasty of the metacarpophalangeal joints in rheumatoid arthritis. *J Hand Surg*, 18B: 1: 81-91

Wirth MA, Agrawal CM, Mabrey JD, Dean DD, Blanchard CR, Miller MA and Rockwood CA Jr (1999): Isolation and characterization of polyethylene wear debris associated with osteolysis following total shoulder arthroplasty. *J. Bone Jt Surg.*, 81(1): 29-37

Wroblewski BM, Siney PD, Dowson D, Collins SN (1996): Prospective clinical and joint simulator studies of a new total hip arthroplasty using alumina ceramic heads and cross-linked polyethylene cups. *J Bone Joint Surg Br.*, 78(2): 280-285.

Wroblewski BM, Siney PD, Fleming PA (1999): Low-friction arthroplasty of the hip using alumina ceramic and cross-linked polyethylene. A ten-year follow-up report. *J Bone Joint Surg Br.*, 81(1): 54-55.

Youm Y, Gillespie TE, Flatt AE and Sprague BL (1978): Kinematic investigation of normal MCP joint. *J Biomech*, 11(3): 109-118.

Zancolli E (1979): *Structural and Dynamic Bases of Hand Surgery, ed 2. Philadelphia, JB Lippincott*, 325-360.

APPENDIX A

Theory section on the Sibly-Unsworth prosthesis

Contact pressure

The contact pressure on the spherical bearing surfaces can be calculated from the internal joint forces. Since the prosthesis is designed for joint replacement in rheumatoid arthritis, it needs to be capable of transmitting the maximum internal load that acts on the MCP joint of a rheumatoid hand. However, internal forces acting on the MCP joint cannot be measured directly, therefore they have to be estimated from external forces. The force across the MCP joint during pinch grip has been given as 3.6P to 5.6P (Weightman and Amis, 1982), which means that if P is the external force measured, the maximum resultant internal force is up to 5.6 times the external force. Therefore, for an average external force of 70 N (Mathiowetz et al., 1985; Walker et al., 1978) which occurs during gripping, the resultant internal force is assumed to be 392 N for a normal hand. However, in a rheumatoid hand, the average external force for pinch grip is approximately 19 N (Walker et al., 1978), which gives a resultant internal "pinch" force of 106 N.

The bearing surfaces were designed such that the radii of the metacarpal and proximal phalanx components were equal, for many different reasons. The main reason is probably the need to minimise the contact stresses on the components by maximising the contact area. The centre of rotation is fixed as the two surfaces are conforming, therefore under the same load the contact area between the two spherical bearing surfaces remains constant no matter what angle of flexion the joint was positioned at. The contact area is also the same no matter what materials are used to manufacture the bearing surfaces.

The contact area between the two components is the phalangeal component area, which could be calculated by integrating the equation of a sphere on the space:

$$z(x,y) = \sqrt{x^2 + y^2 - r^2}$$

on the ellipse domain, where the ellipse is the horizontal projection of the phalangeal component on the plane:

$$\frac{x^2}{a^2} + \frac{y^2}{b^2} = 1$$

with a and b being half value of the relative diagonals of the ellipse.

Thus the integral becomes:

$$A = 4\int_0^a \int_0^{b\sqrt{1-\frac{x^2}{a^2}}} \sqrt{1 + \left(\frac{\partial z}{\partial x}\right)^2 + \left(\frac{\partial z}{\partial y}\right)^2}\, dx \cdot dy = 4\int_0^a dx \int_0^{b\sqrt{1-\frac{x^2}{a^2}}} \sqrt{1 + \left(\frac{x^2 + y^2}{r^2 - x^2 - y^2}\right)}\, dy$$

The integral can also be written as:

$$A = 4\int_{\sigma_{x,y}} \sqrt{\left(\frac{r^2}{r^2 - x^2 - y^2}\right)}\, dx\, dy$$

where $\sigma_{x,y=}\left\{\left(\frac{x}{a}\right)^2 + \left(\frac{y}{b}\right)^2 \le 1\right\}$

If I now change the co-ordinates:

$$u = \frac{x}{a}$$

$$v = \frac{y}{b}$$

the integral becomes:

$$A = 4\int_{\sigma_{u,v}} ab\sqrt{\left(\frac{r^2}{r^2 - a^2u^2 - b^2v^2}\right)}\, du \cdot dv$$

$$\sigma_{u,v=}\left\{u^2 + v^2 \leq 1\right\}$$

It is now possible to simplify the integral using polar co-ordinates:

$$u = \rho\cos\theta$$

$$v = \rho\sin\theta$$

And the integral finally becomes:

$$A = 4\int_0^{\frac{\pi}{2}}\int_0^1 \frac{abr\rho}{\sqrt{r^2 - a^2\rho^2\cos^2\theta - b^2\rho^2\sin^2\theta}} d\rho \cdot d\theta$$

The calculation using Maple V gave the final result:

A= 84.53mm^2

for the 7.5mm-radius prosthesis.

Assuming maximum joint loading conditions (F) of 106 N during "pinch" grip; for a metacarpal radius $(R_x)_1$ of 7.5mm, the mean contact pressure which occurs between two bearing surfaces would therefore be 1.25MPa:

$$\text{Contact pressure (P)} = \frac{\text{Load (F)}}{\text{Area (A)}} = \frac{106\text{N}}{84.53\text{mm}^2} = 1.25\text{MPa}$$

While if the load during flexion-extension is assumed to be L = 10-15N (Tamai et al., 1988), the maximum mean contact pressure during this movement would be:

$$\text{Contact pressure (P)} = \frac{\text{Load (F)}}{\text{Area (A)}} = \frac{15\text{N}}{84.53\text{mm}^2} = 0.18\text{MPa}$$

On the Durham MCP prosthesis production drawings a geometrical tolerance of 0±0.5 has been reported. Therefore if the proximal phalanx bearing surface is 0.05mm larger in radius than the corresponding metacarpal radius, the contact area between the two components could be calculated using the Hertzian theory of elastic contact (Hertz, 1896, Timoshenko and Goodier, 1970). If "a" is the radius of the circular area of contact between the bearing surfaces, we have:

$$a = \sqrt[3]{\frac{3\pi F(k_1 + k_2)}{4\left(\frac{1}{R_H} - \frac{1}{R_C}\right)}}$$

(1)

k_1 and k_2 are defined as:

$$k_1 = \frac{1 - \upsilon_1^{\,2}}{\pi E_1}$$

$$k_2 = \frac{1 - \upsilon_2^{\,2}}{\pi E_2}$$

being E_1 and E_2 the Young's moduli of the two materials, and υ_1 and υ_2 their Poisson's ratios.

The ball (metacarpal head) and socket (phalangeal cup) are pressed together by a force F and the radii of the metacarpal head and phalangeal cup are given by R_H and R_C respectively. In our case, as both the components are manufactured using the same material (XLPE), we have:

$E_1=E_2=1GPa$ $\upsilon_1=\upsilon_2=0.4$

therefore

$k_1=k_2=0.27\cdot10^{-9}$/Pa

The contact radius becomes:

a=5.35mm during "pinch" grip and
a=2.79mm during flexion-extension.

The contact pressure distribution over the contact area is semi-ellipsoidal in shape where the maximum contact pressure "P_o" occurs at the centre:

$$P_o=\frac{3F}{2\pi a^2} \tag{2}$$

and its value is P_o=1.77MPa during "pinch" grip and P_o=0.92MPa during flexion-extension. The materials used in the analysis were assumed to be of an incompressible material, of infinite thickness and possess smooth surfaces. Combining equation (1) and (2) it is possible to notice that as the radius of the proximal phalanx bearing surface is decreased, the contact pressures decrease due to an increase in the contact radius. Thus, the smallest contact pressures are achieved when the radii of the metacarpal and proximal phalanx are equal since this is the design condition where the contact radius is maximum.

Lubrication

The nature of the lubrication of the MCP prosthesis depends on the materials used for the bearing surfaces, the geometry of the bearing surfaces and operating conditions. The formula relating to the case of the semi-infinite solid was used to calculate the minimum film thickness ($h_{s,\,min}$) for the equivalent sphere on a rigid plane (Hamrock and Dowson, 1978):

$$\frac{h_{s,\min}}{2R}=2.789\left(\frac{\eta u}{2E^*R}\right)^{0.65}\left(\frac{F}{4E^*R^2}\right)^{-0.21}$$

where

$$\frac{1}{E^*} = \frac{1}{2}\left(\frac{1-\upsilon^2_1}{E_1} + \frac{1-\upsilon^2_2}{E_2}\right) = \frac{1-\upsilon^2}{E}$$

Unlike a hip or a knee joint, high forces only occur during static conditions. Few situations occur in the MCP joint where high loads are accompanied with movement. During dynamic conditions the forces (F) are quite low and have been estimated at 10-15N (Tamai et al., 1988). The lubricant was assumed to be isoviscous and incompressible with viscosity (h) of 0.001 Pa s, simulating the conditions which occur in hands affected by rheumatoid arthritis (Cooke et al., 1978). The entraining velocity (u) was assumed to be 0.041 ms^{-1}.

The minimum film thickness is primarily dependent on the contact radius. From a lubrication design prospective it is therefore advantageous to increase the contact radius by designing a pair of closely conforming bearing surfaces with a small radial clearance in order to achieve the maximum lubricating film thickness.

The lubrication regime under which the MCP prosthesis operates can be analytically determined by calculating the dimensionless film thickness ratio (Λ). The RMS surface roughness ($R_{q,1 \text{ or } 2}$) can be calculated from the following equation (Hamrock, 1994):

$$R_{q,1or2} = R_a\left(\frac{\pi}{2\sqrt{2}}\right)$$

where R_a is the centre line average surface roughness and is R_a=0.4μm for XLPE. Thus, the effective RMS surface roughness for the bearing surface arrangement can be calculated as (Hamrock, 1994):

$$R_q = \left(R^2_{q,1} + R^2_{q,2}\right)^{1/2}$$

Hence, the dimensionless film thickness ratio (Λ) can be calculated (Hamrock, 1994):

$$\Lambda = \frac{h_{s,\min}}{R_q}$$

If Λ is grater than three, then the prosthesis would operate with a continuous film of lubricant separating the bearing surfaces under an elastohydrodynamic lubrication regime. This is the optimum condition. If Λ is less than three but grater than one, some contact between the bearing surfaces may occur and the prosthesis would operate under a mixed lubrication regime. If Λ is less than one, the bearing surfaces would be in contact and prosthesis would operate under a boundary lubrication regime.

The result of the calculation for XLPE against itself, under conditions which occur in hands affected by rheumatoid arthritis, is:

$$\Lambda = \frac{h_{s,\min}}{R_q} = \frac{0.15 \cdot 10^{-9} m}{0.63 \cdot 10^{-6} m} = 0.24 \cdot 10^{-3}$$

therefore the prosthesis would operate under a boundary lubrication regime.

When designing MCP prosthesis, the smallest contact pressures are required, thus it is better to have equal radii bearing surfaces. This also allows the largest film thickness to be produced.

Material choice

The two-piece all XLPE MCP prosthesis was manufactured with conforming bearing surfaces, thus the contact pressures are the lowest possible also compared with other material combinations. The film thickness is also large relative to other

material combinations due to the rough bearing surfaces (Beevers and Seedhom, 1995).

However, lubrication theory suggests that the prosthesis would operate in the boundary lubrication regime, therefore there may be contact between the two bearing surfaces resulting in wear. Simple wear theory predicts that wear is proportional to load (Archard, 1953; Halling, 1976; Teer and Arnell, 1979), thus since few situations occur when high loads are accompanied with movement, it would seem that wear would not be a significant problem in MCP prosthetic design. However, the surface prosthesis is designed to be implanted at an early stage of rheumatoid arthritis, therefore the life expectancy of the surface prosthesis is much greater than those of current MCP prostheses. Since the wear rate for similar polymer bearing surfaces is high in comparison to other material combination (ref), the choice of the material becomes very important. A study on the comparison between the wear behaviour of UHMWPE sliding against itself and XLPE rubbing against itself was therefore carried out (Joyce and Unsworth, 1996). Non-irradiated UHMWPE showed wear factors over 100 times higher than those of irradiated XLPE against itself. Therefore, considering how important is wear and especially the quantity of wear debris for life expectancy of a prosthetic joint, this result was one of the reason why the combination XLPE against itself was preferred for manufacturing the two pieces Durham MCP joint.

APPENDIX B

Finger Wear Simulator Test Results: Tables of Weight Change

R=7.5mm

NON-IRRADIATED XLPE rubbing against itself in DISTILLED WATER

Initial Weight	Metacarpal Test	Phalangeal Test	Metacarpal Control	Phalangeal Control
mg	361.2	205.3	360.4	204.8

Tab. B.1

Weight Change (in $n \times 10^{-4}$ g)

Cycles	Metacarpal Test	Phalangeal Test	Metacarpal Control	Phalangeal Control
0	0	0	0	0
296,080	0	-1	0	-1
548,600	-1	-1	0	-1
827,110	-2	-1	+1	0
1,025,182	-3	-2	0	0
1,518,925	-3	-2	0	0
2,056,217	-3	-2	0	0
2,567,343	-3	-1	+1	+1
2,991,807	-3	-1	+1	+1
3,580,370	-2	-1	+1	0
4,085,938	-2	-1	+1	0
4,602,937	-2	-1	0	0
5,005,109	-2	-1	0	0
5,524,081	-2	-1	+1	0
5,524,092	-3	0	0	0
6,004,124	-2	-1	0	0
6,509,045	-3	-1	0	0
7,059,709	-3	-1	0	0
7,500,062	-2	-1	0	0
8,000,715	-2	0	+1	+1
8,506,977	-2	-1	+1	0
9,003,117	-2	-1	+1	0
9,556,392	-2	-1	+1	+1
10,021,382	-3	-1	0	0
10,558,483	-3	-1	0	0
11,011,142	-2	-1	+1	0
11,604,121	-3	-1	+1	+1
12,012,153	-7	-2	0	0
12,506,389	-7	-1	0	0
13,046,443	-8	-2	0	0
13,501,562	-9	-1	0	0
14,082,423	-13	-3	0	0
14,506,707	-13	-3	0	0

Tab. B.2

R=8.5mm

NON-IRRADIATED XLPE rubbing against itself in DISTILLED WATER

mg	Metacarpal Test	Phalangeal Test	Metacarpal Control	Phalangeal Control
Initial Weight	479.9	234.7	474.4	232.9

Tab. B.3

Weight Change (in $n \times 10^{-4}$ g)

Cycles	Metacarpal Test	Phalangeal Test	Metacarpal Control	Phalangeal Control
0	0	0	0	0
411,738	+1	0	-2	0
891,388	0	0	-1	+1
1,293,089	0	0	-2	+1
1,650,973	-1	0	-2	+1
2,151,685	0	0	-1	+1
2,652,150	-1	0	-1	+1
3,206,291	-3	-1	-2	0
3,686,115	-3	0	-2	+1
4,156,475	-5	-1	-2	0
4,628,977	-5	-1	-1	+1
5,014,380	-5	0	-1	+1
5,498,171	-5	0	-1	+1
6,015,233	-6	0	-1	+1
6,511,322	-5	0	-1	+2
6,725,891	-6	0	-1	+2
6,725,891	-6	-1	-2	+1
7,082,291	-6	0	-2	+1
7,573,214	-6	-1	-2	+1
8,091,172	-5	0	-1	+2
8,514,715	-5	0	-1	+1
9,132,125	-5	0	-2	+1
9,617,343	-5	0	-1	+2
10,081,001	-6	-1	-2	+1
10,529,121	-4	0	-1	+2
11,019,398	-5	0	-5	+1
11,556,154	-4	+1	-3	+2
12,019,630	-6	0	-4	+2
12,500,150	-9	-1	-4	+2
12,960,997	--12	-2	-4	+2
13,476,001	-17	-2	-5	+2
14,042,768	-19	-3	-5	+1

Tab. B.4

R=9.4mm

GAMMA-IRRADIATED XLPE rubbing against itself in RINGERS SOLUTION

mg	Metacarpal Test	Phalangeal Test	Metacarpal Control	Phalangeal Control
Initial Weight	743.4	229.2	751.7	228.8

Tab. B.5

Weight Change (in $n \times 10^{-4}$ g)

Cycles	Metacarpal Test	Phalangeal Test	Metacarpal Control	Phalangeal Control
0	0	0	0	0
391,353	0	-1	+2	+1
824,149	0	-1	+2	+1
1,195,650	0	-1	+3	+1
1,532,028	-1	-1	+2	+1
2,018,075	-4	-4	+2	+3
2,512,892	-10	-7	+2	+3
3,062,333	-16	-8	+1	+2
3,538,660	-18	-9	+1	+2
4,007,494	-20	-11	0	+2
4,477,407	-22	-11	+1	+2
5,022,960	-22	-11	0	+2
5,497,946	-26	-12	0	+2
6,111,370	-29	-13	-1	+2
6,302,505	-29	-13	0	+2
6,302,505	-29	-13	0	+3
6,530,988	-29	-14	-1	+2
7,054,505	-30	-14	-1	+2
7,568,066	-38	-14	-1	+2
8,016,378	-48	-16	-2	+2
8,485,886	-54	-15	-2	+1

Tab. B.6

R = 9.4 mm

GAMMA-IRRADIATED XLPE rubbing against itself

Tested DRY at FLEX.-EXT. only

mg	Metacarpal Test	Phalangeal Test
Initial Weight	747.5	230.8

Tab. B.7

Weight Change (in $n \times 10^{-4}$ g)

Cycles	Metacarpal Test	Phalangeal Test
0	**0**	**0**
246,150	**+10**	**+2**
508,662	**+12**	**+3**
750,076	**+13**	**+3**
1,062,799	**+15**	**+3**
1,587,945	**+17**	**+4**
1,993,723	**+19**	**+6**
2,586,165	**+30**	**+8**
3,009,628	**+40**	**+15**
3,181,511	**+47**	**+19**

Tab. B.8

R = 9.4 mm

GAMMA-IRRADIATED XLPE rubbing against itself

Tested DRY at FLEX.-EXT. + ROTATION

mg	Metacarpal Test	Phalangeal Test
Initial Weight	650.2	197.6

Tab. B.9

Weight Change (in $n \times 10^{-4}$ g)

Cycles	Metacarpal Test	Phalangeal Test
0	**0**	**0**
145,065	**+2**	**+4**
215,798	**+2**	**+5**
355,859	**+2**	**+7**
504,848	**+4**	**+8**
754,656	**+6**	**+9**
1,009,851	**+9**	**+12**
1,400,274	**+15**	**+20**
1,999,563	**+25**	**+24**
2,518,892	**+29**	**+30**
2,923,585	**+34**	**+33**

Tab. B.10

R=7.5mm

EtO-IRRADIATED XLPE PROSTHESIS rubbing against itself

in DISTILLED WATER

mg	Metacarpal Test	Phalangeal Test	Metacarpal Control	Phalangeal Control
Initial Weight	368.4	206.1	365.2	206.3

Tab. B.11

Weight Change (in $n \times 10^{-4}$ g)

Cycles	Metacarpal Test	Phalangeal Test	Metacarpal Control	Phalangeal Control
0	**0**	**0**	**0**	**0**
262,833	**0**	**0**	**+1**	**0**
500,396	**-3**	**-1**	**+1**	**0**
894,416	**-6**	**-3**	**+1**	**0**
1,517,244	**-11**	**-4**	**+1**	**0**
2,483,822	**-15**	**-6**	**+1**	**0**
3,128,267	**-16**	**-8**	**+1**	**0**
3,575,980	**-19**	**-9**	**+1**	**0**
4,007,094	**-19**	**-10**	**+1**	**+1**
4,539,398	**-19**	**-10**	**+1**	**0**
5,008,729	**-20**	**-10**	**+1**	**0**

Tab. B.12

R=8.5mm

EtO-IRRADIATED XLPE PROSTHESIS rubbing against itself

in DISTILLED WATER

mg	Metacarpal Test	Phalangeal Test	Metacarpal Control	Phalangeal Control
Initial Weight	481.3	233.4	479.8	233.7

Tab. B.13

Cycles	Metacarpal Test	Phalangeal Test	Metacarpal Control	Phalangeal Control
0	**0**	**0**	**0**	**0**
1,214,472	**-25**	**-14**	**+2**	**0**
1,679,465	**-33**	**-18**	**+2**	**0**
2,167,812	**-37**	**-20**	**+2**	**0**
2,696,375	**-40**	**-21**	**+2**	**0**
3,110,097	**-41**	**-21**	**+2**	**0**
3,641,941	**-42**	**-21**	**+2**	**0**
4,152,797	**-44**	**-22**	**+2**	**+1**
4,552,873	**-45**	**-23**	**+3**	**+1**
5,110,889	**-46**	**-23**	**+2**	**+1**

Tab. B.14

R=7.5mm

EtO-IRRADIATED XLPE PROSTHESIS rubbing against itself

in BOVINE SERUM

mg	Metacarpal Test	Phalangeal Test	Metacarpal Control	Phalangeal Control
Initial Weight	379.0	206.5	372.4	206.7

Tab. B.15

Weight Change (in $n \times 10^{-4}$ g)

Cycles	Metacarpal Test	Phalangeal Test	Metacarpal Control	Phalangeal Control
0	**0**	**0**	**0**	**0**
586,935	**+9**	**+5**	**+8**	**+5**
1,093,310	**+11**	**+6**	**+10**	**+5**
1,454,309	**+8**	**+4**	**+10**	**+5**
2,041,159	**+12**	**+6**	**+12**	**+6**
2,536,322	**+10**	**+5**	**+12**	**+6**
3,076,303	**+11**	**+5**	**+13**	**+7**
3,594,675	**+11**	**+5**	**+13**	**+7**
3,736,648	**+10**	**+5**	**+13**	**+7**

Tab. B.16

R=8.5mm

EtO-IRRADIATED XLPE PROSTHESIS rubbing against itself

in BOVINE SERUM

mg	Metacarpal Test	Phalangeal Test	Metacarpal Control	Phalangeal Control
Initial Weight	482.6	224.4	482.6	235.5

Tab. B.17

Cycles	Metacarpal Test	Phalangeal Test	Metacarpal Control	Phalangeal Control
0	**0**	**0**	**0**	**0**
887,841	**+21**	**+11**	**+20**	**+10**
1,171,270	**+23**	**+13**	**+17**	**+7**
1,585,653	**+21**	**+12**	**+16**	**+6**
2,011,248	**+18**	**+11**	**+16**	**+7**
2,523,502	**+12**	**+9**	**+13**	**+5**
3,004,187	**+11**	**+9**	**+14**	**+6**

Tab. B.18

APPENDIX C

Finger Friction Simulator Test Results

Steady state friction test using UHMWPE cup/Ti head in distilled water

N. of Cycles	Friction Factor 1	Friction Factor 2	Friction Factor 3
0	0.06	0.06	0.06
50	0.06	0.06	0.06
100	0.07	0.06	0.06
150	0.07	0.06	0.05
200	0.08	0.07	0.06
250	0.08	0.06	0.06
300	0.08	0.06	0.06
350	0.07	0.06	0.06
400	0.07	0.07	0.06
450	0.08	0.07	0.06
500	0.08	0.07	0.06
550	0.08	0.06	0.06
600	0.09	0.08	0.06
650	0.09	0.08	0.06
700	0.09	0.08	0.07
750	0.09	0.08	0.07
800	0.09	0.08	0.06
850	0.08	0.08	0.06
900	0.08	0.08	0.06
950	0.08	0.08	0.06
1000	0.09	0.08	0.06

Tab. C.1

Stribeck curve for UHMWPE/Ti

N. of Cycles	Friction Factor
40	0.10
80	0.09
120	0.10
Average	**0.10**
Standard Deviation	**0.01**

Tab. C.2

Z	f	f
1.95E-9	0.1	0.12
6.42E-9	0.09	0.09
2.00E-8	0.08	0.09
5.82E-8	0.08	0.07
1.96E-7	0.07	0.06
1.90E-6	0.04	0.03
9.49E-6	0.03	0.03
5.69E-5	0.08	0.07

Tab. C.3

Stribeck curve for UHMWPE/Stainless Steel

N. of Cycles	Friction Factor
40	0.15
80	0.12
120	0.11
Average	**0.13**
Standard Deviation	**0.02**

Tab. C.4

Z	f	f
1.95E-9	0.13	0.10
6.42E-9	0.12	0.09
2.08E-8	0.10	0.09
5.76E-8	0.09	0.08
1.96E-7	0.07	0.07
1.90E-6	0.03	0.04
9.49E-6	0.05	0.05
5.69E-5	0.08	0.07

Tab. C.5

Stribeck curve for Ti/Ti

N. of Cycles	Friction Factor
0	0.33
40	0.30
80	0.33
Avergae	**0.32**
Standard Deviation	**0.02**

Tab. C.6

Z	f	f
1.95E-9	0.32	0.35
6.42E-9	0.26	0.26
2.08E-8	0.23	0.26
5.76E-8	0.17	0.20
1.96E-7	0.18	0.18
1.90E-6	0.20	0.24
9.49E-6	0.13	0.23
5.69E-5	0.07	0.22

Tab. C.7

APPENDIX D

Finger Simulator Wear Debris analysis

MASTERSIZER 2000

Result Analysis Report

Sample Name: 1... **SOP Name:** XLPE Cinzia **Measured:** 28 Oct 1999 15:29:35

Sample Source & type: in vitro = polyethylene **Measured by:** Administrator **Analysed:** 28 Oct 1999 15:29:36

Sample bulk lot ref: **Result Source:** Measurement

Particle Name: Default **Accessory Name:** Hydro 2000SM (A) **Obscuration:** 10.65 %

Particle RI: 1.520 **Absorption:** 0.1 **Analysis model:** General purpose

Dispersant Name: Water **Size range:** 0.020 to 2000.000 um **Weighted Residual:** 1.951 %

Dispersant RI: 1.330

---

centration: 0.0052 %Vol **Vol. Weighted Mean D[4,3]:** 88.466 um **Specific Surface Area:** 1.80473 m²/g

Span (10% - 90%): 13.567 **Uniformity:** 13.4542 **Surface Weighted Mean D[3,2]:** 3.325 um

Result units: Volume

d(0.1): 1.279 um d(0.5): 6.361 um d(0.9): 87.583 um

Particle Size Distribution

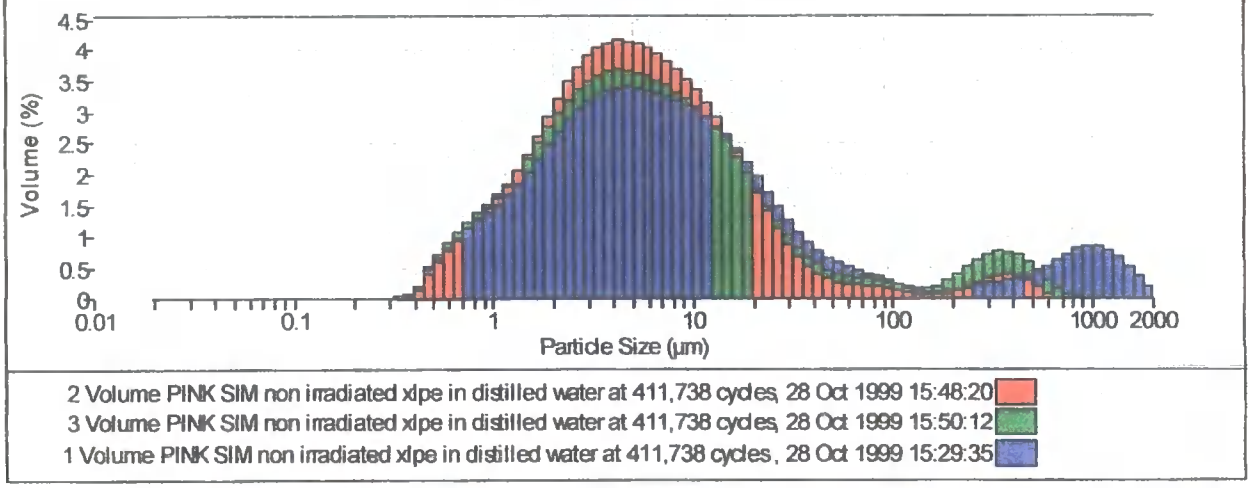

2 Volume PINK SIM non irradiated xlpe in distilled water at 411,738 cycles, 28 Oct 1999 15:48:20

3 Volume PINK SIM non irradiated xlpe in distilled water at 411,738 cycles, 28 Oct 1999 15:50:12

1 Volume PINK SIM non irradiated xlpe in distilled water at 411,738 cycles, 28 Oct 1999 15:29:35

Size (µm)	Volume In %	Size (µm)	Volume In %	Size (µm)	Volume In %	Size (µm)	Volume In %	Size (µm)	Volume In %	Size (µm)	Volume In %
0.020	0.00	0.142	0.00	1.002	1.48	7.096	3.22	50.238	0.55	355.656	0.28
0.022	0.00	0.159	0.00	1.125	1.63	7.962	3.16	56.368	0.48	399.053	0.31
0.025	0.00	0.178	0.00	1.262	1.81	8.934	3.09	63.246	0.43	447.744	0.35
0.028	0.00	0.200	0.00	1.416	2.00	10.024	2.99	70.963	0.38	502.377	0.41
0.032	0.00	0.224	0.00	1.589	2.22	11.247	2.88	79.621	0.33	563.677	0.50
0.036	0.00	0.252	0.00	1.783	2.44	12.619	2.74	89.337	0.28	632.456	0.59
0.040	0.00	0.282	0.00	2.000	2.65	14.159	2.57	100.237	0.22	709.627	0.69
0.045	0.00	0.317	0.00	2.244	2.85	15.887	2.38	112.468	0.16	796.214	0.77
0.050	0.00	0.356	0.03	2.518	3.01	17.825	2.15	126.192	0.12	893.367	0.82
0.056	0.00	0.399	0.17	2.825	3.14	20.000	1.92	141.589	0.09	1002.375	0.81
0.063	0.00	0.448	0.45	3.170	3.24	22.440	1.68	158.868	0.08	1124.683	0.75
0.071	0.00	0.502	0.61	3.557	3.31	25.179	1.44	178.250	0.10	1261.915	0.64
0.080	0.00	0.564	0.80	3.990	3.35	28.251	1.23	200.000	0.13	1415.892	0.50
0.089	0.00	0.632	0.95	4.477	3.36	31.698	1.04	224.404	0.16	1588.657	0.33
0.100	0.00	0.710	1.09	5.024	3.35	35.566	0.88	251.785	0.19	1782.502	0.19
0.113	0.00	0.796	1.22	5.637	3.32	39.905	0.74	282.507	0.22	2000.000	
0.126	0.00	0.893	1.35	6.325	3.28	44.774	0.64	316.979	0.25		
0.142	0.00	1.002		7.098		50.238		355.656			

Operator notes:

MASTERSIZER 2000

Result Analysis Report

mple Name:	3...	**SOP Name:**		**Measured:**	28 Oct 1999 15:50:12
mple Source & type:	ex vivo = polyethylene	**Measured by:**	Administrator	**Analysed:**	29 Oct 1999 17:20:13
mple bulk lot ref:				**Result Source:**	Measurement

rticle Name:	Default		**Accessory Name:**	Hydro 2000SM (A)	**Obscuration:**	8.96	%
rticle RI:	1.520	**Absorption:** 0.1	**Analysis model:**	General purpose			
spersant Name:	Water		**Size range:**	0.020 to 2000.000 um	**Weighted Residual:**	2.028	%
spersant RI:	1.330						

ncentration:	0.0040	%Vol	**Vol. Weighted Mean D[4,3]:**	31.755	um	**Specific Surface Area:**	1.97266 m²/g
an (10% - 90%):	1.367		**Uniformity:**	0.470234		**Surface Weighted Mean D[3,2]:**	3.042 um
sult units:	Number						

d(0.1): 0.449 um d(0.5): 0.632 um d(0.9): 1.312 um

Particle Size Distribution

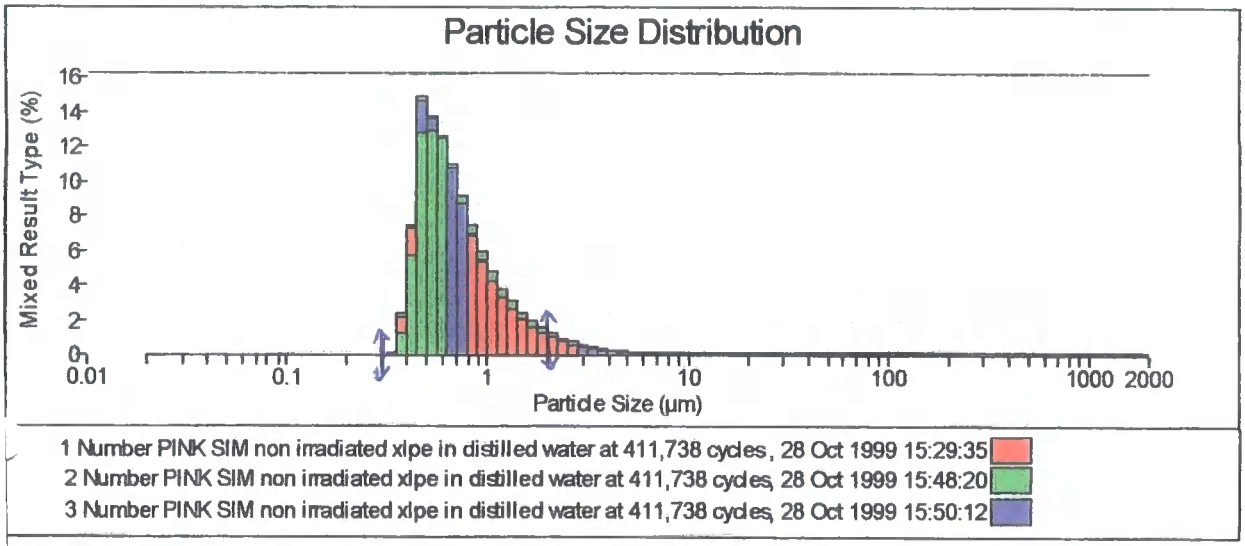

1 Number PINK SIM non irradiated xlpe in distilled water at 411,738 cycles, 28 Oct 1999 15:29:35
2 Number PINK SIM non irradiated xlpe in distilled water at 411,738 cycles, 28 Oct 1999 15:48:20
3 Number PINK SIM non irradiated xlpe in distilled water at 411,738 cycles, 28 Oct 1999 15:50:12

Size (µm)	Volume In %	Size (µm)	Volume In %	Size (µm)	Volume In %	Size (µm)	Volume In %	Size (µm)	Volume In %	Size (µm)	Volume In %
0.020	0.00	0.142	0.00	1.002	4.18	7.096	0.02	50.238	0.00	355.656	0.00
0.022	0.00	0.159	0.00	1.125	3.27	7.962	0.02	56.368	0.00	399.053	0.00
0.025	0.00	0.178	0.00	1.262	2.56	8.934	0.01	63.246	0.00	447.744	0.00
0.028	0.00	0.200	0.00	1.416	2.02	10.024	0.01	70.963	0.00	502.377	0.00
0.032	0.00	0.224	0.00	1.589	1.58	11.247	0.01	79.621	0.00	563.677	0.00
0.036	0.00	0.252	0.00	1.783	1.23	12.619	0.00	89.337	0.00	632.456	0.00
0.040	0.00	0.282	0.00	2.000	0.94	14.159	0.00	100.237	0.00	709.627	0.00
0.045	0.00	0.317	0.01	2.244	0.71	15.887	0.00	112.468	0.00	796.214	0.00
0.050	0.00	0.356	2.31	2.518	0.53	17.825	0.00	126.192	0.00	893.387	0.00
0.056	0.00	0.399	7.37	2.825	0.39	20.000	0.00	141.589	0.00	1002.375	0.00
0.063	0.00	0.448	14.55	3.170	0.29	22.440	0.00	158.868	0.00	1124.683	0.00
0.071	0.00	0.502	13.49	3.557	0.21	25.179	0.00	178.250	0.00	1261.915	0.00
0.080	0.00	0.564	12.42	3.990	0.15	28.251	0.00	200.000	0.00	1415.892	0.00
0.089	0.00	0.632	10.63	4.477	0.10	31.698	0.00	224.404	0.00	1588.657	0.00
0.100	0.00	0.710	8.60	5.024	0.07	35.566	0.00	251.785	0.00	1782.502	0.00
0.113	0.00	0.796	6.88	5.637	0.05	39.905	0.00	282.507	0.00	2000.000	
0.126	0.00	0.893	5.37	6.325	0.04	44.774	0.00	316.979	0.00		
0.142		1.002		7.098		50.238		355.656			

perator notes: the particles present in a number (%) > 10% are 0.4÷0.7 µm in size

MASTERSIZER 2000

Result Analysis Report

Sample Name:	6...	**SOP Name:**	XLPE Cinzia	**Measured:**	29 Oct 1999 14:05:05
Sample Source & type:	In vitro = polyethylene	**Measured by:**	Administrator	**Analysed:**	29 Oct 1999 14:05:06
Sample bulk lot ref:				**Result Source:**	Measurement

Particle Name:	Default		**Accessory Name:**	Hydro 2000SM (A)		**Obscuration:**	8.96 %
Particle RI:	1.520	**Absorption:** 0.1	**Analysis model:**	General purpose			
Dispersant Name:	Water		**Size range:**	0.020 to 2000.000 um		**Weighted Residual:**	1.588 %
Dispersant RI:	1.330						

centration:	0.0056 %Vol	**Vol. Weighted Mean D[4,3]:**	33.770 um	**Specific Surface Area:**	1.37839 m²/g
Span (10% - 90%):	8.104	**Uniformity:**	2.85424	**Surface Weighted Mean D[3,2]:**	4.353 um
Result units:	Volume				
d(0.1):	1.654 um	d(0.5):	10.384 um	d(0.9):	85.799 um

Particle Size Distribution

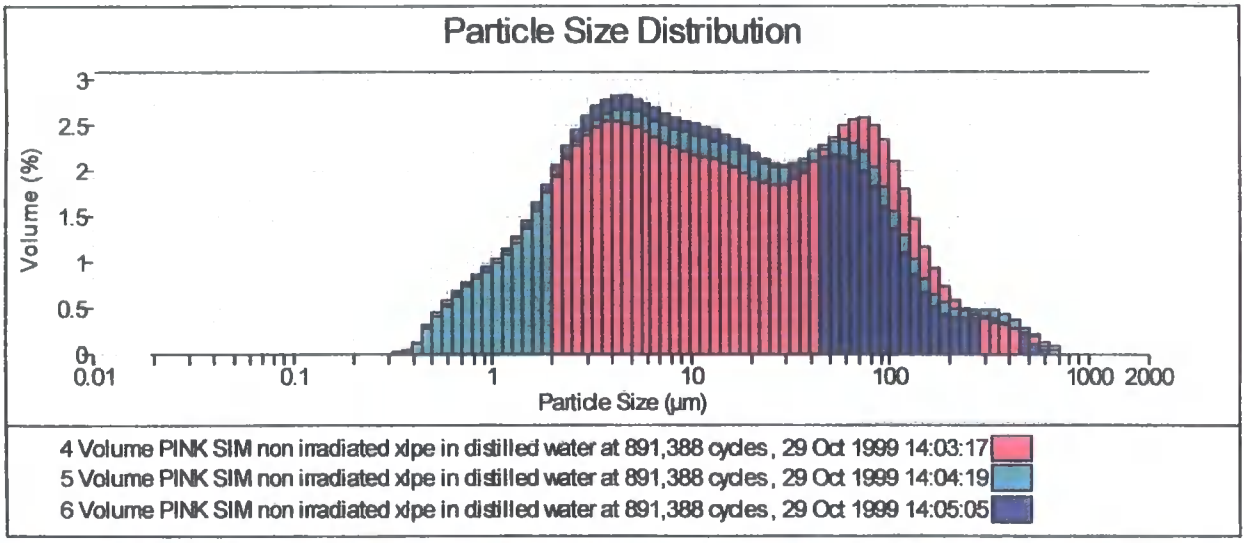

Size (µm)	Volume In %	Size (µm)	Volume In %	Size (µm)	Volume In %	Size (µm)	Volume In %	Size (µm)	Volume In %	Size (µm)	Volume In %
0.020	0.00	0.142	0.00	1.002	1.03	7.096	2.62	50.238	2.16	355.656	0.34
0.022	0.00	0.159	0.00	1.125	1.14	7.962	2.57	56.368	2.15	399.053	0.28
0.025	0.00	0.178	0.00	1.262	1.28	8.934	2.53	63.246	2.09	447.744	0.20
0.028	0.00	0.200	0.00	1.416	1.44	10.024	2.50	70.963	1.99	502.377	0.09
0.032	0.00	0.224	0.00	1.589	1.64	11.247	2.47	79.621	1.82	563.677	0.03
0.036	0.00	0.252	0.00	1.783	1.84	12.619	2.43	89.337	1.60	632.456	0.00
0.040	0.00	0.282	0.00	2.000	2.06	14.159	2.39	100.237	1.36	709.627	0.00
0.045	0.00	0.317	0.00	2.244	2.26	15.887	2.33	112.468	1.09	796.214	0.00
0.050	0.00	0.356	0.03	2.518	2.44	17.825	2.26	126.192	0.86	893.367	0.00
0.056	0.00	0.399	0.11	2.825	2.59	20.000	2.19	141.589	0.66	1002.375	0.00
0.063	0.00	0.448	0.28	3.170	2.70	22.440	2.13	158.866	0.51	1124.683	0.00
0.071	0.00	0.502	0.41	3.557	2.77	25.179	2.08	178.250	0.43	1261.915	0.00
0.080	0.00	0.564	0.54	3.990	2.80	28.251	2.05	200.000	0.39	1415.892	0.00
0.089	0.00	0.632	0.65	4.477	2.80	31.698	2.05	224.404	0.38	1588.657	0.00
0.100	0.00	0.710	0.76	5.024	2.77	35.566	2.07	251.785	0.39	1782.502	0.00
0.113	0.00	0.796	0.85	5.637	2.73	39.905	2.10	282.507	0.40	2000.000	
0.126	0.00	0.893	0.94	6.325	2.67	44.774	2.14	316.979	0.38		
0.142	0.00	1.002		7.096		50.238		355.656			

Operator notes: this prediction present in 0 % of [illegible] = 2.5 %
and 12.8 : 10 [illegible] in size

MASTERSIZER 2000

Result Analysis Report

Sample Name: 6... **SOP Name:** XLPE Cinzia **Measured:** 29 Oct 1999 14:05:05

Sample Source & type: in vitro = polyethylene **Measured by:** Administrator **Analysed:** 29 Oct 1999 17:21:50

Sample bulk lot ref: **Result Source:** Measurement

Particle Name: Default **Accessory Name:** Hydro 2000SM (A) **Obscuration:** 8.96 %

Particle RI: 1.520 **Absorption:** 0.1 **Analysis model:** General purpose

Dispersant Name: Water **Size range:** 0.020 to 2000.000 um **Weighted Residual:** 1.588 %

Dispersant RI: 1.330

Concentration: 0.0056 %Vol **Vol. Weighted Mean D[4,3]:** 33.770 um **Specific Surface Area:** 1.37839 m²/g

Span (10% - 90%): 1.439 **Uniformity:** 0.496704 **Surface Weighted Mean D[3,2]:** 4.353 um

Result units: Number

d(0.1): 0.450 um d(0.5): 0.641 um d(0.9): 1.372 um

Particle Size Distribution

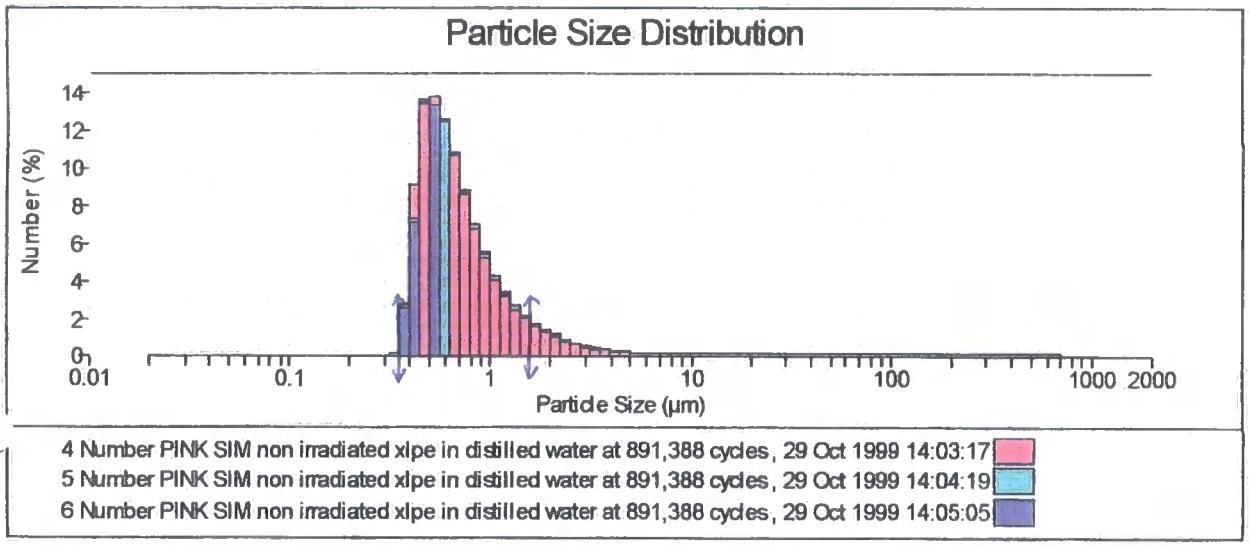

4 Number PINK SIM non irradiated xlpe in distilled water at 891,388 cycles, 29 Oct 1999 14:03:17

5 Number PINK SIM non irradiated xlpe in distilled water at 891,388 cycles, 29 Oct 1999 14:04:19

6 Number PINK SIM non irradiated xlpe in distilled water at 891,388 cycles, 29 Oct 1999 14:05:05

Size (µm)	Volume In %	Size (µm)	Volume In %	Size (µm)	Volume In %	Size (µm)	Volume In %	Size (µm)	Volume In %	Size (µm)	Volume In %
0.020	0.00	0.142	0.00	1.002	4.23	7.098	0.03	50.238	0.00	355.656	0.00
0.022	0.00	0.159	0.00	1.125	3.32	7.962	0.02	56.368	0.00	399.053	0.00
0.025	0.00	0.178	0.00	1.262	2.63	8.934	0.01	63.246	0.00	447.744	0.00
0.028	0.00	0.200	0.00	1.416	2.11	10.024	0.01	70.963	0.00	502.377	0.00
0.032	0.00	0.224	0.00	1.589	1.68	11.247	0.01	79.621	0.00	563.677	0.00
0.036	0.00	0.252	0.00	1.783	1.35	12.619	0.00	89.337	0.00	632.456	0.00
0.040	0.00	0.282	0.00	2.000	1.08	14.159	0.00	100.237	0.00	709.627	0.00
0.045	0.00	0.317	0.01	2.244	0.83	15.887	0.00	112.468	0.00	796.214	0.00
0.050	0.00	0.356	2.51	2.518	0.63	17.825	0.00	126.192	0.00	893.367	0.00
0.056	0.00	0.399	7.01	2.825	0.47	20.000	0.00	141.589	0.00	1002.375	0.00
0.063	0.00	0.448	13.53	3.170	0.35	22.440	0.00	158.866	0.00	1124.683	0.00
0.071	0.00	0.502	13.22	3.557	0.25	25.179	0.00	178.250	0.00	1261.915	0.00
0.080	0.00	0.564	12.40	3.990	0.18	28.251	0.00	200.000	0.00	1415.892	0.00
0.089	0.00	0.632	10.72	4.477	0.13	31.698	0.00	224.404	0.00	1588.657	0.00
0.100	0.00	0.710	8.72	5.024	0.09	35.566	0.00	251.785	0.00	1782.502	0.00
0.113	0.00	0.796	6.94	5.637	0.06	39.905	0.00	282.507	0.00	2000.000	
0.126	0.00	0.893	5.42	6.325	0.04	44.774	0.00	316.979	0.00		
0.142		1.002		7.098		50.238		355.656			

Operator notes: the particles present in a number (%) > 10% are 0.4 ÷ 0.7 µm in size

MASTERSIZER 2000

Result Analysis Report

Sample Name: 9... **SOP Name:** XLPE Cinzia **Measured:** 29 Oct 1999 14:56:30

Sample Source & type: in vitro = polyethylene **Measured by:** Administrator **Analysed:** 29 Oct 1999 14:56:31

Sample bulk lot ref: **Result Source:** Measurement

Particle Name: Default **Accessory Name:** Hydro 2000SM (A) **Obscuration:** 1.76 %

Particle RI: 1.520 **Absorption:** 0.1 **Analysis model:** General purpose

Dispersant Name: Water **Size range:** 0.020 to 2000.000 um **Weighted Residual:** 2.592 %

Dispersant RI: 1.330

Concentration: 0.0025 %Vol **Vol. Weighted Mean D[4,3]:** 44.721 um **Specific Surface Area:** 0.623601 m²/g

Span (10% - 90%): 2.363 **Uniformity:** 0.74041 **Surface Weighted Mean D[3,2]:** 9.622 um

Result units: Volume

d(0.1): 4.435 um **d(0.5): 38.264 um** d(0.9): 94.845 um

Particle Size Distribution

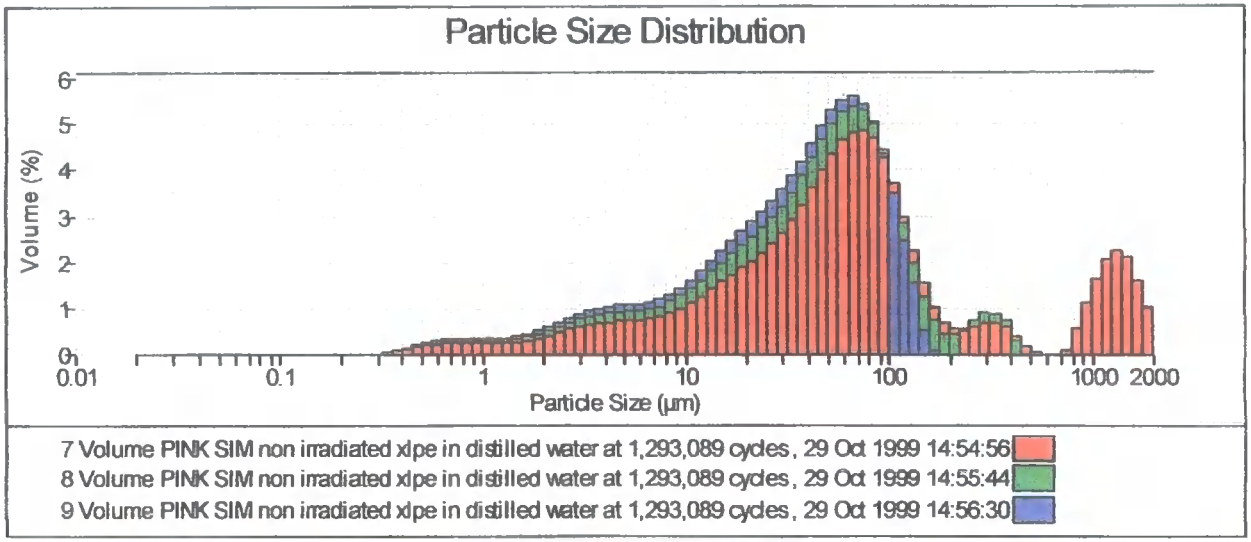

Size (µm)	Volume In %	Size (µm)	Volume In %	Size (µm)	Volume In %	Size (µm)	Volume In %	Size (µm)	Volume In %	Size (µm)	Volume In %
0.020	0.00	0.142	0.00	1.002	0.31	7.096	1.17	50.238	5.25	355.656	0.00
0.022	0.00	0.159	0.00	1.125	0.31	7.962	1.27	56.368	5.47	399.053	0.00
0.025	0.00	0.178	0.00	1.262	0.32	8.934	1.41	63.246	5.54	447.744	0.00
0.028	0.00	0.200	0.00	1.416	0.35	10.024	1.58	70.963	5.39	502.377	0.00
0.032	0.00	0.224	0.00	1.589	0.40	11.247	1.78	79.621	4.99	563.677	0.00
0.036	0.00	0.252	0.00	1.783	0.47	12.619	2.00	89.337	4.33	632.456	0.00
0.040	0.00	0.282	0.00	2.000	0.56	14.159	2.22	100.237	3.46	709.627	0.00
0.045	0.00	0.317	0.00	2.244	0.66	15.887	2.44	112.468	2.44	796.214	0.00
0.050	0.00	0.356	0.07	2.518	0.75	17.825	2.65	126.192	1.53	893.367	0.00
0.056	0.00	0.399	0.13	2.825	0.85	20.000	2.85	141.589	0.50	1002.375	0.00
0.063	0.00	0.448	0.20	3.170	0.92	22.440	3.06	158.866	0.08	1124.683	0.00
0.071	0.00	0.502	0.24	3.557	0.98	25.179	3.28	178.250	0.00	1261.915	0.00
0.080	0.00	0.564	0.28	3.990	1.01	28.251	3.53	200.000	0.00	1415.892	0.00
0.089	0.00	0.632	0.30	4.477	1.03	31.698	3.83	224.404	0.00	1588.657	0.00
0.100	0.00	0.710	0.32	5.024	1.05	35.566	4.16	251.785	0.00	1782.502	0.00
0.113	0.00	0.796	0.32	5.637	1.05	39.905	4.54	282.507	0.00	2000.000	
0.126	0.00	0.893	0.31	6.325	1.10	44.774	4.91	316.979	0.00		
0.142	0.00	1.002		7.096		50.238		355.656	0.00		

Operator notes: this condition produced a [illegible] (%) > 4% CNE. 35.5 = 89.3 [illegible] in size

MASTERSIZER 2000

Result Analysis Report

Sample Name: 9... **SOP Name:** XLPE Cinzia **Measured:** 29 Oct 1999 14:56:30

Sample Source & type: in vitro = polyethylene **Measured by:** Administrator **Analysed:** 29 Oct 1999 17:23:19

Sample bulk lot ref: **Result Source:** Measurement

Particle Name: Default **Accessory Name:** Hydro 2000SM (A) **Obscuration:** 1.76 %

Particle RI: 1.520 **Absorption:** 0.1 **Analysis model:** General purpose

Dispersant Name: Water **Size range:** 0.020 to 2000.000 um **Weighted Residual:** 2.592 %

Dispersant RI: 1.330

Concentration: 0.0025 %Vol **Vol. Weighted Mean D[4,3]:** 44.721 um **Specific Surface Area:** 0.623601 m²/g

Span (10% - 90%): 1.090 **Uniformity:** 0.429838 **Surface Weighted Mean D[3,2]:** 9.622 um

Result units: Number

d(0.1): 0.398 um **d(0.5):** 0.533 um d(0.9): 0.979 um

Particle Size Distribution

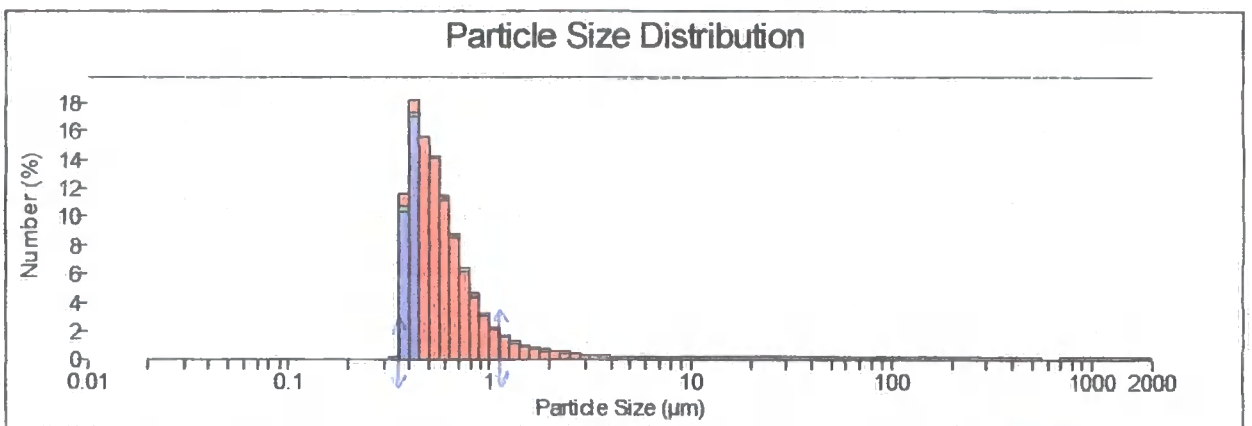

7 Number PINK SIM non irradiated xlpe in distilled water at 1,293,089 cycles, 29 Oct 1999 14:54:56

8 Number PINK SIM non irradiated xlpe in distilled water at 1,293,089 cycles, 29 Oct 1999 14:55:44

9 Number PINK SIM non irradiated xlpe in distilled water at 1,293,089 cycles, 29 Oct 1999 14:56:30

Size (µm)	Volume In %
0.020	0.00
0.022	0.00
0.025	0.00
0.028	0.00
0.032	0.00
0.036	0.00
0.040	0.00
0.045	0.00
0.050	0.00
0.056	0.00
0.063	0.00
0.071	0.00
0.080	0.00
0.089	0.00
0.100	0.00
0.113	0.00
0.126	0.00
0.142	0.00

Size (µm)	Volume In %
0.142	0.00
0.159	0.00
0.178	0.00
0.200	0.00
0.224	0.00
0.252	0.00
0.282	0.00
0.317	0.03
0.356	10.21
0.399	16.88
0.448	15.44
0.502	14.05
0.564	11.30
0.632	8.63
0.710	6.35
0.798	4.51
0.893	3.15
1.002	

Size (µm)	Volume In %
1.002	2.19
1.125	1.56
1.262	1.15
1.416	0.89
1.589	0.72
1.783	0.60
2.000	0.50
2.244	0.42
2.518	0.34
2.825	0.27
3.170	0.21
3.557	0.16
3.990	0.11
4.477	0.08
5.024	0.06
5.637	0.04
6.325	0.03
7.096	

Size (µm)	Volume In %
7.096	0.02
7.962	0.02
8.934	0.01
10.024	0.01
11.247	0.01
12.619	0.01
14.159	0.01
15.887	0.00
17.825	0.00
20.000	0.00
22.440	0.00
25.179	0.00
28.251	0.00
31.698	0.00
35.566	0.00
39.905	0.00
44.774	0.00
50.238	

Size (µm)	Volume In %
50.238	0.00
56.368	0.00
63.248	0.00
70.963	0.00
79.621	0.00
89.337	0.00
100.237	0.00
112.468	0.00
126.192	0.00
141.589	0.00
158.866	0.00
178.250	0.00
200.000	0.00
224.404	0.00
251.785	0.00
282.507	0.00
316.979	0.00
355.656	

Size (µm)	Volume In %
355.656	0.00
399.053	0.00
447.744	0.00
502.377	0.00
563.677	0.00
632.456	0.00
709.627	0.00
796.214	0.00
893.387	0.00
1002.375	0.00
1124.683	0.00
1261.915	0.00
1415.892	0.00
1588.657	0.00
1782.502	0.00
2000.000	0.00

Operator notes:

MASTERSIZER 2000

Result Analysis Report

Sample Name: 12... **SOP Name:** XLPE Cinzia **Measured:** 29 Oct 1999 15:05:11

Sample Source & type: in vitro = polyethylene **Measured by:** Administrator **Analysed:** 29 Oct 1999 15:05:12

Sample bulk lot ref: **Result Source:** Measurement

Particle Name: Default **Accessory Name:** Hydro 2000SM (A) **Obscuration:** 1.38 %

Particle RI: 1.520 **Absorption:** 0.1 **Analysis model:** General purpose

Dispersant Name: Water **Size range:** 0.020 to 2000.000 um **Weighted Residual:** 8.572 %

Dispersant RI: 1.330

Concentration: 0.0011 %Vol **Vol. Weighted Mean D[4,3]:** 285.855 um **Specific Surface Area:** 1.27399 m²/g

Span (10% - 90%): 13.114 **Uniformity:** 4.3609 **Surface Weighted Mean D[3,2]:** 4.710 um

Result units: Volume

d(0.1): 1.385 um **d(0.5): 62.439 um** d(0.9): 820.220 um

Particle Size Distribution

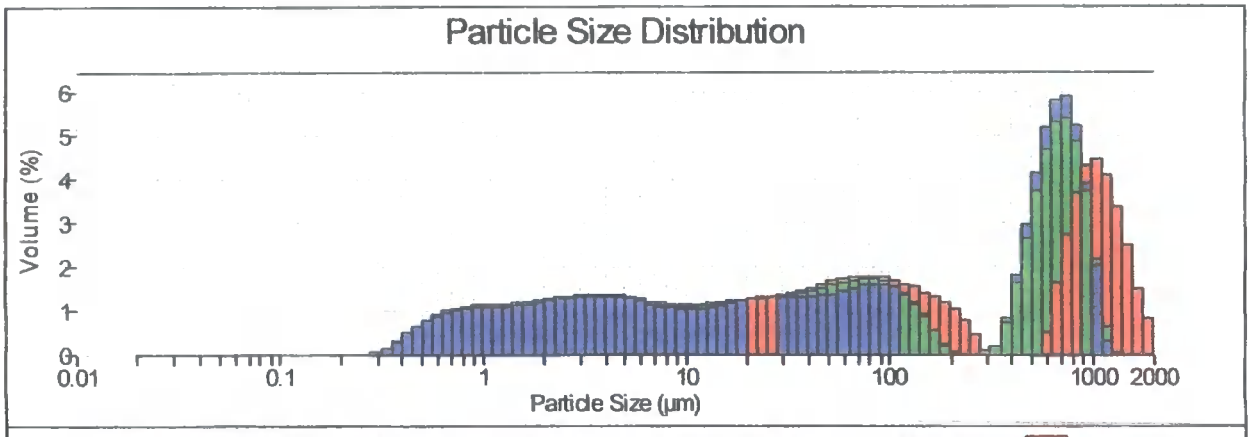

Size (µm)	Volume In %
0.020	0.00
0.022	0.00
0.025	0.00
0.028	0.00
0.032	0.00
0.036	0.00
0.040	0.00
0.045	0.00
0.050	0.00
0.056	0.00
0.063	0.00
0.071	0.00
0.080	0.00
0.089	0.00
0.100	0.00
0.113	0.00
0.126	0.00
0.142	0.00

Size (µm)	Volume In %
0.142	0.00
0.159	0.00
0.178	0.00
0.200	0.00
0.224	0.00
0.252	0.00
0.282	0.01
0.317	0.09
0.356	0.27
0.399	0.46
0.448	0.60
0.502	0.73
0.564	0.85
0.632	0.93
0.710	0.99
0.796	1.03
0.893	1.05
1.002	1.06

Size (µm)	Volume In %
1.002	1.06
1.125	1.06
1.262	1.07
1.416	1.09
1.589	1.12
1.783	1.15
2.000	1.19
2.244	1.23
2.518	1.26
2.825	1.29
3.170	1.31
3.557	1.31
3.990	1.30
4.477	1.28
5.024	1.24
5.637	1.19
6.325	1.13
7.096	1.08

Size (µm)	Volume In %
7.096	1.08
7.962	1.05
8.934	1.03
10.024	1.02
11.247	1.04
12.619	1.08
14.159	1.12
15.887	1.17
17.825	1.21
20.000	1.25
22.440	1.27
25.179	1.29
28.251	1.29
31.698	1.29
35.566	1.29
39.905	1.29
44.774	1.30
50.238	1.32

Size (µm)	Volume In %
50.238	1.32
56.368	1.36
63.246	1.42
70.963	1.48
79.621	1.55
89.337	1.58
100.237	1.58
112.468	1.51
126.192	1.36
141.589	1.14
158.866	0.86
178.250	0.53
200.000	0.18
224.404	0.01
251.785	0.00
282.507	0.00
316.979	0.00
355.656	0.16

Size (µm)	Volume In %
355.656	0.16
399.053	0.79
447.744	1.78
502.377	2.92
563.677	4.12
632.456	5.16
709.627	5.81
796.214	5.86
893.367	5.19
1002.375	3.90
1124.683	2.03
1261.915	0.31
1415.892	0.00
1588.657	0.00
1782.502	0.00
2000.000	0.00

Operator notes:

MASTERSIZER 2000

Result Analysis Report

Sample Name:	12...	**SOP Name:**	XLPE Cinzia	**Measured:**	29 Oct 1999 15:05:11
Sample Source & type:	in vitro = polyethylene	**Measured by:**	Administrator	**Analysed:**	29 Oct 1999 17:24:54
Sample bulk lot ref:				**Result Source:**	Measurement

Particle Name:	Default		**Accessory Name:**	Hydro 2000SM (A)	**Obscuration:**	1.38	%
Particle RI:	1.520	**Absorption:** 0.1	**Analysis model:**	General purpose			
Dispersant Name:	Water		**Size range:**	0.020 to 2000.000 um	**Weighted Residual:**	8.572	%
Dispersant RI:	1.330						

Concentration:	0.0011	%Vol	**Vol. Weighted Mean D[4,3]:**	285.856	um	**Specific Surface Area:**	1.27399	m²/g
Span (10% - 90%):	1.096		**Uniformity:**	0.383655		**Surface Weighted Mean D[3,2]:**	4.710	um
Result units:	Number							
d(0.1):	0.366	um	d(0.5):	0.505	um	d(0.9):	0.919	um

Particle Size Distribution

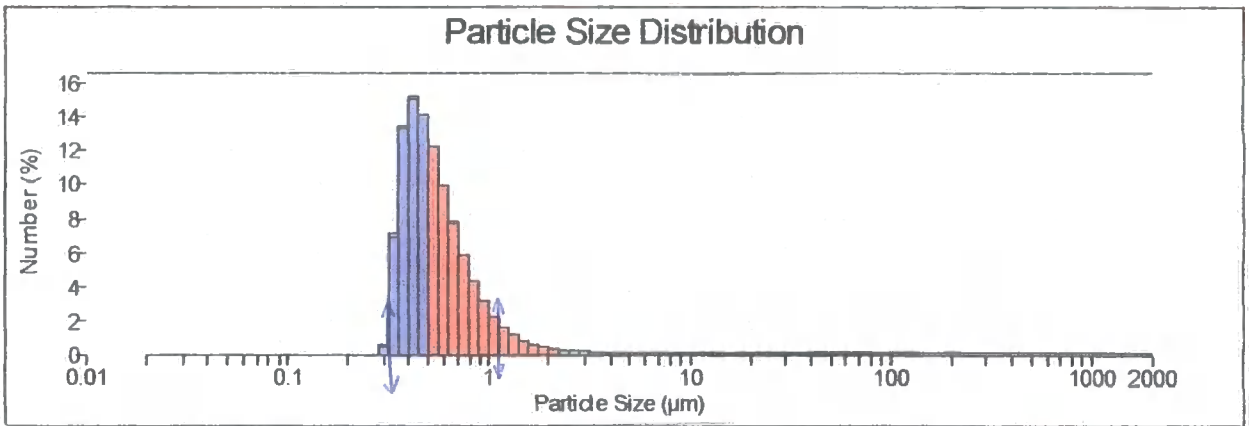

10 Number PINK SIM non irradiated xlpe in distilled water at 1,650,973 cycles, 29 Oct 1999 15:03:37
11 Number PINK SIM non irradiated xlpe in distilled water at 1,650,973 cycles, 29 Oct 1999 15:04:23
12 Number PINK SIM non irradiated xlpe in distilled water at 1,650,973 cycles, 29 Oct 1999 15:05:11

Size (µm)	Volume In %	Size (µm)	Volume In %	Size (µm)	Volume In %	Size (µm)	Volume In %	Size (µm)	Volume In %	Size (µm)	Volume In %
0.020	0.00	0.142	0.00	1.002	2.19	7.096	0.01	50.238	0.00	355.656	0.00
0.022	0.00	0.159	0.00	1.125	1.56	7.962	0.00	56.368	0.00	399.053	0.00
0.025	0.00	0.178	0.00	1.262	1.11	8.934	0.00	63.246	0.00	447.744	0.00
0.028	0.00	0.200	0.00	1.416	0.80	10.024	0.00	70.963	0.00	502.377	0.00
0.032	0.00	0.224	0.00	1.589	0.58	11.247	0.00	79.621	0.00	563.677	0.00
0.036	0.00	0.252	0.00	1.783	0.43	12.619	0.00	89.337	0.00	632.456	0.00
0.040	0.00	0.282	0.45	2.000	0.31	14.159	0.00	100.237	0.00	709.627	0.00
0.045	0.00	0.317	6.79	2.244	0.23	15.887	0.00	112.468	0.00	796.214	0.00
0.050	0.00	0.356	13.15	2.518	0.17	17.825	0.00	126.192	0.00	893.367	0.00
0.056	0.00	0.399	14.98	2.825	0.12	20.000	0.00	141.589	0.00	1002.375	0.00
0.063	0.00	0.448	14.04	3.170	0.09	22.440	0.00	158.866	0.00	1124.683	0.00
0.071	0.00	0.502	12.16	3.557	0.06	25.179	0.00	178.250	0.00	1261.915	0.00
0.080	0.00	0.564	9.85	3.990	0.04	28.251	0.00	200.000	0.00	1415.892	0.00
0.089	0.00	0.632	7.68	4.477	0.03	31.698	0.00	224.404	0.00	1588.657	0.00
0.100	0.00	0.710	5.79	5.024	0.02	35.566	0.00	251.785	0.00	1782.502	0.00
0.113	0.00	0.796	4.28	5.637	0.01	39.905	0.00	282.507	0.00	2000.000	0.00
0.126	0.00	0.893	3.07	6.325	0.01	44.774	0.00	316.979	0.00		
0.142	0.00	1.002		7.096		50.238		355.656			

Operator notes:

n Instruments Ltd.
n, UK
+[44] (0) 1684-892456 Fax +[44] (0) 1684-892789